Norges miljø- og
biovitenskapelige
universitet

Master's Thesis 2017 30 ECTS
Department of Mathematical Science and Technology

Mechanical and Electrochemical Prelithiation of Silicon Nanoparticles in Lithium-Ion Battery Anodes

Alise Johannessen Hjellbrekke
Environmental Physics and Renewable Energy

Preface

This master's thesis marks the end of the five year long Master of Science in Environmental Physics and Renewable Energy at NMBU.

Leaving high school five years ago, the only thing I knew for sure was that I did not want to become an engineer and that I wanted to study something relevant for a more sustainable future. Never had I imagined that five years later I would be leaving NMBU with a Master of Science in the university's most theoretical, and in my opinion most future-oriented, science degree. I can not be anything but impressed, proud and a bit surprised by myself.

The work was done in collaboration with the Institute for Energy Technology (IFE) as part of the project called Siproco Fobeliba (Silicon Production Control For Better Lithium Ion Batteries). The Research Council of Norway is acknowledged for the funding of this project through the ENERGIX Project No. 255116.

During the thesis work I got the opportunity to present my work as a poster presentation at the 3rd Nordic Battery Conference in Kokkola, Finland 1.-3. of November 2017. This poster took home the Best Poster Award and can be found in Appendix A.

Kjeller, 14.12.2017

Alise Johannessen Hjellbrekke

Acknowledgements

First of all I want to thank Samson Lai, post-doc and my technical supervisor at IFE, for optimistic support, excellent guidance and so patiently answering all my (at times silly) questions. I would also like to give a big thank you to my supervisor at NMBU, Arne Grimenes, for his enthusiasm, encouraging advice and time.

I am very grateful for the opportunity to write my master's thesis in collaboration with IFE. I have not only learned a lot about batteries, but also a lot about solar energy by following the dedicated researchers at the Solar Department. I am grateful that I got the opportunity to be a part of the multidisciplinary project group Siproco Fobeliba, which provided a useful arena for feedback and helped put a greater meaning into my thesis work. I also want to thank Jan Petter Mæhlen and Asbjørn Ulvestad from the Energy Systems Department, who have been my coo-supervisors and provided me with invaluable help with interpreting and understanding the electrochemical data when needed. I also need to thank Marius Nagell, lab engineer at IFE, for training and allowing me access to the battery labs.

Last but not least I want to thank my friends and family. An immensely big thank you to my two best friends, Malin and Johanne, for countless hours of scientific discussions, silly girl talks, delicious dinners, wine "tasting," etc. A big thank you to my family for always supporting and believing in me, and an especially big thank you to my boyfriend, Bård, for encouraging and keeping me sane these last couple of months.

Samandrag

Silisium (Si) har vist seg å vere eit av dei mest lovande anodemateriala for neste generasjons litium-ionbatteri. Silisium har ei høg legeringsevne med litium, og kan i teorien levere opp til ti gongar så mykje kapasitet som den meir tradisjonelle grafittanoden. Men, med denne legeringsevna følgjer ei enorm volumendring som resulterer i degresjon av kapasitet i tideleg sykling. Lang nok levetid for batteria til å bli kommersielle er endå ikkje nådd.

I denne studia har prelitiering blitt undersøkt som ei mogeleg løysing for å redusere det irreversible kapasitetstapet sett i tideleg sykling, samt potensielt sett forlenge levetida til cellene. To prelitieringsmetodar har blitt utvikla: elektrokjemisk prelitiering (EP) og mekanisk prelitiering (MP). I EP prosessen blei kvar celle sykla ein gong i ein batteritestar med ein rate på C/20, før dei blei demonterte, vaska og remonterte til nye, no prelitierte, halvceller. I MP prosessen blei litiumfolie lagt direkte oppå Si elektrodane med berre elektrolytt imellom, og klemt saman mellom to glasskåler.

Begge metodane viste suksessfull prelitiering, og ein litieringsgrad på omlag 100 % blei nådd med både EP og MP. Gjennom ei tidsavhengig studie, blei det sett at litieringsgraden aukar med prelitieringstid, og det blei vist at prelitiering potensielt sett kan bli regulert ved hjelp av tids- og massemålingar. Resultata viste òg at ein litieringsgrad > 90 % kan bli nådd med berre 60 min MP.

Både referanse- og prelitierte Si elektrodar blei monterte i halvceller med litium-metall som referanse-elektrode, og elektrokjemisk sykla i ein batteritestar. Resultata viste ingen forskjell i elektrokjemisk syklingsignatur mellom dei prelitierte og ikkje-prelitierte cellene. Dette blei vidare forklart av elektronmikroskopi (SEM) som viste at Si nanopartiklane overlevde prelitiering utan betydelige endringar i nanostruktur. Sjølv om degraderinga av kapasiteten i dei første syklusane blei redusert, oppnådde dei prelitierte cellene same levetid som referansecellene på $\sim$ 50 syklusar. To av MP cellene med høgast litieringsgrad blei vist å nå ein noko lenger levetid opp mot 60 syklusar.

I tillegg blei dei prelitierte cellene sykla på to forskjellige program med avgrensa kapasitet. Det eine programmet avgrensa litieringskapasiteten, mens det andre programmet avgrensa delitieringskapasiteten. Begge programma var avgrensa av kapasiteten 372 mAh/g_{Si}, som er den teoretiske kapasiteten til grafittanoden. Alle cellene sykla med neglisjerbar kapasitetsdegresjon for 500 syklusar.

Abstract

Silicon (Si) is one of the most promising anode materials for the next generation lithium ion batteries, as it can store up to ten times the capacity compared to the conventional graphite anode. However, with its alloying capacity follows great volume expansions resulting in capacity fade during the early cycles.

In this study, prelithiation was studied as a possible solution to reduce the irreversible capacity loss seen during the first cycle, and to potentially increase cycle life. Two methods for prelithiation of silicon nanoparticles (SiNPs) were developed: electrochemical prelithiation (EP) and mechanical prelithiation (MP). In the EP process the half-cells were electrochemically cycled one cycle with a rate of C/20, before disassembled, washed, and reassembled into new, now prelithiated, half-cells. In the MP process a Si electrode with electrolyte was sandwiched with a piece of Li foil between two glass dishes.

Both methods were shown to successfully prelithiate the Si electrodes, and a degree of prelithiation close to 100 % was obtained with both EP and MP. Through a time-dependent study it was seen that the degree of prelithiation increases with prelithiation time, and that prelithiation potentially can be regulated by time and mass measurements. The results showed that a degree of prelithiation > 90 % could be reached in just 60 min of MP.

Both reference and prelithiated Si electrodes were assembled into coin cells with lithium metal as the counter electrode, and electrochemically cycled. The results showed no significant change in electrochemical cycling signature, and scanning electron microscopy (SEM) measurements showed that the structure of the SiNPs was maintained during prelithiation. Even though the discharge capacity decay was seen reduced for the prelithiated cells during the first cycles, they retained as poor cycle life as the reference cells of $\sim$ 50 cycles. Two of the MP cells with the highest degree of prelithiation showed however slightly increased cycle lives up to $\sim$ 60 cycles.

Additionally, prelithiated cells were cycled on two different limited capacity cycling programs, one limiting the lithiation process, the other limiting the delithiation process. Both were limited by the capacity of 372 mAh/g_{Si}, similar to the theoretical value of the graphite anode. All cells cycled 500 cycles with no significant decrease in discharge capacity.

Contents

Preface iii

Acknowledgements v

Samandrag vii

Abstract ix

1 Introduction 1
1.1 Aim of this work . . . 3

2 Theoretical Background 5
2.1 Development of Batteries Through History . . . 5
2.2 The Electrochemical Cell . . . 6
2.2.1 Battery vs. Cell . . . 6
2.2.2 Standard Components of the Electrochemical Cell . . . 7
2.2.3 Standard Operation of the Electrochemical Cell . . . 7
2.2.4 Primary Cells and Secondary Cells . . . 8
2.2.5 Full Cells and Half-Cells . . . 9
2.3 Lithium-Ion Batteries . . . 9
2.3.1 Electrochemical principle . . . 10
2.3.2 Choosing Components for Lithium-Ion Batteries . . . 11
Electrode Materials . . . 11
Electrolyte . . . 12
Solid Electrolyte Interphase layer . . . 13
2.4 Silicon as Anode Material . . . 14
2.4.1 Lithiation Mechanism of Silicon . . . 14
2.4.2 Challenges of Silicon Anode . . . 17
Material Pulverisation . . . 17
Morphology and Volume Change of the Electrode . . . 17
Formation of Unstable SEI . . . 18
Low Initial Coulombic Efficiency . . . 18
2.5 Strategies to Overcome Si Anode Challenges . . . 19
2.5.1 Prelithiation . . . 20
2.5.2 Limited capacity cycling . . . 21
2.5.3 Carbon Coating . . . 22
2.6 Electrochemical Characterization . . . 23
2.6.1 Capacity and Coulombic Efficiency . . . 24
Theoretical and Practical Capacity . . . 24
Reversible Capacity . . . 24

Coulombic Efficiency 25
2.6.2 Cycle Life 26
Charge/Discharge Rate 26
2.6.3 Voltage-Capacity Curves 26
2.6.4 Galvanostatic Techniques 27
2.6.5 Differential Capacity 28

3 Experimental and Analytic Methodology 31
3.1 Slurry and Electrode Preparation 31
3.2 Cell Assembly 32
Electrolyte 33
3.3 Prelithiation 33
3.3.1 Electrochemical Prelithiation 34
3.3.2 Mechanical Prelithiation 34
3.4 Galvanostatic Cycling 36
3.4.1 Standard Cycling Program 37
3.4.2 Limited Capacity Cycling Programs 37
Limited Delithiation Cycling 38
Limited Lithiation Cycling 38
3.5 Analysis Methods 39
3.5.1 Cycling Data 40
Accuracy of Arbin 40
3.5.2 Mass Measurements 40
3.5.3 Scanning Electron Microscopy 40

4 Results 43
4.1 Prelithiation 43
4.1.1 Degree of Prelithiation 43
4.1.2 Change in Mass 46
4.2 Electrochemical Performance 48
4.2.1 Reference Cells 48
4.2.2 Electrochemical Prelithiation 53
4.2.3 Mechanical Prelithiation 58
4.2.4 Summary of Performance 66
4.3 Limited Capacity Cycling 68

5 Discussion 75
5.1 Prelithiation over time 75
5.1.1 Degree of Prelithiation 75
5.1.2 Potential Sources of Error in the Determination of the Calculation of the Degree of Prelithiation 76
5.1.3 Washing of the Prelithiated Electrodes 76
5.1.4 Mass Change and Prelithiation Time 77
5.2 Electrochemical Cycling 78
5.2.1 Variation in Mass Loading 79
5.2.2 Coulombic Efficiency and HC Efficiency 79
Coulombic Efficiency 79
HC Efficiency 81

5.2.3 Voltage-Capacity Cycles 82
5.2.4 Differential Capacity 83
5.2.5 Cell Failure 83
5.2.6 Performance 84
5.3 Limited Capacity Cycling 86
5.4 Evaluation of the Prelithiation and Galvanostatic Cycling Methods 87
5.4.1 Electrochemical Prelithiation 87
5.4.2 Mechanical Prelithiation 87
5.4.3 Galvanostatic Cycling 89

6 Conclusion **91**

7 Further Work **93**

A Best Poster Award at the Nordic Battery Conference 2017 **101**

B Galvanostatic Cycling **103**
B.1 Elecrochemical Prelithiation Program 103
B.2 Standard Cycling Program 103
B.3 Limited Capacity Cycling Programs 104
B.3.1 Limited Delithiation Cycling: 104
B.3.2 Limited Lithiation Cycling: 105

C Complete list of cells **107**

List of Abbreviations

2DS	Two-Degree-Scenario
Ar	Argon
a-Si	Amorphous Silicon
B2DS	Beyond-Two-Degree-Scenario
BEV	Battery Electric Vehicle
C	Carbon
CE	Coulombic Efficiency
CMC	Carboxymethyl Cellulose
Co	Cobalt
c-Si	Crystalline Silicon
Cu	Copper
CVD	Chemical Vapour Deposition
DMC	Dimethyl Carbonate
EC	Ethylene Carbonate
EDS	Energy-Dispersive X-Ray Spectroscopy
EP	Electrochemical Prelithiation
EV	Electric Vehicle
F	Fluorine
FC	Full cell
FEC	Fluorethylene Carbonate
FSR	Free Space Reactor
HC	Half-cell
HEV	Hybrid Electric Vehicle
ICL	Irreversible Capacity Loss
IEA	International Energy Agency
IFE	Institute for Energy Technology
IR	Internal Resistance
KOH	Potassium Hydroxide
Li	Lithium
LIB	Lithium-Ion Battery
MP	Mechanical Prelithiation
Ni-Cd	Nikkel-Cadmium
Ni-MH	Nikkel-Metalhydrid
NMBU	University of Life Science
O	Oxygen
OCV	Open Circuit Voltage
OEM	Original Equipment Manufacturer
Pb-acid	Lead-acid
PC	Propylene Carbonate

PHEV	Plug-in Hybrid Electric Vehicle
Redox	Reduction-Oxidation
RTS	Reference Technology Scenario
SEI	Silicon Electrolyte Interphase
SEM	Scanning Electrode Microscopy
SHE	Standard Hydrogen Electrode
Si	Silicon
SiO	Silicon Mono-Oxide
SiNP	Silicon Nanoparticle
SiNW	Silicon Nanowire
SLMP	Stabilized Lithium Metal Powder
SOC	State of Charge
VC	Vinylene Carbonate

List of Symbols

E	electrical energy	$\mathrm{W\,h\,kg^{-1}}$ or $\mathrm{W\,h\,l^{-1}}$
C	Celsius	$^{\circ}$
C_i	capacity measured in cycle *i*	$\mathrm{W\,h\,kg^{-1}}$
C_{rev}	reversible capacity	$\mathrm{W\,h\,kg^{-1}}$
C_{Th}	theoretical capacity	$\mathrm{W\,h\,kg^{-1}}$ or $\mathrm{C\,kg^{-1}}$
C′	differential capacity	$\mathrm{A\,h\,g^{-1}\,V^{-1}}$
I	current density	$\mathrm{A\,m^{-2}}$
M	molecular mass	$\mathrm{kg\,mol^{-1}}$
n	number of electrons	-
P	power	$\mathrm{W\,m^{-2}}$ ($\mathrm{J\,s^{-1}\,m^{-2}}$)
Q	charge capacity	$\mathrm{A\,h\,kg^{-1}}$
Q_{in}	charge flowing into electrode during lithiation	$\mathrm{A\,h\,kg^{-1}}$
Q_{out}	charge flowing out of electrode during delithiation	$\mathrm{A\,h\,kg^{-1}}$
R	internal resistance	Ω
V	potential	V
wt%	mass fraction, percentage by mass/weight	%
x	cycle number	-
η	coulombic efficiency	%

1 Introduction

According to the International Energy Agency (IEA)'s 2017 CO_2 Emission outlook, the energy sector accounts for about two-thirds of the world's total greenhouse gas emissions, and almost 80 % of CO_2 emissions [14]. The most effective way to combat climate change is to reduce the emission of greenhouse gasses. If the 2 °C goal of the 2015 Paris Agreement is going to be achieved, great efforts need to be put into the decarbonisation of the energy sector.

Decarbonisation of the energy sector goes hand in hand with electrification. According to the Exxon Mobil 2017 Outlook for Energy [31], electricity generation will be the largest and fastest growing demand sector, with an expected rise of 60 % by 2040. Furthermore, the transport sector alone accounts for about 34 % of the total greenhouse gas emissions, making it clear that a transition from a fossil fuel-based to an electricity-based transport sector will be an important step towards a carbon-free future [15]. With the expected increase in electricity demand and the obvious need for a more electricity-based transport sector, the demand for energy storage is naturally significant.

Today, energy storage is all around us, used in device such as the TV control to the electric busses soon driving around in Oslo. A wide range of batteries are used, each specially designed for a specific purpose. The lithium-ion battery (LIB) is the most widely used battery in portable electronics. It is also on the way to becoming an equally important battery for electric vehicles (EVs), and is already used in both Tesla and Nissan Leaf cars [48].

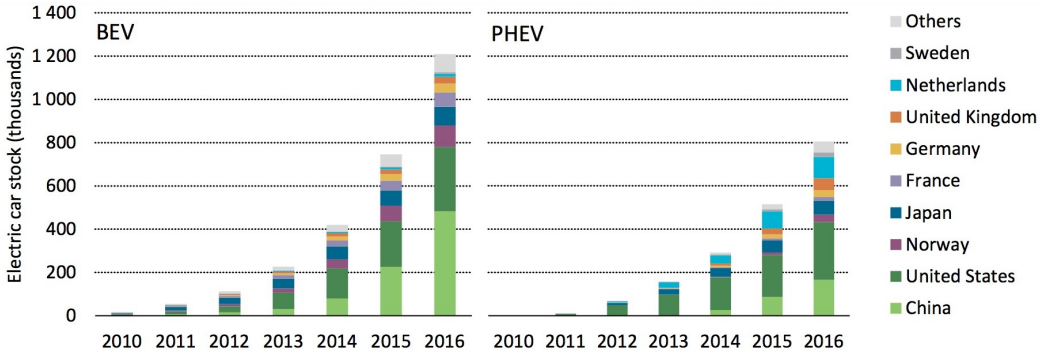

FIGURE 1.1: Evolution of the global electric car stock from 2010 to 2016. BEV is battery electric vehicles and PHEV is plug-in hybrid electric vehicles. Illustration originally appeared in IEA's Global EV 2017 Outlook [15].

The electrification of the energy sector has already started, and has been most remarkable in the transport sector. Since 2010 there has been an enormous growth in the use of EVs and hybrid electric vehicles (HEVs) (see Figure 1.1), and in 2016 the 2-million-vehicle threshold was surpassed [15]. Norway is the leading country, holding 29 % of the market share, with EVs and HEVs accounting for as much as 40 % of the personal vehicles sold in the country in 2016 [11]. The global stock of EVs and HEVs is projected to continue to grow at an exponential rate, and is expected to reach a number between 40 and 70 millions by 2025 (Figure 1.2) [15].

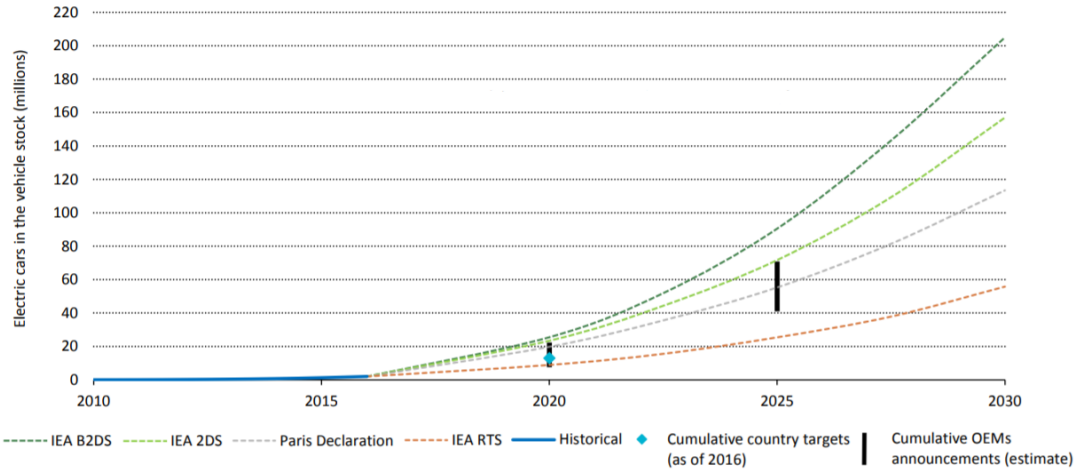

FIGURE 1.2: IEA's projection of the stock of electric cars until 2030. The different scenarios are: the beyond-two-degree scenario (B2DS), the two-degree scenario (2DS), the Paris declaration scenario, and the reference technology scenario (RTS). Illustration originally appeared in IEA's Global EV 2017 Outlook [15].

However, there is concerns regarding the amount of resources available. Both lithium and cobalt (cobalt is a key material in most commercialised LIBs) are finite resources, and this limits how many batteries that can be produced using the existing technology. Cobalt is a particular concern due to its scarcity of supply. In an estimation done by the Battery Innovation Centre in Belgium, it was found that if the production of LIBs continues with the expected rate and the same technology as today, the annual production of cobalt will not be sufficient for more than 10 years [37]. Another supply and demand projection displayed by LiCo Energy Metals is presented in Figure 1.3 [16]. The message is that the production of cobalt is not enough to answer the battery demand. The future of the LIB and EV production relies on the mining sector to find new deposits, however this is a process partly hindered by political instability and ethical concerns [13]. It is thus becoming clear that today's LIB technology is not a sustainable solution, and to be able to answer to the enormous demand for batteries, alternatives must be developed. This is not seen upon lightly by energy researchers, and research groups all over the world are putting great effort into the development of the next-generation LIB.

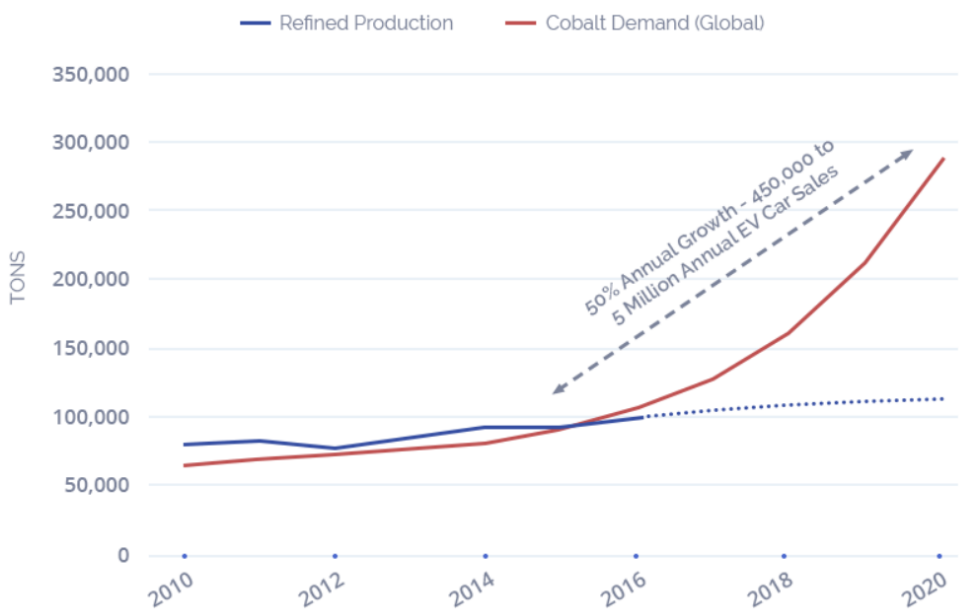

FIGURE 1.3: Projected supply and demand of cobalt until 2020. Illustration originally displayed by LiCo Energy Metals Inc. [16].

Using silicon as an anode material has emerged as one of the most promising solutions for the next-generation LIBs. Silicon is abundant in Earth's crust and has the capacity to store ten times the amount of lithium ions compared to the graphite anode traditionally used in LIBs [1]. Silicon as an anode material will also reduce the need for cobalt. However, with its alloying capacity follows a volume expansion of ~ 300 %, which tends to lead to cracking of the particles upon repeated cycling and eventually battery failure. Before good enough silicon-lithium-ion batteries can become a reality, the challenges related to these volume changes must be solved.

1.1 Aim of this work

In order to use silicon as anode material in LIBs and benefit from its high energy density, the issues related to the volume change occurring during cycling must be solved. In this thesis work, prelithiation will be studied as a possible solution.

Prelithiation is the process in which the electrodes are lithiated before being assembled into cells, and has been seen to reduce the irreversible capacity loss (ICL) in the first cycle [12, 26, 58]. Pairing prelithiated silicon electrodes with lithium-free cathodes is also a promising method to remove the requirement that LIB cathodes must contain lithium in its original state [26]. Thus, prelithiation may become an important step towards the development of the next generation high-energy LIBs, however only limited research has been done on the subject [1].

This study will be done in collaboration with the Institute for Energy Technology (IFE) as part of the project called Siproco Fobeliba (Silicon Production Control For Better Lithium Ion Batteries). Researchers at IFE are putting great effort into studying the the use of silicon particles as anode material [32], however nothing is yet being done on prelithiation. The main aim of this study is to develop simple prelithiation methods in the IFE lab, and to study the effect of prelithiation on cell performance.

Two methods for prelithiation of silicon nanoparticles will be developed in this study: electrochemical prelithiation and mechanical prelithiation, hereafter referred to as EP and MP, respectively. Despite it being a costly and time-consuming process, a silicon electrode can be electrochemically prelithiated in cells, disassembled and extracted, before being reassembled into new cells. Silicon electrodes can also be mechanically prelithiated by sandwiching the electrode and a piece of lithium metal foil, effectively short-circuiting the cell. Compared to EP, MP is a simpler and more cost-efficient method, but lacks control of the stress applied to the silicon and the degree of prelithiation. This study will compare the two methods each other and to a set of reference cells. It will also discuss if there is a way to control MP, and if prelithiation can reduce the ICL seen during the first cycles, and eventually improve the overall cyclability of the cells.

2 Theoretical Background

2.1 Development of Batteries Through History

A battery is a device that stores energy by converting chemical energy into electrical energy through redox (reduction and oxidation) reactions. The first battery was invented by Alessandro Volta, professor of physics at the University of Pavia in Italy, in 1800. His invention became known as the "Voltaic Pile," in which an electric current is produced by connecting the two ends of a stack of two metal discs separated by a cloth soaked in an alkaline solution [8, 39]. Volta's invention set the starting point for the development of the batteries as we know them today, and throughout the past 200 years various batteries have been studied and commercialised.

Batteries are classified as primary (non-rechargeable) or secondary (rechargeable), depending on their ability to reuse the chemicals and become charged/ discharged multiple times. The primary battery is the simplest type, and the one first developed. The first widely used primary battery was the Leclanché battery, invented by French chemist Georges Leclanché in 1866 [8]. The battery had a negative electrode of zinc and a positive electrode of carbon, both immersed in a solution of ammonium chloride, resulting in a working voltage of 1.5 V. This level of working voltage allowed the Leclanché battery to be used in a wide range of applications. Later the electrolyte was replaced with an alkaline electrolyte, resulting in the alkaline battery [39]. After the development of the Laclanché battery other primary batteries were developed, such as the zink-air battery (1.4 V) and the silver oxide battery (1.5 V). The first secondary battery, the lead-acid battery, was demonstrated in 1859 by the French chemist Gaston Planté [8]. With the commercialisation of the 3 V primary lithium battery (using lithium as the anode material) in the 1970s, the battery technology greatly improved, which finally led to the development of the lithium secondary batteries widely used today.

Today the lithium secondary battery (Li-ion battery – LIB) has exceeded competing technologies like the nikkel-metalhydrid (Ni-MH) battery, nikkel- cadmium (Ni-Cd) battery and lead-acid (Pb-acid) battery, in terms of energy density, as illustrated in Figure 2.1. This attractive property, coupled with its long cycle life, have led to a revolution of the battery technology, and the LIB is now the battery most frequently used in portable electronics, and is regarded to be the battery of choice for the next generation EVs and HEVs[10].

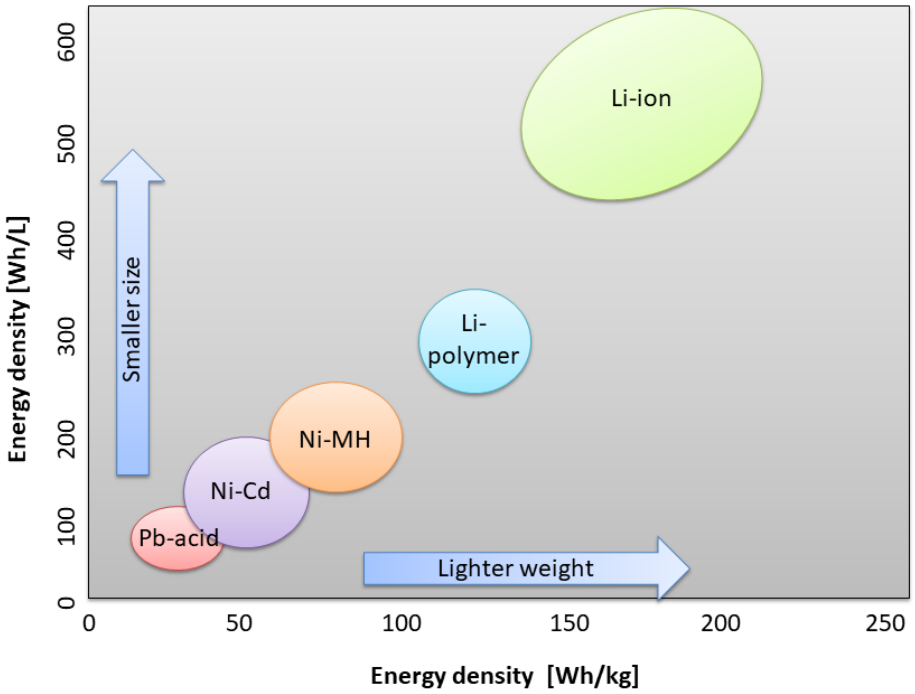

FIGURE 2.1: Changes in volumetric and gravimetric energy density for various secondary batteries. Illustration adapted from [39, 10, 47].

2.2 The Electrochemical Cell

This section will describe the basic components and operation of an electrochemical cell, whereas the next section will go into detail on how the LIB works. The theory is obtained from Dell and Rand [8] and Linden and Reddy [24], unless other is specified.

2.2.1 Battery vs. Cell

The basic electrochemical unit is called an electrolytic cell, or more commonly an electrochemical cell. A battery consists of one or several electrochemical cells, electrically connected in series or parallel to achieve the desired output voltages and capacities. It is common to refer to the term "battery" when talking about the product manufactured and sold to the users, while the term "cell" is used when talking about the cell component of the battery and its chemical properties. For the rest of this thesis the term "cell" will primarily be used.

2.2.2 Standard Components of the Electrochemical Cell

There are three main components in an electrochemical cell:

1. **Anode** - the electrode where an oxidation process, i.e. electron donation, takes place during discharge. During discharge, the negative electrode is the anode.
2. **Cathode** - the electrode where a reduction process, i.e. electron acceptance, takes place during discharge. During discharge, the positive electrode is the cathode.
3. **Electrolyte** - the medium providing ionic conductivity between the anode and cathode so that charge can be balanced between the two. It is typically a concentrated aqueous solution of salts, acids or alkalis. The electrolyte must be electrically insulating to prevent the cell from self-discharging and/or short-circuiting.

In addition to the components mentioned above, the cell consists of a separator and the housing. The separator is a thin and usually porous and insulating material, mechanically preventing contact between the two electrodes. Together with the electrolyte this mechanism protects the cell from short-circuiting. The pores in the separator will be filled with electrolyte allowing ionic current to flow through, thus maintaining the ionic conductivity between the electrodes. The housing of the cell will differ depending on what kind of cells are being built (cylindrical, flat, button, prismatic, etc.). The housings is also designed to prevent leakage and dry-out of the electrolyte.

2.2.3 Standard Operation of the Electrochemical Cell

When a chemical reaction occurs at the electrode, the electrode is said to undergo a half-cell reaction. It is when a half-cell reaction occurs on both electrodes that electricity is generated. Each electrode consists of an active material and a current collector. The active material is the chemical/metal that undergoes oxidation or reduction during the half-cell reaction, and the current collector is the metal component collecting the electrons and leading them through an external circuit. The driving force of the current in the external circuit is the difference in electrode potentials between the two half-cell reactions. When the electrochemical cell produces a current it is called a galvanic cell (Figure 2.2).

During discharge electrons are transported from the negative electrode to the positive electrode through a load in the external circuit (like demonstrated in Figure 2.2). The electric circuit is completed in the electrolyte where positive ions (cations) move towards the cathode and negative ions (anions) move towards the anode. The chemistry describing the two half-cell reactions during discharge can be represented as the following:

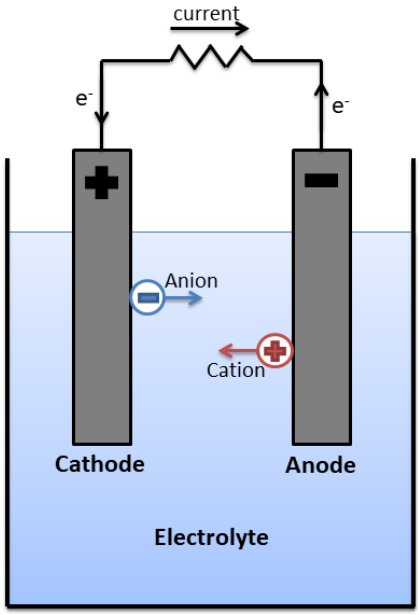

FIGURE 2.2: A galvanic cell. Illustration adapted from [8].

Negative electrode - oxidation/anodic reaction:

$$\mathrm{M} \rightarrow \mathrm{M}^{n+} + n\mathrm{e}^{-} \tag{2.1}$$

Positive electrode - reduction/cathodic reaction:

$$n\mathrm{X} + n\mathrm{e}^{-} \rightarrow n\mathrm{X}^{-} \tag{2.2}$$

where M is a metal, X is an oxidising agent/metal oxide and e^{-} is an electron.

During charge the flow of ions and electrons is reversed.

2.2.4 Primary Cells and Secondary Cells

Electrochemical cells and batteries can be defined as primary or secondary cells/batteries. Primary cells are not rechargeable and will be discarded after the first discharge. Secondary cells are rechargeable and are capable of repeated charging and discharging.

In secondary cells both oxidation and reduction occur on both electrodes depending on whether the cell is charging or discharging, thus the anode and cathode naming will switch every time charge/discharge changes. To avoid confusion the general operation mode of a cell has been defined as the discharge mode, and the anode and cathode named accordingly.

2.2.5 Full Cells and Half-Cells

Figure 2.2 is a demonstration of a full cell (FC) with working cathode and anode. A half-cell (HC) is, as the name indicates, only half of the full cell, that is only one of the electrodes in an electrolytic environment. To collect data from the half-cell, i.e. activity and working voltage, a reference electrode is required. For the experimental part of this study lithium (Li) will be used as the reference electrode when studying the effect of silicon (Si) as anode material. Using half-cells each electrode can be studied separately to understand the reactions occurring on each electrode. Experiments can be done with both full cells and half-cells, depending on purpose [39]. In this study, the effect of Si as anode material has been studied in half-cells.

2.3 Lithium-Ion Batteries

The lithium-ion battery was first commercialised by Sony in 1991, and quickly grew to become one of today's most well known and used battery types, in addition to the lead-acid battery [42]. Being a rechargeable battery and having a high energy density, it is ideal for use in portable electronics, and EVs and HEVs. With the enormous expansion in these markets, great resources are aimed at further development and optimisation of the Li-ion technology all over the world.

Li is the most electropositive (-3.04 V vs. the standard hydrogen electrode (SHE)) and the lightest (equivalent weight M = 6.94 g/mol) metal, making it suitable for high energy density storage [47]. These unique characteristics make LIBs the most promising rechargeable battery technology for meeting today's power demand. The main advantages making LIBs favourable can be summarised as:

- High specific energy and energy density
- High average operating voltage (3.6 V)
- Good lifetime >500 cycles
- Low self-discharge rate
- No memory effect
- High coulombic efficiency and energy efficiency
- Rapid recharge capability
- High rate and rapid discharge capability
- Uses Li compounds $\rightarrow$ safer than pure Li-metal cells

A big disadvantage is that Li is hazardous and highly reactive causing safety issues when placed in flammable electrolyte. The problems especially occur in the case of a leak, degradation at high temperatures or capacity loss

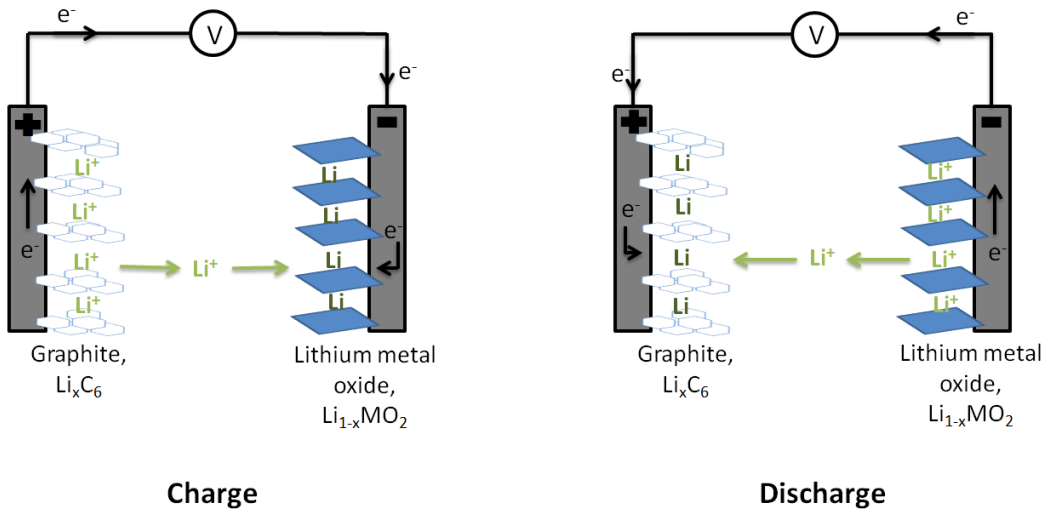

FIGURE 2.3: Working principal of a lithium-ion cell during charge and discharge.

when overcharged. Unstable decomposition of the electrolyte on the electrode surfaces can also cause challenges for the LIBs as further described in section 2.3.2. Other disadvantages specific to the choice of anode, cathode and electrolyte materials exist, and the main challenges related to the use of Si-based anodes in LIBs will be described in section 2.4.2.

2.3.1 Electrochemical principle

The working principle of a LIB is based on Li-ions being able to intercalate (absorb) into the crystal lattice of certain materials, such as trivalent cobalt, nickel oxides or graphite, to form intercalation compounds. Both electrodes in a LIB consist of such Li intercalation compounds. As LIB is a secondary battery, it can charge/discharge multiple times, and the working principle is similar to other rechargeable battery systems and to what was described in section 2.2.3.

During cycling Li-ions exchange between the positive and negative electrode. This movement of Li-ions has also been referred to as "rocking" forwards and backwards between the electrodes, given LIBs the nickname "rocking chair cells." Figure 2.3 gives a graphical demonstration of how the LIB works during charge and discharge.

The electrode materials are typically of layered structure and are commonly a metal oxide for the positive electrode and carbon graphite for the negative electrode. During charge and discharge the Li-ions move in and out of interstitial space between the atomic layers in the electrode materials.

An example of the chemical reactions in a typical LIB is represented by equations 2.4, 2.3 and 2.5.

Negative electrode:

$$\mathrm{C} + x\mathrm{Li}^+ + x\mathrm{e}^- \underset{\text{charge}}{\overset{\text{discharge}}{\rightleftharpoons}} \mathrm{Li}_x\mathrm{C} \tag{2.3}$$

Positive electrode:

$$\mathrm{LiMO_2} \underset{\text{charge}}{\overset{\text{discharge}}{\rightleftharpoons}} \mathrm{Li}_{1-x}\mathrm{MO_2} + x\mathrm{Li}^+ + x\mathrm{e}^- \tag{2.4}$$

Overall:

$$\mathrm{LiMO_2} + \mathrm{C} \underset{\text{charge}}{\overset{\text{discharge}}{\rightleftharpoons}} \mathrm{Li}_x\mathrm{C} + \mathrm{Li}_{1-x}\mathrm{MO_2} \tag{2.5}$$

where M is a metal/alloy, $0 < x < 1$, and e^- are the electrons taking place in the reaction.

The movement of Li-ions in and out of the interstitial layers in the electrodes can also be referred to as lithiation and delithiation, where lithiation describes the process of inserting Li-ions into the electrode, and delithiation describes the process of extracting Li-ions from the electrode.

2.3.2 Choosing Components for Lithium-Ion Batteries

The amount of active material on each electrode are crucial when deciding a cell's capacity, yet the total capacity will only be a fraction of this as all other components, i.e. separator, electrolyte and housing, effect the performance. Developing the optimal cell all components must be optimised. In this section some of the most central components in a LIB will be described, however, the details as to the use of Si as anode material will be thoroughly described in section 2.4.

Electrode Materials

LIB electrode materials can be divided into three groups: intercalation materials, conversion materials and alloys [38]. In intercalation materials the lithiation process involves Li-ions being intercalated into the interstitial sites of the crystalline lattice of the electrode material without destroying the crystal structure. This is the case with graphite anodes. In conversion materials, the process is similar, but the crystal structure is reversibly destroyed, resulting in a a compound without Li in addition to the compound storing the Li. Conversion anodes can typically be metal oxides, fluorides, sulfides etc. An alloy is a composition of two or more metallic components, and for a Li-alloy the lithiation occurs through the alloying between lithium and the electrode material. All these material groups are suitable for LIBs, but the most traditionally used are the intercalation materials. However, as alloying reactions induce higher storage of Li than intercalation or conversion reactions, alloy

anodes are now of growing interest [38]. Silicon is an alloy material and has for that reason become a promising anode material, as will be described in section 2.4.

The choice of electrode materials decides the potential of the cell, and for LIBs the anode material should have as low redox potential as possible with respect to Li^+/Li to achieve high energy density. With a low anode potential with respect to Li^+/Li the potential difference between the electrodes in the cell will increase resulting in a higher total cell potential, which is important for ensuring a high diffusion rate in the cell. Some additional general requirements for the choice of electrode materials mentioned by Linden and Reddy[24] are:

- High electronic conductivity and Li-ion diffusion rate.
- Host as many Li-ions as possible per host atom.
- High electrode potential and high electrochemical equivalence (high coulombic efficiency).
- Minimal structural change during reaction.
- Environmentally friendly, easily available and cost efficient.

Electrolyte

As Li is reactive in aqueous solutions, nonaqueous electrolytes are required. For LIBs, polar organic solutions are the most common electrolyte solvent. The most important function of the electrolyte is to conduct Li-ions efficiently between the electrodes, and avoid large internal resistance (IR) polarisation losses. General requirements for the choice of electrolyte given by Linden and Reddy[24] are:

- Good ionic conductivity, and low electronic conductivity.
- Chemically stable electrolyte salts and solvent.
- Low reactivity with both electrode materials, especially with Li. If it is reactive it must form some type of coating to prevent further formation.
- Thermally stable over a broad range of temperatures to assure cell operation at different temperatures, especially at low temperatures.
- A wide electrochemical window.
- Nontoxic and nonflammable.

Depending on preferences and demand, the electrolyte can be of many forms, such as organic, inorganic, polymer, aqueous or solid-state. Examples of polar organic electrolytes commonly used in LIBs are lithium hexafluorphosphate ($LiPF_6$), dioxolane ($C_3H_6O_2$), propylene carbonate ($C_4H_6O_3$) and ethylene carbonate ($C_3H_4O_3$) [24].

Additionally, additives are added in the electrolyte to enhance electrolyte properties and improve LIB performance. A review study done by Zhang in 2006 [54] concluded that even though different additives have their own unique properties to improve cell performance, each also introduces other functions negatively impacting the overall performance. As an example, one common additive used to control SEI formation (see next section) and prolong cycle-life is vinylene carbonate (VC), however, excess VC has the opposite effect. Zhang also concluded that a combination of additives could cause desirable improvements, however, this is provided that the additives do not interact with each other.

Solid Electrolyte Interphase layer

The solid electrolyte interphase (SEI) layer is a passivation layer that develops as the electrolyte irreversibly decomposes on the electrode surface. At anode potentials below $\sim$1 V versus Li^+/Li, decomposition of organic electrolyte on the electrode surface is thermodynamically favourable [51]. LIBs have a varying working potential over the anode/electrolyte surface, and it is lowest when it is fully charged (close to 0 vs. Li^+/Li). This results in the formation of the SEI layer occurring during recharge [52, 40, 55].

Initially, the SEI layer protects the electrode against further solvent decomposition, and plays an important role in determining the cell's performance. The SEI layer is electronically insulating, but permeable to Li-ions, hence inhibiting electron transfer between the electrode and the electrolyte providing kinetic stability, at the same time as transfer of Li-ions is preserved [46]. As the SEI layer is permeable to Li-ions, an ongoing discharge process is allowed. Unstable formation of the SEI layer may lead to uneven Li deposition upon charge with dendrite formation that eventually may lead to short-circuiting of the cell [41]. When electrode expansion is minimised, the SEI formation is self-limiting, however, during continuous exposure to fresh electrode surface continual SEI growth and irreversible capacity loss is encouraged. In extreme cases, this might lead to overheating effects with thermal runaway and explosions/fire. The loss of Li-ions related to the uncontrolled formation of SEI has been known as one of the most fundamental sources of capacity fade in LIBs [40].

The SEI layer is a composition of organic and inorganic components, including LiF, Li_2O, Li_2CO_3, semicarbonates, created by the reduction of electrolyte as shown in Figure 2.4 [29]. In these components the anions typically originate from the reductive decomposition of the electrolyte, while the Li-ions originate from the electrolyte or the electrode [55]. The exact composition of SEI depends on type of electrolyte, additives in the electrolyte, electrode material etc.

The stability of the SEI layer at the interface between the electrode and the electrolyte is not only an important safety issue for the LIB, but is also crucial for obtaining long cycle life [52]. An effective SEI layer should thus be

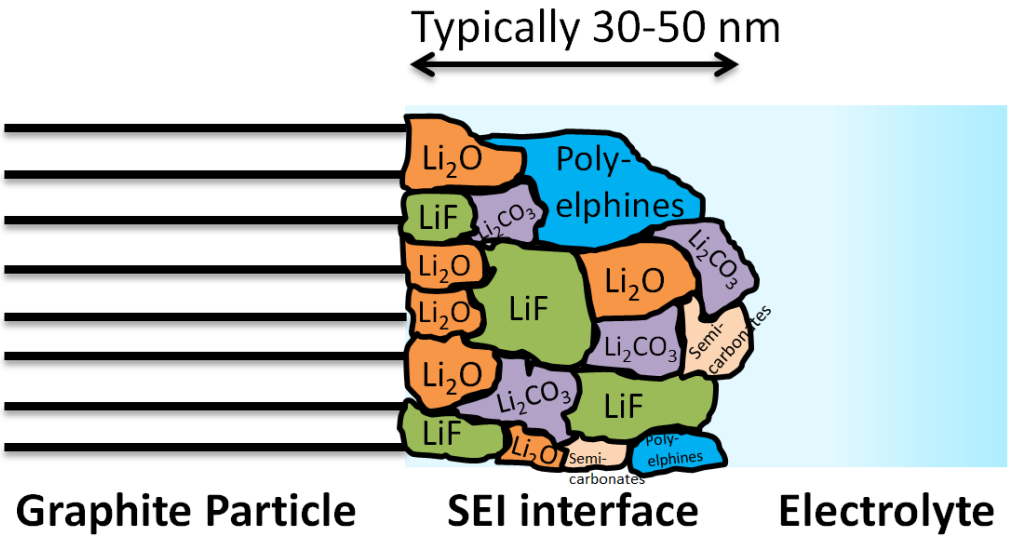

FIGURE 2.4: A graphical representation of the composites of a SEI layer. Illustration adapted from [29].

both mechanically and chemically stable, permeable to Li-ions and electrically insulating. However, obtaining a stable SEI layer may be challenging, especially when electrode material undergoes mechanical fracture issues, i.e. in the case of Si anodes. Great effort is put into the study of both composition and controlled formation of SEI [52, 34, 49, 55, 40].

2.4 Silicon as Anode Material

One of the most promising anode materials for the next generation LIB is silicon (Si). Si has a relatively low working potential (0.4 V vs. Li^+/Li), is the second most abundant element in earth's crust and has the highest known gravimetric and volumetric capacity among the feasible anode materials [1, 50, 38]. Its theoretical capacity of 3,579 mAh/g_{Si} for the fully lithiated state of the alloy $Li_{15}Si_4$ at room temperature, is about an order of magnitude higher than that of the common graphite based anode (372 mAh/g_C for lithiated state of LiC_6). This capacity can even increase to a maximum of 4,200 mAh/g_{Si} corresponding to the formation of $Li_{22}Si_5$ at high temperatures, though this is not a stable nor practical Li-Si alloy state [1, 38]. Nevertheless, these high capacities place Si as the best anode material studied, except for pure Li metal itself.

2.4.1 Lithiation Mechanism of Silicon

Silicon is an elemental semiconductor, and belongs to the group IV in the periodic table. Solids are generally divided into three groups: amorphous, single- and poly-crystalline, as schematically described in Figure 2.5. Si can

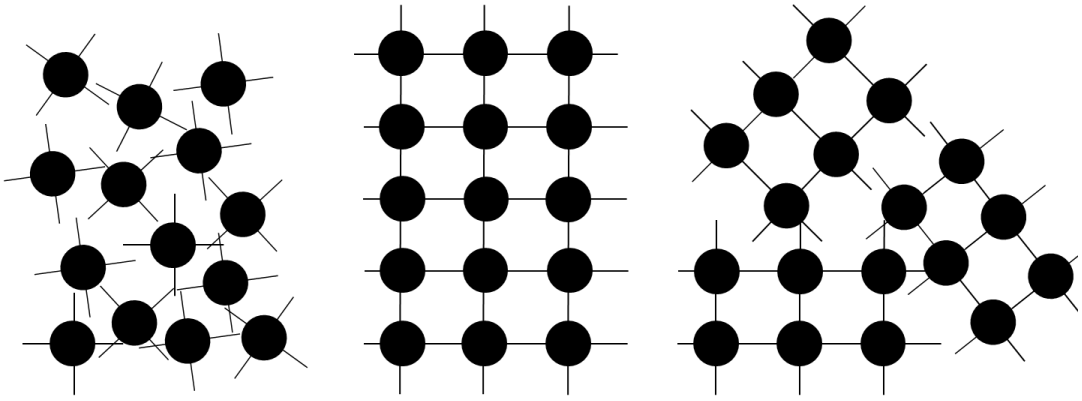

FIGURE 2.5: Schematics of the three general types of crystal structures: amorphous, single crystalline and polycrystalline.

be found in both amorphous form (a-Si) and single- and poly-crystalline form (c-Si), and it has been shown to have a diamond structure [33]. These properties have made Si the most common semiconductor in integrated circuits today [33]. As an electrode material, Si is categorised an alloy material, and together with Li forms Si-Li alloys. During lithiation and delithiation, the transport of Li is driven by the diffusion of Li-ions and the amount of electrons in the Si material.

Li is defined as a n-type doping impurity in c-Si. In contrast to normal group-V donors, which are substitutional impurities in the silicon lattice, lithium is incorporated in interstitial configurations, which leads to the high diffusion capability that makes Li prior to other doping impurities in Si [38]. As a dopant in Si, Li acts as a shallow donor, meaning that its additional energy level is negligible, resulting in the Si-Li alloy electrically acting like Si, but with increased electron concentration due to the inserted Li. This ensures electrical conductivity of the alloy, and free electrons for the Li-ions to couple with.

The Li diffusion rate is just as important as the electric conductivity of the active material, and plays an important role deciding the speed at which the cell may be charged and discharged. When the Si material is in contact with a Li rich material (i.e. Li_2O), Li-ions will diffuse on the surface of the Si particles, followed by a radial flow from the surface towards the centre of the particles (Figure 2.6).

By a simple thermodynamic estimation, it can be shown that Li metal will react spontaneously with c-Si. The electrochemical reaction corresponding to $Li_{15}Si_4$ can be expressed as:

Reduction:

$$\text{c-Si} + 3.75\text{Li}^+ + 3.75\text{e}^- \rightarrow \text{Li}_{3.75}\text{Si} \tag{2.6}$$

Oxidation:

$$3.75\text{Li} - 3.75\text{e}^- \rightarrow 3.75\text{Li}^+ \tag{2.7}$$

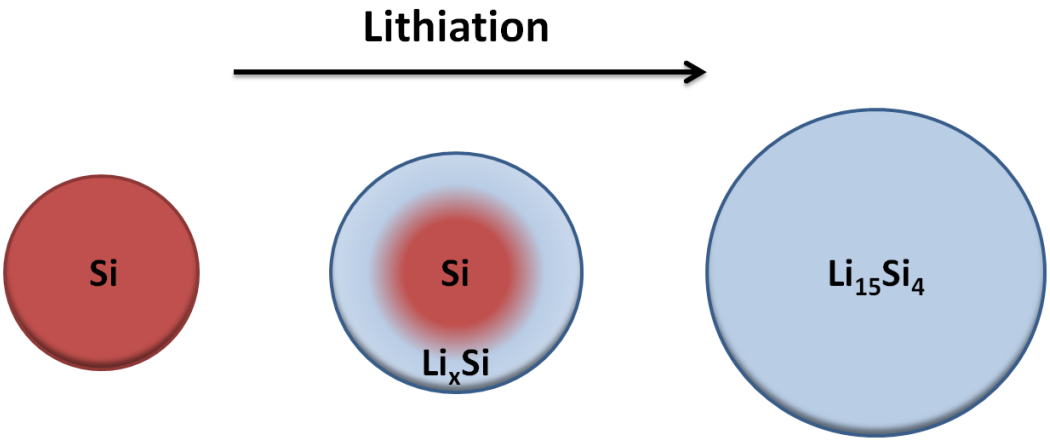

FIGURE 2.6: Lithiation of a silicon particle. c-Si undergoes a phase transition before $Li_{15}Si_4$ is formed upon full lithiation.

Net reaction:

$$3.75\text{Li} + \text{c-Si} \rightarrow \text{Li}_{3.75}\text{Si} \tag{2.8}$$

Gibbs free energy:

$$\Delta\text{G} = \text{nEF} \approx -36\text{kJ/mol} \tag{2.9}$$

where ΔG is Gibbs free energy of the total reaction, E is the potential of the reaction and is assumed to be 0.1 V according to experimental data [5], F is the Faraday constant, and n is the number of electrons involved in the reaction. As ΔG is negative the reaction is spontaneous.

According to the equilibrium Li-Si phase diagram, the insertion of Li into Si at elevated temperatures should result in Si undergoing multiple phase transitions, with distinct voltage plateaus occurring for each two-phase region. The different possible Li-Si alloys are Li_xSi with x = 1.00, 1.71, 2.33, 3.25, 3.75 or 4.40 [9]. When cycling c-Si at room temperature however, only a single plateau between 0.0 and 1.0 V has been observed [35]. This plateau indicates that only one phase transformation of the single c-Si occurs during lithiation at room temperature. The process reported by multiple studies states that c-Si first undergoes an amorphisation process to form a Li_xSi alloy, which further crystallises into the poly-crystalline $Li_{15}Si_4$ upon full lithiation [1, 27, 28, 35, 38]. $Li_{15}Si_4$ is the Li-Si alloy phase without any Si-Si bonds, that is, all Si atoms are surrounded by Li atoms. A more detailed description of the electrochemical chemistry of the c-Si during lithiation/delithiation can be found in Obrovac and Christensen [35]. In addition to the crystallographic deformation, mechanical deformation occurs during the lithiation process (Figure 2.6) as a result of Li taking up great space in the interstitial space in the Si lattice. This and other challenges as to the use of Si as anode material will be discussed next.

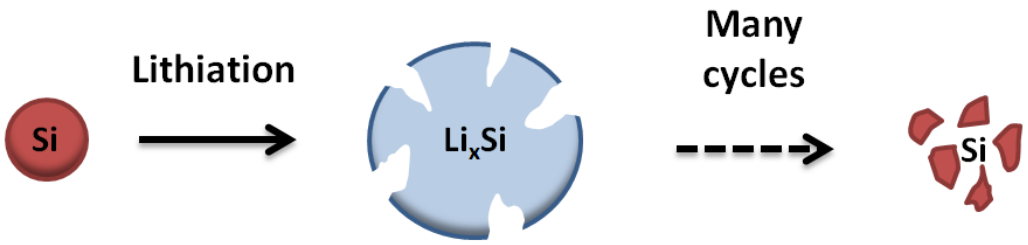

FIGURE 2.7: As the Si-particles expand and contract during cycling, they will experience great stress resulting in cracking and eventually pulverisation upon multiple cycles. Illustration adapted from [51].

2.4.2 Challenges of Silicon Anode

The practical use of Si as anode material is hindered by multiple challenges that need to be overcome before commercialisation can be an option. The main challenges are related to the enormous volume expansion (300 – 400 %) occurring during lithiation/delithiation, leading to reduced electric conductivity and unstable formation of the SEI layer [1, 18]. It was early shown that Si anode-based cells suffer from poor capacity retention, even though they achieve a high initial capacity during the first lithiation [46, 3]. The capacity typically decrease with number of cycles, and can decrease as much as 70 % after only the first few cycles. Such a decrease is naturally too high for practical applications.

In a review article by Wu and Cui [51] the fundamental material challenges of Si anodes were discussed, and divided into three main groups: *i)* Material pulverisation (Figure 2.7), *ii)* Morphology and volume change of the electrode (Figure 2.8), and *iii)* Formation of unstable SEI (Figure 2.9). Each of these will shortly be presented in this section, in addition to the challenges regarding low initial coulombic efficiency.

Material Pulverisation

The volume change of 300 – 400 % of the SiNPs on the anode during cycling induces great stress. Great stress can result in cracking and pulverisation of the Si material, which leads to loss of electric contact with the current collector, poor electron transport and eventually capacity fading. This mechanism is likely to account for most of the capacity fading in Si anodes [51]. Studying the surface of Si anodes during cycling shows that the cracking occurs during the extraction of the Li-ions [51, 44].

Morphology and Volume Change of the Electrode

The volume changes of the particles during cycling will also induce volume and morphology changes on the electrode as a whole. As the Si particles

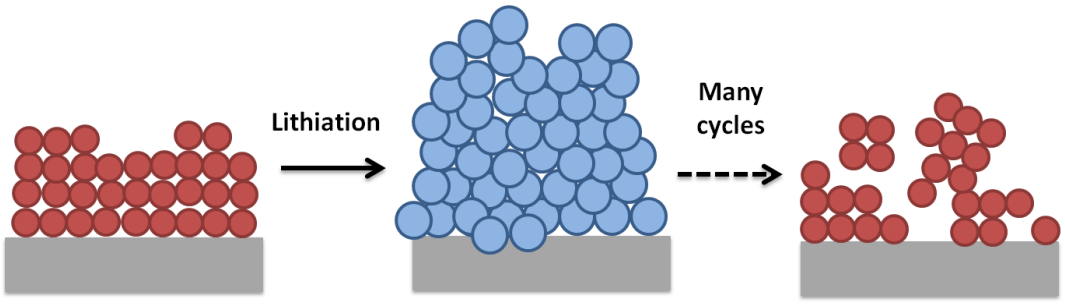

FIGURE 2.8: As the Si-particles expand and contract during cycling, the electrode experiences volume and morphology changes. The particles impinge on each other and the result morphology is different from the initial morphology. Illustration adapted from [51].

grow during lithiation, they will impinge on each other, and during delithiation they might contract differently to the initial morphology (see Figure 2.8). These changes can result in material peeling off of the current collector, loss of electric contact and eventually further capacity fading. Large volume changes of the electrode can also cause problems to the designing of full cells.

Formation of Unstable SEI

Due to repeated volume changes, fraction and re-formation of the SEI layer on the Si particles occur each cycle (Figure 2.9). This leads to a continuous availability of free Si surface, continuous consumption of the electrolyte, increased impedance and eventually capacity fading [1]. After the first cycle, at which the SEI formation is greatest causing high ICL (with corresponding coulombic efficiency (CE) as low as 25 – 75 % depending on the structure of the silicon and the composition of the anode [18]), SEI will continue to reform and slowly grow thicker. The result is degradation of the cell performance, which occurs due to *i)* continuous consumption of Li-ions and electrolyte, *ii)* reduced electrical contact between current collector and Si anode due to the electrically insulating nature of SEI, *iii)* long Li-ion diffusion length through the thickening SEI layer, and *iv)* degradation of Si anode caused by mechanical stress from the SEI [52].

Low Initial Coulombic Efficiency

The enormous volume change and the formation of SEI during the first cycle, result in a low initial coulombic efficiency (CE). Low initial CE indicates that the number of Li-ions flowing out of the anode during delithiation, is small compared to the number of Li-ions flowing in during lithiation. As this number is small, the cell's capacity has been drastically reduced and can never go back to the original level. After the first cycle the CE is typically stable at a high level, even as high as 97 % depending on structure and composition of the anode, for many cycles. For example, for a pristine graphene electrode

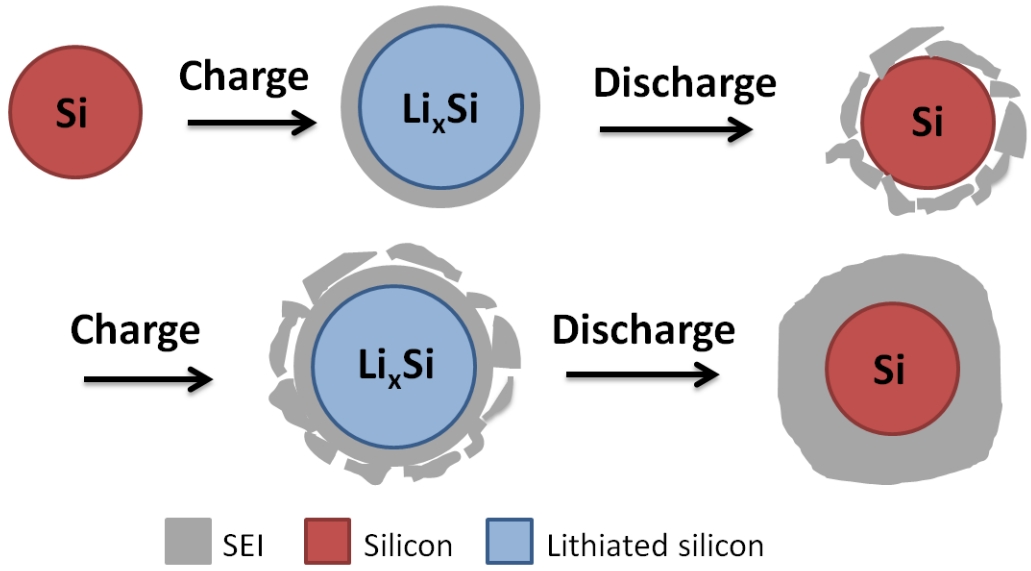

FIGURE 2.9: Unstable SEI formation on Si surface. Illustration adapted from [52].

the initial CE was shown to be ∼22 %, but after 10 cycles the CE was close to 97 % [6]. The same study showed that for a nanosize Si/graphene composite electrode the initial CE was 73 %, and after 30 cycles retained an average CE of 93 %. The value of the CE thus depend on anode structure and composition, electrolyte binder and additives, electrode surface area, etc.

2.5 Strategies to Overcome Si Anode Challenges

Significant efforts and multiple papers and review papers have been published addressing the issues mentioned above. Some widely studied solutions are:

- **Adjusting Si particle size and morphology -** a method that has been shown to reduced the volume change each Si particle experiences, and hence increase electric contact and cycle life. Various material designs are being studied, e.g. different nanostructures, porous structures and nanocomposites [4, 5, 6, 27, 52].
- **Coating of Si particles -** a method that has been shown to reduce continuous growth of unstable SEI and hence improving cyclability and cycle life. Examples of commonly studied coating materials are: carbon, silicon oxide and copper [6, 22, 19, 30].
- **Addition of electrolyte additives -** there are many different additives available for LIBs, each with different functions such as improveing stable SEI formation, reducing Li deposition in electrolyte, safety etc.

Addition of certain additives can hence significantly improve cyclability and cycle life, however each additive also has its limitations [49, 54, 57].

- **Use of novel binders -** as in the case with the additives, different binders used in the slurry coating of the Si electrode can have different functions, such as accommodating the particle's volume changes, improving electric contact, improving stable SEI formation etc. The right choice of binder will then improve the battery cycle life [20, 21, 56, 57].
- **Controlled SEI formation -** a stable SEI layer is a protective layer formed on the interface between the electrolyte and the Si electrode, and cycle life, cyclability, irreversible capacity losses and safety higly depend on the quality of the SEI layer. Different methods are studied and shows promising results, e.g. by creating artificial SEI layers or by forming an ion-permeable silicon oxide shell around Si nanotubes [49, 52, 58].
- **Prelithiation**[1] **-** a method in which the Si electrode gets lithiated before assembled into cells. The method is considered a solution for improving initial irreversible capacity losses [9, 12, 22, 26, 28, 58].

The list goes on, and to even more unorthodox methods, meaning they have unique features, structures and designs not fitted in the categories above or not yet widely studied. One examples is pomegranate-inspired silicon nanoparticles, which is being studied in the Siproco Fobeliba project group at IFE, and limited capacity cycling [43].

As this study will address both prelithiation of SiNPs and limited capacity cycling, a further introduction of these two methods will be given next. Carbon coating will also be addressed as it can be a natural step for further work.

2.5.1 Prelithiation

One strategy compensating for the Li-ion loss primarily associated with the formation of SEI during the first charging cycle, is prelithiation. Several prelithiation methods are being studied [12, 9, 22, 26], but the general principle is that the electrode material becomes lithiated before assembled into cells. It is during the lithiation process the expansion occurs, and a fully prelithiated material will be at its maximal volume. The idea is that prelithiation will induce a pre-volume-expansion of Si, so that the relative change in volume of Si is decreased and sufficient space is created before electrode and cell fabrication. Such suppression should improve cyclability and coulombic efficiency of the Si electrode by reducing the volume and morphology challenges described above.

To date, the only commercialised prelithiation reagent in powder form is stabilised lithium metal powder (SLMP) from FMC Lithium Corp., which shows

[1] Prelithiation is not yet a widely studied solution, but the interest is growing and as it is the topic of this thesis it is mention alongside the other widely studied solutions.

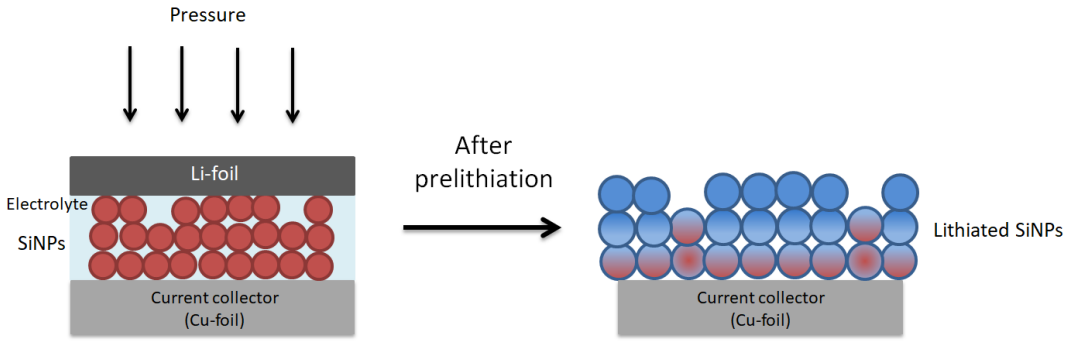

FIGURE 2.10: Schematics of prelithiation of Si particles by direct contact between the particles and a piece of Li-foil. Li diffuses into the Si particles, and how much time it takes before all the particles are fully lithiated depends on the diffusion rate. In this illustration not all the Si particles have managed to become fully lithiated.

promising results when used on different anode materials such as graphite, silicon monoxide (SiO) and silicon nanowire (SiNW) compositions [12, 22, 57]. A study by Li and Fitch [22] showed that the coulombic efficiency of a hard graphite/spinel $LiMn_2O_4$ anode increased as much as 50 % when SLMP was used. Nevertheless, SLMP is expensive and not easily available, and a cheaper and facile method is desired.

An alternative method studied by Liu et al. [26], prelithiates the anode material by a self-discharge mechanism, which occurs due to direct contact between the anode material and a piece of Li-foil. Figure 2.10 illustrates the principle of this method. Zhao et al. [58] have developed another method growing artificial SEI around Li_xSi nanoparticles before prelithiating graphite anode materials with these coated nanoparticles. Both studies showed improved cycle life for the prelithiated cells, indicating that prelithiation might be an important step towards the next generation high-energy-density LIBs. A more recent study by Domi et al. [9] shows the same results, but pointed out that only appropriate prelithiation will improve coulombic efficiency, as excess prelithiation will decrease the efficiency. The group considered that the discharge process tended to stop before the electrochemically stored Li was completely extracted from the Si anode, thus leading to reduced efficiency.

2.5.2 Limited capacity cycling

It has been shown by Sethuraman et al. [43] that Si undergoes elastic deformation during lithiation and delithiation, inducing rapid rise of stress in the lattice, and that the degree of stress evolves continuously with the concentration of Li. This mechanical stress cannot be completely avoided, but can be retarded to a significant extent by limiting the amount of Li inserted into and out of the Si lattice, in other words, by limited capacity cycling. These results

indicate that limited capacity cycling can be an effective method to improve cycle life of the Si anode cells.

A partly limited capacity cycling is already in use since the lower capacity Li-Si alloy phase $Li_{3.75}Si$ (3,579 mAh/g_{Si}) is obtained rather than $Li_{4.4}Si$ (4,200 mAh/g_{Si}). Even cycling at this capacity level has not yet been proven to provide long enough cycle life for the Si anode cells. A further reduction of the discharge capacity (down to that of graphite anodes of $\sim$320 mAh/g_C) will drastically improve the performance of today's Si anodes.

Chakrapani et al. [4] has demonstrated this. By cycling SiNWs in ionic electrolyte at a capacity of 321 mAh/g_{Si}, a cycle life > 650 cycles and a coulombic efficiency tending towards 100 %, was achieved. The group also cycled similar electrodes with a somewhat higher capacity of 1000 mAh/g_Si in organic electrolyte, which cycled > 200 cycles without cell degradation and morphology change of the SiNWs.

Even though it might seem like a waste assembling high capacity Si anode cells, only to limit the capacity during cycling, the method reveals more advantages than disadvantages. The main advantages of limited capacity cycling can be summarised as: constant volumetric variation in Si anode during each cycle, the reduced amount of Li reduces the extent of lattice strain, a more stable SEI is preserved, and unwanted consumption of electrolyte is reduced.

2.5.3 Carbon Coating

Coating of Si is a widely studied strategy overcoming volume and morphology challenges, and multiple methods have and are being developed [30, 51, 53, 56]. The poor cell lifetime of a LIB is mainly rooted in the side reactions occurring at the electrode-electrolyte interface, and the general principle behind coating the particles with a protective layer, is to prevent direct contact between the particles and the electrolyte. Avoiding direct contact, especially during the enormous volume changes, the continuous re-formation of SEI can be prohibited, however, the coating must allow Li-ions to pass through to ensure a functioning LIB. Multiple coating materials are being explored, i.e. metal oxides (Al_2O_3, ZnO, MgO, SiO_2 etc.), metal phosphate, metal fluoride, glass composites and carbon [19]. The most important criteria for a good coating material are: good electric and ionic conductivity, low volume expansion, and mechanical stability [1, 56]. A coating layer providing these properties will be able to improve cyclability, reversible capacity and rate capability.

Of the coating materials mentioned above, carbon is one of the most promising alternatives as it provides great electronic conductivity. Its superiority lays in it being an excellent current collector, in which it decreases the internal resistance of the electrode [56]. Looking at power ability ($P = UI$, where U is cell voltage and I is current density) it can be understood that minimal

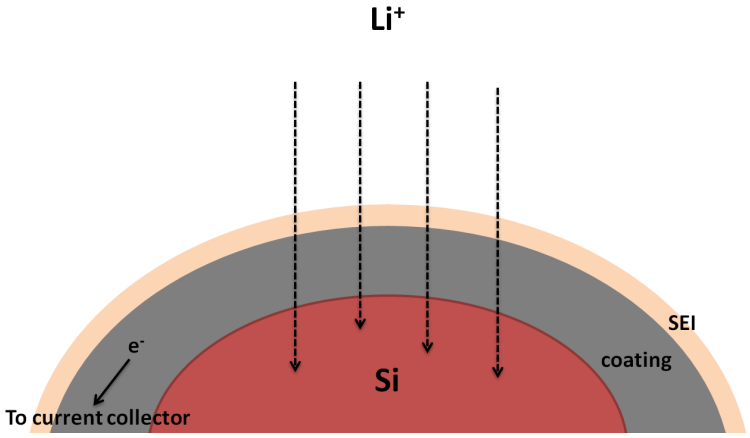

FIGURE 2.11: Coating of a Si particle. The coating material must be ionic and electric conductive, mechanically stable, have low volume expansion and allow Si to expand inside it without fracturing. Example of such a material is carbon [56].

internal resistance is required to achieve high power density. Accomplished with the charge/discharge process, heat is generated due to the I^2R losses (where I is current density and R is total internal resistance) as current flows through the internal resistance. This process is known as joule heating or ohmic heating. High internal resistance would lead to a more rapid decline of cell voltage and accelerated degradation of cell life.

Another method widely investigated is silicon oxide (SiO_x) coatings, which is studied in combination with various structural Si anode designs [51]. A layer of Si_xO is mechanically strong and successfully allow Li-ions to pass through while Si is prevented from expanding out. Applied on i.e. Si nanotubes, results in prolonged cycle life, high specific charge capacity and fast charge/discharge rates as commented by Wu and Cui [51]. A very different method was studied by McDowell et al. [30], who used copper as coating material. Copper has a high electronic conductivity and was shown to create a more stable SEI layer than non-coated Si, increasing coulombic efficiency and rate capability. However the group did not manage to create a coating layer withstanding the large volume changes, and it fractured and re-exposed Si to the electrolyte.

2.6 Electrochemical Characterization

Electrochemical testing can involve a number of techniques to evaluate a cell's performance. The performance is most commonly characterised by the electrical energy it is able to deliver, which is either expressed per unit weight (*Wh/kg*) or per unit volume (*Wh/L*). The energy is a function of cell potential (V) and charge capacity (Q), $E = QV$, both directly related to the chemistry of the cell. As the chemistry of the cell is complex, many methods have been developed to study the cell's performance. This section will further give a

description of the most important methods for electrochemical characterisation that will be used in this study. The theory is based on Bard et al. [2] and Linden and Reddy [24] unless other is specified.

2.6.1 Capacity and Coulombic Efficiency

Theoretical and Practical Capacity

The theoretical capacity is determined by the amount of active material in the cell. It is defined by the total quantity of electricity involved in a specific reaction, and is usually expressed in terms of ampere-hours per kg (Ah/kg) or coulombs per kg (C/kg). The general expression for the theoretical capacity (in Ah/kg) for a given anode and cathode material combined in a full cell is:

$$\mathrm{C}_{Th} = \frac{n\mathrm{F}}{\mathrm{M}} \tag{2.10}$$

where C_{Th} is the theoretical specific capacity, n is the number of electrons involved in the chemical reaction, M is the molecular weight of the active materials and F is Faraday's constant.

Only the active material in the anode and cathode is considered when calculating the theoretical capacity, ignoring the electrolyte, separator, water and any other materials that may be involved in the cell reaction.

The practical, or actual capacity of a cell is lower than the theoretical capacity. It is defined as the amount of electric energy actually drawn from the cell under given discharge conditions. Several factors contribute to the reduction compared to the theoretical case. Firstly, there are other materials, such as electrolyte, separator and housing, affecting the total capacity of the cell. These materials add to the total weight and volume of the cell, which reduces its capacity per mass compared to theoretical value. Secondly, the cell is not fully discharged and charged each cycle, thus lowering the average voltage and reducing delivered ampere-hours. The active materials in a cell are not perfectly stoichiometrically balanced, thus reducing specific energy as an excess amount of one of the active materials is used. The practical capacity is also dependent on the kinetics of the energy transfer, the temperature, the cut-off voltage and the electrode and cell design. Even for "good" cells the practical capacity is only about 25 – 35 % of the active material's theoretical capacity.

Reversible Capacity

High degradation of the capacity is normally seen during the first cycles. Figure 2.12 demonstrates a general capacity versus number of cycles plot [45]. The rate of capacity fade is initially high, as demonstrated by region A, but quickly slows down in region B and C. The slow degradation rate seen in

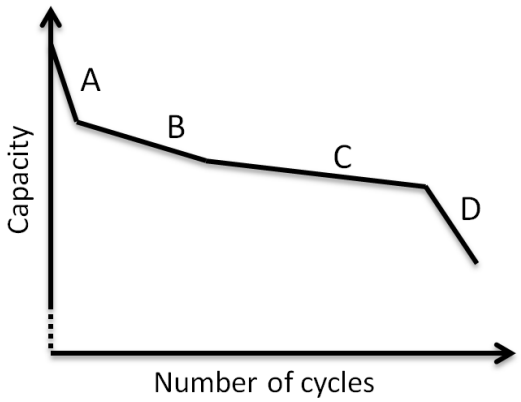

FIGURE 2.12: Schematics of typical capacity fade during cycling of a cell. Illustration adapted from [45].

region C typically occurs after about a few hundred cycles in good cells. Finally, the end-of-life of the cell is reached, resulting in a very rapid degradation in region D. End-of-life is defined as the point where the cell can no longer achieve the required performance criteria, i.e. when it reaches 80 % of its initial capacity [45]. Often, the capacity fade from regions A through C is approximated as a linear function and expressed in terms of capacity fade per cycle.

In the discussion section of this thesis it will be referred to reversible capacity as the average capacity seen when the capacity stabilises relative to the degradation during the first cycles, thus as the average capacity of region B through C in Figure 2.12.

The high degradation might last for as much as 20 cycles, but might also stabilise earlier, depending on the cell components. Calculation of the reversible capacity can be done by equation 2.11,

$$C_{rev} = \frac{\sum_{x_1}^{x_2} C_i}{x_2 - x_1} \tag{2.11}$$

where C_{rev} is the reversible capacity, x_1 and x_2 are the first and last cycle with relative stable capacity, and C_i is the capacity in each cycle *i*.

Coulombic Efficiency

Coulombic efficiency (η) is defined as the ratio between the amount of electric charge delivered during discharge and the amount of electric charge consumed during the previous charge. In other words, it is the ratio between how much electric charge flows in and out of the electrodes each cycle. The coulombic efficiency (CE) essentially says something about how much charge/capacity get lost in each cycle.

$$\eta = \frac{\mathrm{Q}_{out}}{\mathrm{Q}_{in}} \tag{2.12}$$

where Q_{in} and Q_{out} are the amount of charge in and out of the electrodes.

CE should be as high as possible to assure well performing cells. Commonly, the CE is preferred to be > 90% for high specific density anodes, to ensure viable cells when the anode and a cathode are paired in full cells [12].

2.6.2 Cycle Life

The cycle life of a rechargeable cell is the number of charge-discharge cycles the cell can withstand before it fails to meet predefined performance criteria. The performance criteria may vary depending on what the data collected is to be used for, and how they are to be compared with other cells. The lifetime depends on structure and type of cell, and on cycling parameters such as charge-discharge rates and loading.

Charge/Discharge Rate

The charge/discharge rate is the pace at which current is inserted and extracted, respectively, from the electrodes. It is given in either amperes per gram of active material or coulombic rate (C-rate). During cycling the charge-discharge rate is most commonly given as a fraction or multiple of the C-rate.

The C-rate is expressed relative to the rated capacity, and is defined as the rate at which the entire capacity of the electrode is charged or discharged during one hour. It is commonly written as C/t, where t represents the time it takes to fully charge/discharge the cell. From this definition it can be understood that a C-rate of 1C means that a fully charged cell rated at 1 Ah should provide 1 A for one hour. A cell discharged at a C/2 rate will require two hours to completely discharge, and a discharge rate of C/10 will require 10 hours to completely discharge.

Charging/discharging at very high C-rates causes great stress on the electrodes, which gradually reduces the capacity that can be obtained from the cell. This reduces the cell's overall performance. C-rates higher than 1C (i.e. completely discharged in less than one hour for a 1 Ah cell) are commonly considered as high rates.

2.6.3 Voltage-Capacity Curves

Cell voltage can be thought of as the potential the cell has to deliver a certain charge, i.e. a measure of the cell's power. Capacity can be thought of

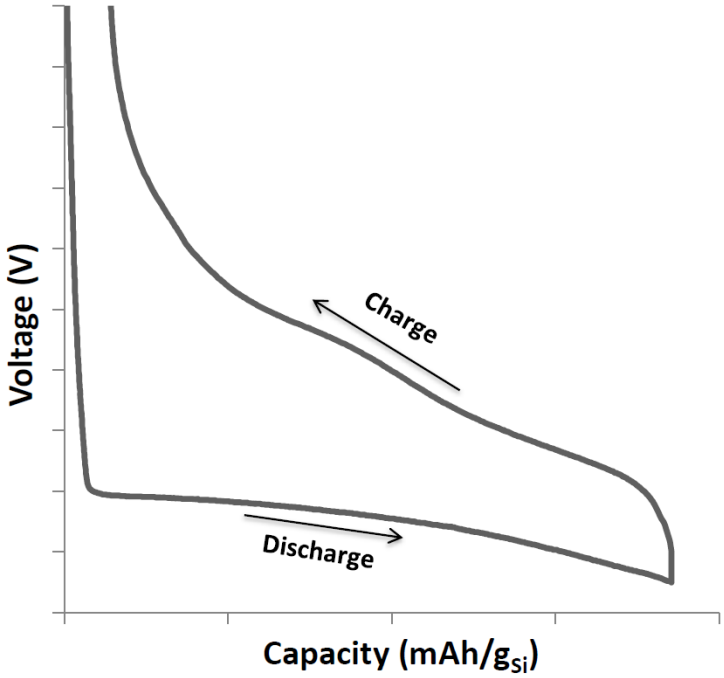

FIGURE 2.13: Schematics of a voltage-capacity plot with both the charge and discharge curve.

as how long the cell can provide this voltage, i.e. a measure of the cell's endurance. Combined in a plot, they provide important information about the cell's chemical characteristics.

The voltage-capacity curves are commonly plotted with voltage along the y-axis and capacity or time of discharge along the x-axis at constant charge current or power. They can be plotted in various ways, e.g. as voltage cycles including both the charge and discharge curve (see Figure 2.13), or with only one of the charge/discharge curves. The exact shape of the curves and the nominal voltage will vary depending on the electrochemical system, construction of the cell, temperature and other discharge conditions.

For cells with a sloping discharge curve, the power delivered will fall progressively throughout the discharge cycle, while for cells with a flat curve, the power delivered will stay relatively stable until the end of the discharge cycle. A flat area in the curve represents a two-phase transition. Most modern LIBs have a relative flat discharge curve similar to the example seen in Figure 2.13.

2.6.4 Galvanostatic Techniques

Electrochemical characterisation by galvanostatic techniques is a common method for determining the performance of an electrode and its active material. It is a constant current method and holds the current between the anode and the cathode constant or stepped, controlled by a pre-designed program,

so that the potential can be measured as a function of time. Plotted against cycle number or voltage it can be used to determine cycle life or voltage profiles of the cell. It can also be used to determine specific capacity and stability of load capabilities.

Galvanostatic testing is a two step process with one constant-current step and one constant-voltage step. The cycling starts with constant current, usually determined by C-rate, and during discharge (lithiation) the cell voltage will decrease until a cut-off voltage is reached. The cut-off voltage is determined based on the capacity of the cell, and will limit electrolyte decomposition, and hence SEI growth, on the electrodes. When the cell voltage reaches the cut-off value, the constant-current step is finished, and the process switches into the constant-voltage mode. The voltage is held constant to give Li-ions time to completely diffuse into the material, and the time is either controlled by a set-time in the pre-designed program, or lasts until the current has reached a certain fraction of its discharging value (e.g. 10 % of initial value).

Usually a low current is used during the first few cycles to ensure relatively controlled formation of SEI on the anode surface. After the initially low constant-current cycles have finished, the current is increased, and the cell can be cycled with either limited or unlimited capacity.

Important information about the cell's reversibility can be found from the galvanostatic cycling data. By comparing the amount of charge obtained after the first lithiation to the amount of charge obtained after the subsequent delithiation the cell's irreversible capacity loss can be determined. High capacity retention throughout the cycling reveals good reversibility.

2.6.5 Differential Capacity

Differential capacity can be used to study the cell beyond what can be studied through a capacity plot. It is defined as the increment of charge going into or out of the cell over a given voltage increment:

$$\mathrm{C}' = \frac{\mathrm{dQ}}{\mathrm{dV}} \tag{2.13}$$

where C' is the differential capacity, Q is the excess charge stored in the electrode and V is the electrode potential.

From data collected during galvanostatic cycling, capacity-voltage curves for each cycle can be plotted. The differential capacity plot can then be found by differentiating these capacity-voltage curves like shown in Figure 2.14.

Each peak in the differential capacity plot corresponds to a plateau in the capacity-voltage curve. These plateaus represent a phase transition, i.e. from A to B like demonstrated in Figure 2.14, and can for many cells be hard to quantify by observation. The derivatives of these curves however, will detect even the small plateaus, and can be easier to understand. Peaks in a

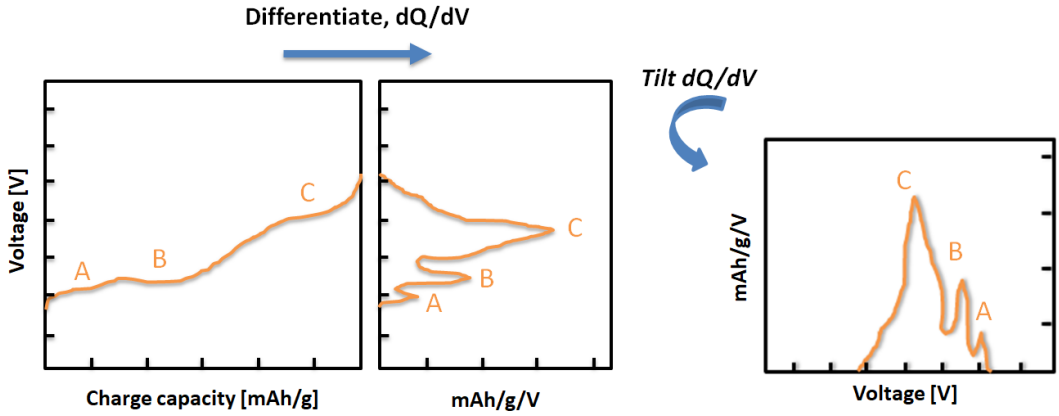

FIGURE 2.14: Illustration of how to obtain a differential capacity plot from cycling data.

differential capacity plot will be somewhat different for intercalation materials and alloy materials due to the different phase transitions occurring during cycling.

Differentiating the capacity-voltage curve for each discharge-charge cycle can give a better understanding of the physical and chemical development inside the cell over time. As a cell ages, features in the plot might shift in position, and by studying the dQ/dV curves, these changes can be tracked and analysed.

3 Experimental and Analytic Methodology

This chapter will describe the process from slurry and electrode preparation to electrochemical testing and characterisation of the assembled coin cells. The slurry, electrode preparation, coin cell assembly, and electrochemical characterisation were performed according to established techniques used at IFE. The two prelithiation methods (EP and MP), and the limited capacity cycling program were developed by the author.

3.1 Slurry and Electrode Preparation

Silicon nanoparticles (SiNPs) produced by chemical vapour deposition (CVD) in a Free Space Reactor (FSR) at IFE were used as active material on the Si-electrodes in the experimental work of this thesis [32]. A big challenge when using SiNP-based electrodes is to ensure electrical contact between the nanoparticles and the current collector after repeated volume changes. The composition of the electrode slurry coating is tailored to this challenge, thus conductive carbon and various binder additives are commonly used in the slurry for Si electrodes. In the slurry used in this thesis, graphite and carbon black were used as conductive additives, and sodium carboxymethyl cellulose (CMC) as binder. The exact composition of the slurry powders was 60 wt% silicon, 10 wt% graphite (Timcal, KS6L), 15 wt% carbon black (Timcal, Super-C65) and 15 wt% CMC. The buffer solution made at IFE of potassium hydroxide (KOH) and citric acid was added as four times the mass of the powders. This composition resulted in a viscous mass that was mixed in a THINKY Planetary Centrifugal Mixer to reach a homogeneous state. The slurry was then tape casted onto a dendritic copper (Cu) foil current collector and left for drying overnight. Finally, it was dried at 120 °C in an argon (Ar) filled environment to remove the remaining moisture.

From the slurry, 15 mm diameter electrodes (see Figure 3.1) were punched out using a Hohsen punch. The electrodes were weighed, making sure they had approximately the same masses for comparing purposes, and so that the active mass load could be calculated. Finally, the electrodes were moved inside an Ar-filled glove box where further prelithiation experiments and/or cell assembly could take place.

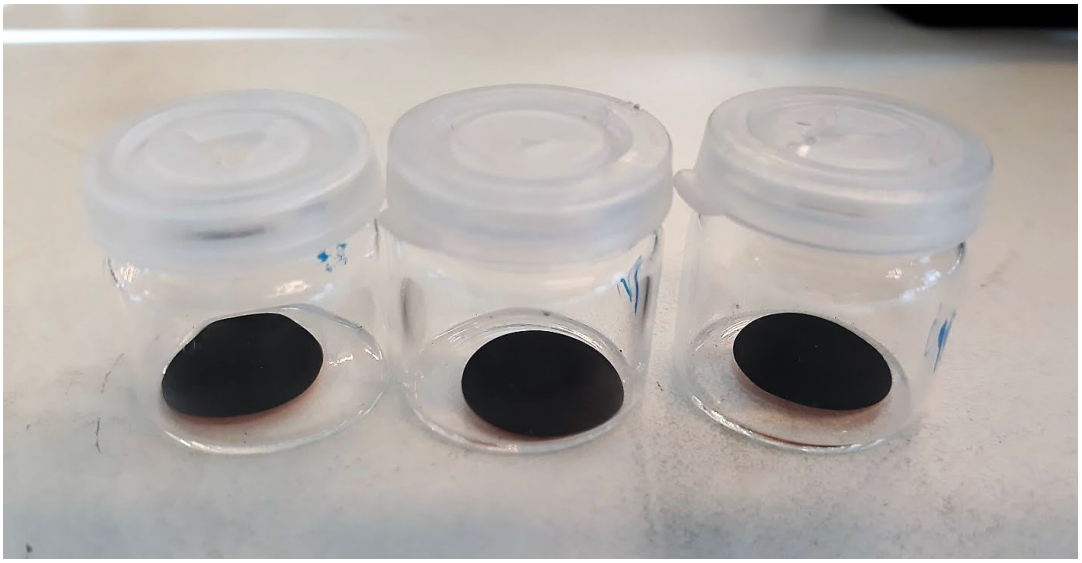

FIGURE 3.1: 15 mm diameter Si electrodes ready to be moved into the glove box for prelithiation and/or cell assembly.

3.2 Cell Assembly

As only the Si-electrode is of interest in this study, half-cells were made. As the counter electrode, a Li-foil disk was used, thus providing an excess of Li-ions so that only the capacity of the Si limits the performance of the cell. The half-cells were assembled in an Ar-filled glove box with stainless steel CR2032 cells from Hohsen Corp. In the glove box the concentration of H_2O and O_2 were < 0.1 ppm.

The schematics of the coin cell components are shown in Figure 3.2. Using a micropipette, 5 μl electrolyte was dropped into the bottom case of the coin cell to help hold the electrode in place while assembling the cell. The electrode was placed with the Cu-foil down on the drop of electrolyte. 20 μl electrolyte was then dropped on top of the electrode, followed by a 18 mm diameter Celgard separator (2045 propylene, 20 μm thick). Another 15 μl electrolyte was added on top of the separator, to fully soak it, before a gasket was placed on top. The gasket was added to prevent electrical contact between the positive and negative sides of the coin cell. Finally, a piece of Li-foil was placed on top of the separator. Before assembly, the Li-foil was carefully scraped free from any oxides that formed on the surface using a scalpel. After the Li-foil was placed on the separator, a stainless spacer and a washer spring was added, filling up any extra volume in the coin cell, and adding pressure to ensure good contact between all the components. Finally the top casing was placed over the spring, and the cell was sealed in a crimping machine.

Both reference cells and prelithiated cells were assembled.

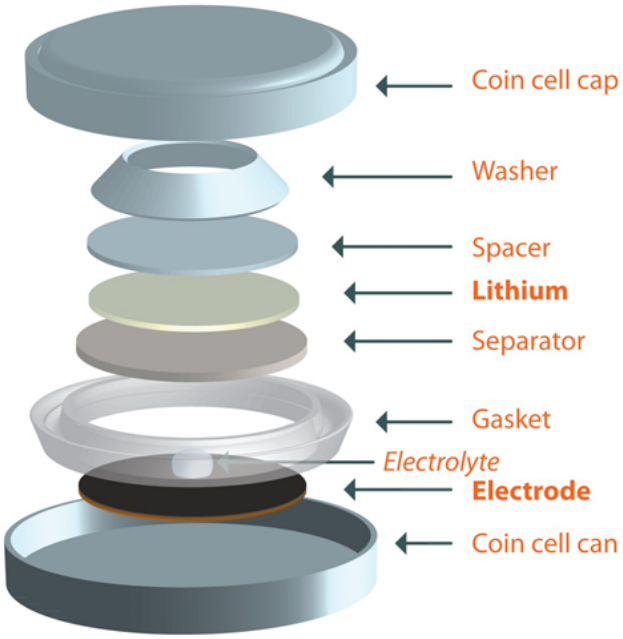

FIGURE 3.2: Components of a coin cell. Illustration by Jan Petter Mæhlen (IFE).

Electrolyte

The electrolyte used in this thesis work was called "G1." It was an organic electrolyte with 1 M of $LiPF_6$ in a 1:1:3 ethylene carbonate (EC)/propylene carbonate (PC)/dimethyl carbonate (DMC) weight ratio, with 1 wt% vinylene carbonate (VC) and 5 wt% fluoroethylene carbonate (FEC) as additives.

3.3 Prelithiation

Two different methods of prelithiation were developed in this thesis: electrochemical prelithiation and mechanical prelithiation. For simplification they will be referred to as EP and MP, respectively, throughout this thesis.

A simple way to prelithiate SiNPs in the lab is to attach a piece of Li directly onto a Si electrode, i.e. MP. Despite being a simple process, it lacks control of the degree of prelithiation and the stress applied to the SiNPs. For a good understanding of this method it was seen as necessary to compare it to another prelithiation method, and EP was chosen. In industry, using a form for EP is preferable, even though it is a costly and time-consuming process. EP can be performed in the same facilities simply by cycling the assembled cells once, disassemble them and re-assemble the prelithiated electrodes into new, now prelithiated cells. By designing a computer-controlled cycling-program, the EP method could be studied and used for comparison purposes.

These two methods were explored in this study and a description of how the cells were prelithiated in each method will be described bellow. After prelithiation they were cycled on similar cycling-programs to study cycle life and cell performance. Reference cells were also made to see whether prelithiation has an improving effect on cycle life or not.

3.3.1 Electrochemical Prelithiation

The EP cells were first assembled like normal (see Section 3.2), cycled for one and a half cycle with a rate of C/20 in a computer-controlled multi-channel battery tester (Arbin), and stopped at lithiated state. This method was designed by the author and is equal to the first cycle in the standard cycling program (will be described in section 3.4). The charge rate was chosen similar to those of the reference cells for comparison purposes. For a detailed description of the EP cycling program see Appendix B.1.

The lithiated cells were carefully disassembled in an Ar-filled glove box, and all components except the Si electrodes were disposed of. The Si electrodes were washed with DMC to remove salts and the SEI layer formed during cycling, and left overnight to dry. The dried, washed and now prelithiated Si electrodes were then weighed and re-assembled into new coin cells.

3.3.2 Mechanical Prelithiation

The MP process developed in this study was inspired by Liu et al. [26] who prelithiated SiNW-based anodes by sandwiching the anode and a piece of Li-foil manually between two glass slides.

Prelithiation of the SiNP-based electrodes was performed inside an Ar-filled glove box to avoid Li reacting with H_2O. Inside the glove box, pieces of Li-foil were first carefully scraped free from any oxides before directly attached on top of the Si electrodes, with 15 μl electrolyte between. Glass dishes were used to sandwich the pieces, and pressure was added by putting a small weight (133 g) on top to induce electrical short-circuiting between the SiNPs and the Li-foil. After chosen time interval of MP (see Table 3.1), the Si electrode was carefully peeled off from the Li foil. The prelithiated Si electrodes were washed with DMC to remove any salts, and left to dry overnight, before weighed and assembled into coin cells. The MP tools used are shown in Figure 3.3.

TABLE 3.1: Time of mechanical prelithiation.

Time of prelithiation (min)
3
9
27
81
243
1027

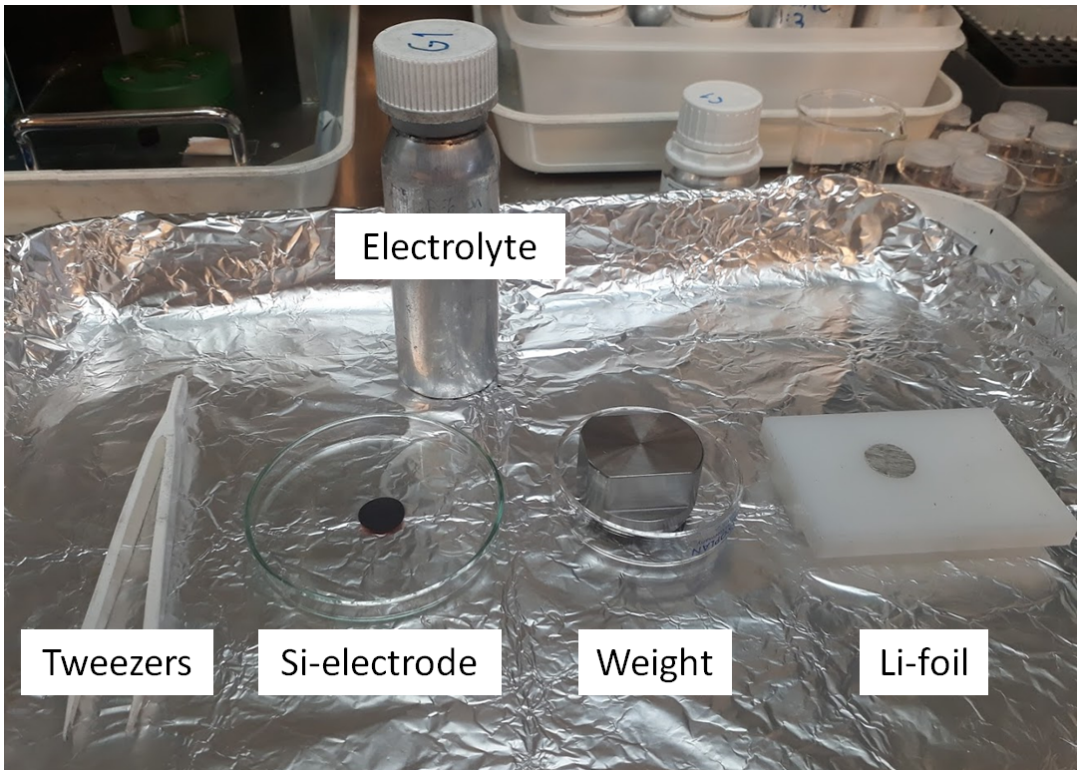

FIGURE 3.3: Mechanical prelithiation tools: the tweezers are used to put the Li-foil carefully on top of the Si-electrode with only 15 μl electrolyte in between. The weight is put on top to add pressure and to induce electrical shorting.

3.4 Galvanostatic Cycling

The half-cells were galvanostatically charged and discharged in a computer-controlled multi-channel battery tester (Arbin, see Figure 3.4) to determine capacity and cycling stability of the cells. The cells were run on different cycling programs (described bellow), but all the programs started with discharge (lithiation). With this initial discharge step, the non-prelithiated cells should obtain a high initial discharge capacity close to 3,579 mAh/g_{Si}, while the fully prelithiated cells should obtain an initial discharge capacity close to zero. By comparing the first cycle discharge capacity for prelithiated and non-prelithiated cells the degree of prelithiation could be calculated. A detailed description of each program, including the electrochemical prelithiation (EP) program, can be found in Appendix B.

Table 3.2 shows what program the different prelithiation methods were cycled at. For comparison purposes 9 min and 27 min MP were chosen for limited capacity cycling, as early results showed that they had a relative big difference in degree of prelithiation. One cell prelithiated for 81 min was also cycled on LC, as it was assumed to have a degree of prelithiation close to 100 %. This sample was only tested on one of the LC programs due to the time limitation of this thesis work.

FIGURE 3.4: Coin cells cycling in the multi-channel battery tester Arbin.

TABLE 3.2: Prelithiation method and cycling programs. "standard" is the cycling program all cells were cycled at, "LC (lithiation)" is the limited capacity program where lithiation was limited, "LC (delithiation)" is the limited capacity program where delithiation was limited.

Prelithiation Method	Cycling program
none	standard
EP	standard LC (lithiation) LC (delithiation)
MP (3min)	standard
MP (9min)	standard LC (lithiation) LC (delithiation)
MP (27min)	standard LC (lithiation) LC (delithiation)
MP (81min)	standard LC (delithiation)
MP (243min)	standard
MP (1027min)	standard

3.4.1 Standard Cycling Program

After undergoing prelithiation (either electrochemically or mechanically), the cells were cycled on a program here referred to as "the standard cycling program." This program was already made and used by scientists at IFE. It is an unlimited capacity cycling program with a formation loop of three cycles at C/20, followed by a loop of 100 cycles at C/10. The program has no capacity limits, but is limited by the voltage range of 0.05 – 1 V (vs. Li^+/Li). See Appendix B.2 for the detailed description of the program. The reference cells were also cycled on this program.

3.4.2 Limited Capacity Cycling Programs

In addition to the standard cycling test, two limited capacity (LC) cycling programs were tested on the prelithiated cells, one limiting the degree of prelithiation, and one limiting the degree of delithiation (described below). These programs were designed by the author for this study. In contrast to the standard cycling program, the capacity is limited, i.e. the amount of Li-ions inserted/extracted into/from the Si electrode is limited. Limited capacity

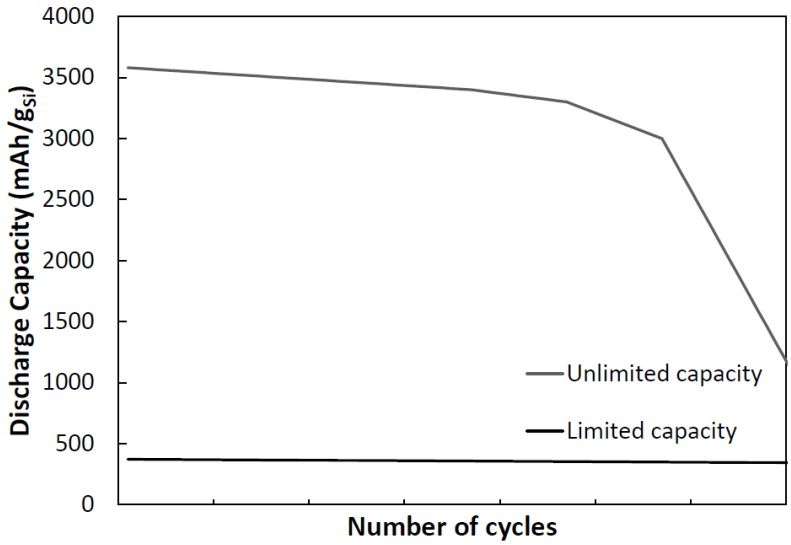

FIGURE 3.5: Expected form of discharge capacity curves for cells cycled with unlimited capacity and limited capacity.

cycling normally results in a prolonged cycle life, and the aim of the testing was to see if and how the prelithiated cells performed over extended cycling. For both LC programs the limited capacity was chosen to be 372 mAh/g_{Si}, similar to the theoretical capacity of the graphite anode, for comparison purposes. Similar to a standard cycling program, they cycled within the voltage range of 0.05 – 1 V (vs. Li^+/Li).

The expected shape of the discharge capacity curves for the cells cycled with LC versus the cells cycled with unlimited capacity (the standard cycling program) is demonstrated in Figure 3.5.

Limited Delithiation Cycling

The limited delithiation program had a formation loop of two and a half cycles at rate C/20. Then followed a loop of 500 cycles at C/10, where delithiation was limited by the capacity of 372 mAh/g_{Si}. Thus, the 500 cycles loop started when the Si electrode was in the lithiated state.

Limited Lithiation Cycling

The limited lithiation program had a formation loop of three cycles at C/20, followed by a 500 cycles loop at C/10, where the lithiation was limited by the capacity of 372 mAh/g_{Si}. Thus, the 500 cycles loop started when the Si electrode was in the delithiated state.

3.5 Analysis Methods

Characterisation of the Si electrode material before and after prelithiation, and before and after electrochemical cycling was done by collecting cycling data, study the electrodes with scanning electron microscopy (SEM), mass measurements and visual observations. Cycling data was also used to study cell performance.

All cells analysed in this study are plotted in Table 3.3 with corresponding cycling program and load of active material (i.e. Si). More cells were made but not analysed in this study due to cycling at wrong C-rates and/or the cell failure during the first 10 cycles due to unknown failure mechanisms[1]. The complete list of cells made during this study can be found in Appendix C.

TABLE 3.3: List of cells analysed in this study, with corresponding cycling program and load of active material (i.e. Si).

Cell	**Cycling program**	**Load of active material (mg_{Si}/cm^2)**
ref_01	standard	0.38
ref_02	standard	0.42
EP_04	standard	0.38
EP_05	standard	0.32
EP_06	standard	0.38
EP_07	LC (delithiation)	0.42
EP_08	LC (delithiation)	0.42
EP_09	LC (lithiation)	0.37
EP_10	LC (lithiation)	0.38
MP_04	standard	0.38
MP_05	standard	0.34
MP_06	standard	0.40
MP_07	standard	0.42
MP_08	standard	0.42
MP_09	standard	0.34
MP_10	LC (delithiation)	0.36
MP_12	standard	0.31
MP_13	standard	0.34
MP_14	LC (delithiation)	0.42
MP_15	LC (delithiation)	0.40
MP_16	LC (lithiation)	0.37
MP_17	LC (lithiation)	0.45

[1]The cells MP_06 and MP_08 reached unsafe voltage levels after about 20 cycles, however their initial cycling data was analysed

3.5.1 Cycling Data

Cycling data was exported from the Arbin-connected computer to Excel files so that various plots (discharge capacity, differential capacity (dQ/dV), IR plots, CE etc.) could be made for visualisation and analysing purposes. These plots were useful when comparing the methods, evaluating the performance and lifetime of the cells, and the electrochemical process inside the cells during cycling.

Two efficiencies were calculated for the cells: CE and HC. The CE was calculated comparing the delithiation capacity to the lithiation capacity in the same cycle. This value describes the efficiency of the lithiation/delithiation process of the Si electrode in the cell, and is similar to the CE value the cell would have obtained if assembled in a FC. The HC efficiency was calculated by comparing the charge capacity (delithiation) in the first cycle and the discharge capacity (lithiation) in the following cycle. This value describes how much charge is flowing out of the HC compared to how much was flowing in, and gives information about the HC's working principle. As the effect of prelithiation mainly will be visible in the first cycle, initial CE and HC efficiency were calculated to study the effect of prelithiation on initial cycling.

For the voltage-capacity and dQ/dV plots, the measured values correspond to one lithiation/delithiation cycle. The capacity is given per gram of active material on the electrode (i.e. per gram of Si). All other plots are obtained after the lithiation step, i.e. when the Si electrode is in the lithiated state.

Accuracy of Arbin

The cycling data collected from Arbin is of high precision. All cells were cycled on channels with a current range of 0 – 10 mA. According to the specifications given by Arbin Instruments [17], the measurement precision is < 100 ppm, and the control accuracy is < 0.02 % of 10 mA.

3.5.2 Mass Measurements

The mass of the the Si electrodes before and after prelithiation were measured to look for a correlation between increase in mass and prelithiation time. By theoretical calculations the change in mass is expected to increase with degree of prelithiation. The uncertainty of the scale used inside the glove box was 0.1 mg, and 0.01 mg for the scale used outside the glove box.

3.5.3 Scanning Electron Microscopy

The Si electrodes were studied in a scanning electron microscope (SEM) before and after prelithiation, to study the surface changes due to prelithiation.

In order to study the prelithiated electrodes in SEM, they had to be taken out of the Ar-filled glove box and into the SEM. For most of the movement, the electrodes were placed in a sealed container, however they were exposed to air for a few seconds when moved out off the container and into the SEM's working chamber. By using SEM the idea was to study the changes in nanostructure of the SiNPs for the two methods.

When studying the electrodes in SEM an elemental analysis of the electrode surface could be performed by energy-dispersive X-ray spectroscopy (EDS). The EDS analysis provides information about the chemical composition on the surface, however it can not detect Li as Li is too light for the sensor to detect its signal. EDS was performed on the reference electrode and one of the prelithiated electrodes.

4 Results

This chapter will present results that indicate whether or not prelithiation occurred, to what degree it occurred, and how the different prelithiation methods effected the Si electrodes differently. SEM micrographs will show what the electrodes looked like before and after prelithiation, and cycling data will show how the prelithiated cells behaved during cycling. This chapter will also present limited capacity cycling results, which give information about how/if prelithiation affects the performance of the cells during extended cycling.

4.1 Prelithiation

Signs of prelithiation were seen quite early in the process, that is, between the prelithiation process and cell assembly. Before assembling the prelithiated Si electrodes into coin cells, signs of stress were observed in form of change in surface colour, scratches (in the MP case), and rougher surfaces. By visually comparing the reference electrodes with the prelithiated electrodes, small areas of darker colours were seen on most of the prelithiated electrodes, and most frequently on the MP electrodes.

After cell assembly the open circuit voltage (OCV) was measured. Prelithiated cells had an OCV of 100 – 200 mV, while reference cells had an OCV of ~ 3 V. This is reasonable because the insertion of Li-ions reduces the electrochemical potential of Si; hence, this difference in OCV indicated that prelithiation was successful, and the coin cells were ready for cycling.

Beyond these qualitative observations, capacity and mass measurements were made to calculate the degree of prelithiation and the mass change seen as a result of prelithiation, respectively. These two topics will be presented below.

4.1.1 Degree of Prelithiation

The degree of prelithiation was calculated by comparing the first cycle discharge capacity of the prelithiated cells with the average first cycle discharge capacity of the reference cells. It was assumed that the electrodes were identical so that the average first cycle discharge capacity of the reference cells was the maximum discharge capacity that the prelithiated cells would have reached if not prelithiated. With this assumption, the difference between the

discharge capacity values was used to calculate the degree of prelithiation. The degree of prelithiation is plotted in Table 4.1 for MP and in Table 4.2 for EP.

The results show that the degree of prelithiation is > 97 % for all the EP cells except one. For the MP cells the degree of prelithiation varies but follows an overall trend of asymptotic increase with time of prelithiation. For all MP cells prelithiated for 81 min or more the degree of prelithiation is > 95 %.

Figure 4.1 depicts the degree of prelithiation for MP graphically with a corresponding trendline. It can be seen that the degree of prelithiation increases quickly for the first $\sim$ 80 min, before it flattens completely out. With this observation, an asymptotic trendline was found with a non-linear least squares analysis. The equation for the trendline was

$$SOC = \frac{1}{at^{-b} + 1} * 100\% \tag{4.1}$$

where SOC is the state of charge (degree of prelithiation), t is time of prelithiation, and a and b are fitting parameters, which were found by least squares fitting to be 18.93424 and 1.272757, respectively.

By this estimation the MP method reaches a degree of prelithiation of 90 % after 57 min of MP, and 99 % after 370 min.

TABLE 4.1: Degree of prelithiation for the MP cells.

MP Time (min)	**Cell**	**Discharge Capacity 1. cycle (mAh/g$_{Si}$)**	**Degree of Prelithiation (%)**
3	MP_04	2506	33
	MP_07	2719	27
9	MP_05	1395	63
	MP_08	2491	34
	MP_14	2628	30
	MP_16	2624	30
27	MP_06	290	92
	MP_09	330	91
	MP_10	737	80
	MP_17	1199	68
81	MP_15	205	95
243	MP_12	79	98
1027	MP_13	31	99

TABLE 4.2: Degree of prelithiation for the EP cells

Cell	Discharge Capacity 1. cycle (mAh/g_{Si})	Degree of Prelithiation (%)
EP_04	1011	73
EP_05	77	98
EP_06	66	98
EP_07	65	98
EP_08	59	98
EP_09	109	97
EP_10	71	98

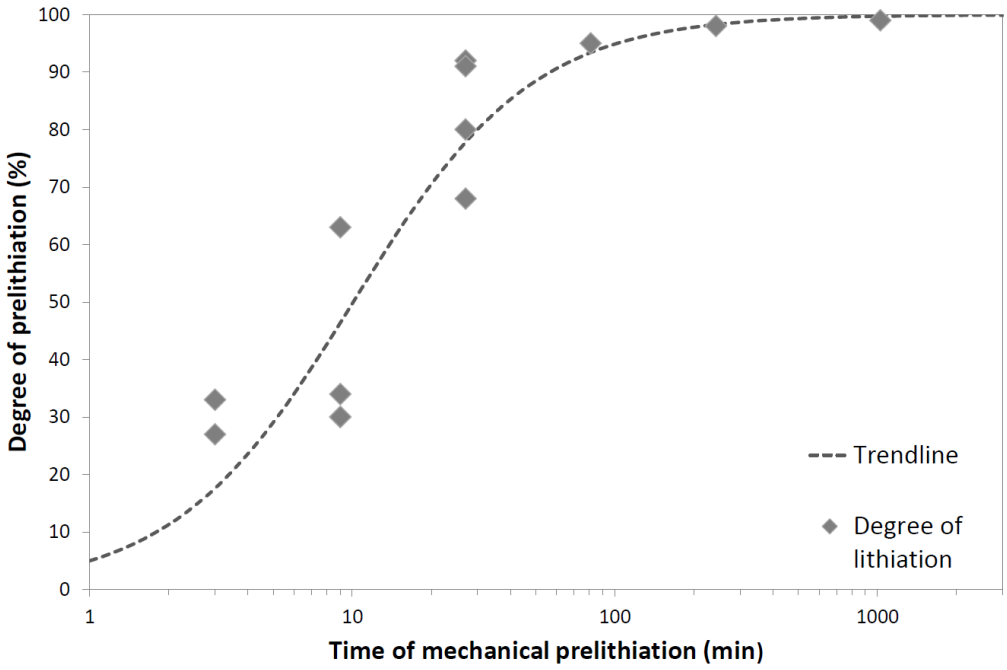

FIGURE 4.1: Degree of prelithiation with time of mechanical prelithiation.

4.1.2 Change in Mass

Before prelithiation the electrode masses were measured outside the glove box. After prelithiation they were left overnight to dry and measured on a scale inside the Ar-filled glove box the next day. The mass of the current collector was measured to be 28.7 mg, and was subtracted from the measured electrode masses to obtain the mass of only the electrode material before and after prelithiation. The change in mass is given as percentage change relative to the initial mass, and can be found in Table 4.3 for EP and Figure 4.2a for MP.

All EP electrodes experienced a mass increase ranging from 50 to 90 %, while for MP the change in mass ranged from 10 to 120 %. The highest mass change for a MP electrode was seen for an electrode mechanically prelithiated for only 27 min.

In Figure 4.2b the MP results for the first 81 min are shown. A linear trendline was plotted to correlate time of prelithiation and degree of mass change. According to the trendline the mass change increases with time of prelithiation, but so does the variation.

TABLE 4.3: Change in electrode material mass for electrochemically prelithiated electrodes. The electrodes were lithiated in the Arbin battery tester with a rate of C/20.

Electrode	**Change in mass (%)**
pre_01	76
pre_02	66
pre_03	92
pre_04	66
pre_05	72
pre_06	49

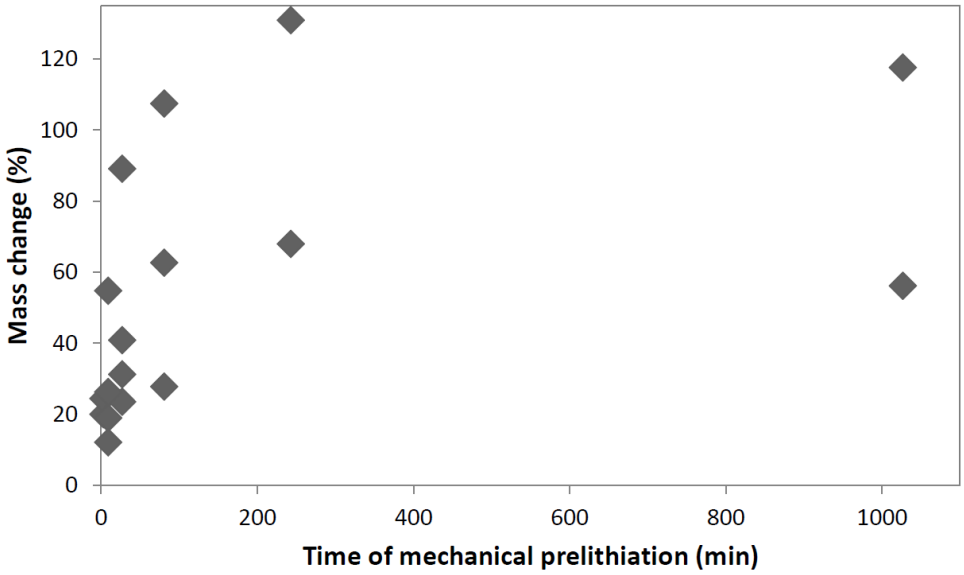

(a)

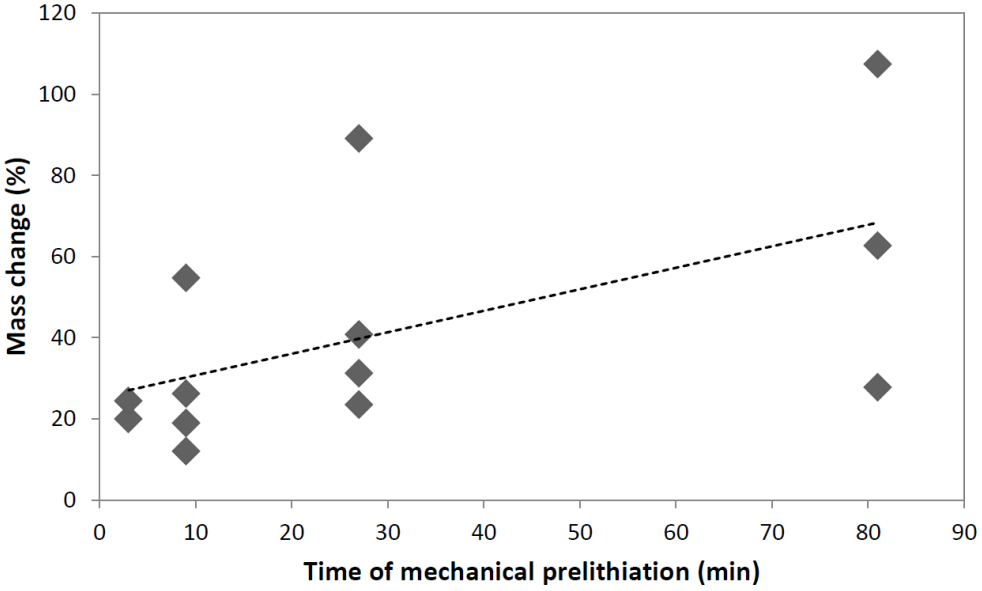

(b)

FIGURE 4.2: Change in electrode material mass as a function of time of MP.
a) Shows the change in mass for all the MP electrodes, and b) a subset showing MP up to 81 min.

4.2 Electrochemical Performance

4.2.1 Reference Cells

A total of four reference cells without any prelithiation were cycled on the standard cycling program, however two of them experienced cell failure and was not furthered used in this study. The remaining two were used as the baseline for comparison, and to calculate the degree of prelithiation for the MP and EP cells (Table 4.1 and 4.2) as seen in the previous section. As both reference cells showed similar results, graphs presented in this section show only the cycling data for one of the reference cells for clarity. SEM micrographs of a reference electrode will also be presented in this section.

Figure 4.3 shows the voltage-capacity relation for the ten first cycles in the reference cell. As the Si electrode is lithiated the cell voltage decreases quickly and flattens out as the electrode is filling up with Li-ions. When Si is nearing full lithiation, the potential drops further until it reaches the cut-off voltage of 0.05 V (vs. Li^+/Li). During delithiation the cell voltage increases until it reaches the cut-off voltage of 1 V (vs. Li^+/Li).

By studying the voltage-capacity curves it can be seen that the cell capacity is highest in cycle one and decreases significantly in the second cycle. The third and final formation cycle is nearly identical to the second cycle, before another significant decrease is seen for the fourth cycle cell capacity as the faster cycling commences. After the three formation cycles in the standard cycling program, the capacity decreases slowly each cycle. Each shift/decrease in the voltage-capacity plot corresponds to a drop in the discharge capacity, which can be seen in Figure 4.4. The discharge capacity curve drops quickly during the three first cycles before it flattens out. The less decay seen in the discharge capacity curve, the longer cycle life can be expected. A voltage-capacity figure with minimal difference between the cycles, and a nearly flat discharge capacity curve, are signs of the cell having long cycle life.

The differential capacity (dQ/dV) plot for the two first cycles in the reference cell is shown in Figure 4.5. Again it can be seen that the cell voltage decreases during lithiation and increases during delithiation. The peaks correspond to phase transitions occurring in the process of transforming the SiNPs into fully lithiated $Li_{3.75}Si$. These points are difficult to detect in the voltage-capacity figure (Figure 4.3), and is only visible in a differential capacity plot like this. The areas under the curves, which correspond to the amount of lithium transferred in and out of the silicon, are similar in size, which is confirmed by the high CE (Figure 4.6), as expected from a rechargeable battery.

The calculated initial CE and HC efficiencies for the two reference cells are shown in Table 4.4. It can be seen that the initial CE is > 90 % for both reference cells. A high initial CE is related to a small irreversible loss of lithium, and should ideally be as close to 100 % as possible. Figure 4.6 shows the calculated CE for all the the cycles in the two reference cells. Just after the

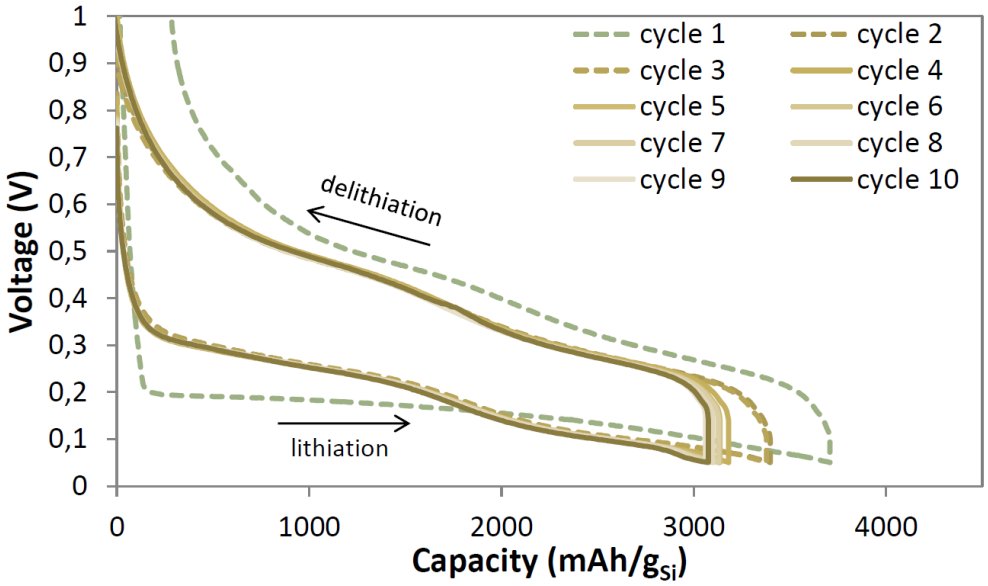

FIGURE 4.3: Voltage-capacity for the ten first cycles in reference cell one. Load of active material: 0.38 mg/cm^2.

formation cycles the CE drops, before it increases and stabilises at $\sim$ 100 %. The CE maintains this level for $\sim$ 40 cycles before it starts to slowly decrease. The initial HC efficiency was for both reference cells > 97 %, indicating that the charge/discharge ratio of the HC is high, and hence its rechargeability is good.

TABLE 4.4: Initial Coulombic Efficiency (CE) and HC efficiency in the reference cells.

Cell	CE (%)	HC efficiency (%)
ref_01	99.2	99.2
ref_02	94.0	97.4

From the discharge capacity curve in Figure 4.4 it can be seen that after $\sim$ 50 cycles the discharge capacity falls below 80 % of post-formation discharge capacity. This corresponds well with the CE just reported. The discharge capacity is high and reference cell one has a reversible capacity of $\sim$ 3,000 mAh/g$_{Si}$ for cycles 4 – 49. This value was calculated based on the discharge capacity in each cycle. The sharpest decay in discharge capacity is seen during the first three cycles as noted in the voltage-capacity cycles. From cycle 2 to 10 the discharge capacity decayed with 9 %.

At what point the discharge capacity starts to decay with a high rate often corresponds to increase of IR in the cell. Figure 4.7 shows the IR measured for the reference cells. Some variation is seen, especially for the ref_01 cell but the general trend is that the IR is low to start with, and slowly increases

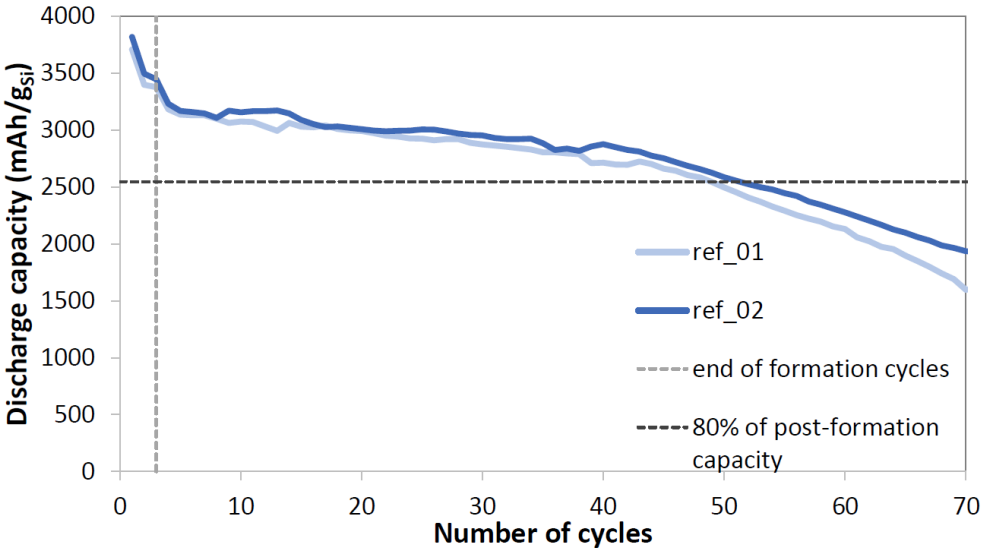

FIGURE 4.4: Discharge capacity and cycle life plot for the reference cells. Load of active material: 0.38 mg/cm^2 (ref_01) and 0.42 mg/cm^2 (ref_02).

cycle by cycle. The variation in IR for the ref_01 cell seems to have had little effect on its overall cycle life.

A reference electrode was studied in SEM to get an understanding of what the surface of the Si electrode looks like before prelithiation. SEM micrographs of the reference Si electrode are shown in Figure 4.8.

It can be seen that the electrode surface consist of quite polydisperse and agglomerated nanoparticles. By an elemental analysis of the surface with energy-dispersive X-ray spectroscopy (EDS), it was confirmed that the light particles on the micrographs are Si and the big, darker chunks are carbon (C). The SiNPs vary in size and distribution over the electrode surface, and many of the particles have merged to form larger secondary particles with irregular shapes. The variation in particle size and distribution mainly comes from the Si powder used and the composition of the electrode slurry. The electrode slurry contains 60 % Si and 25 % C, so it is quite natural to detect C when studying the electrode with SEM.

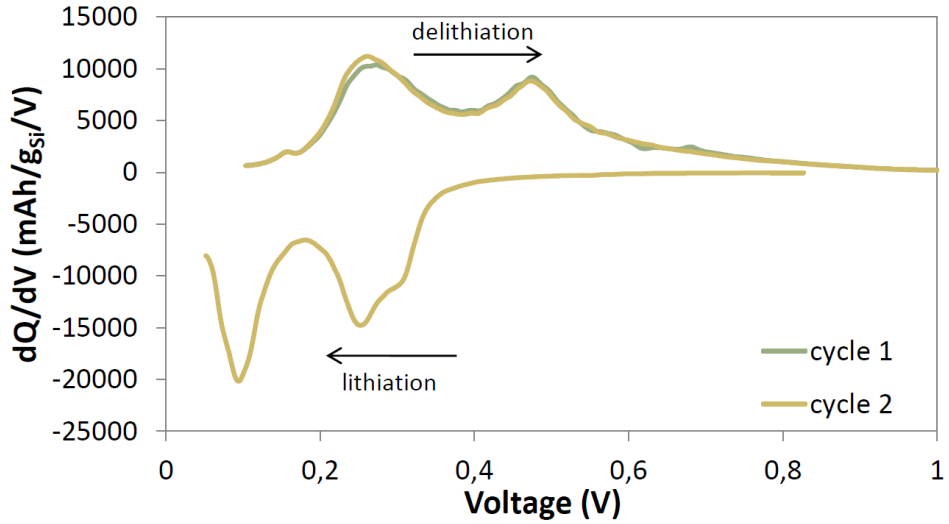

FIGURE 4.5: Differential capacity (dQ/dV) plot for reference cell one. Load of active material: 0.38 mg/cm^2.

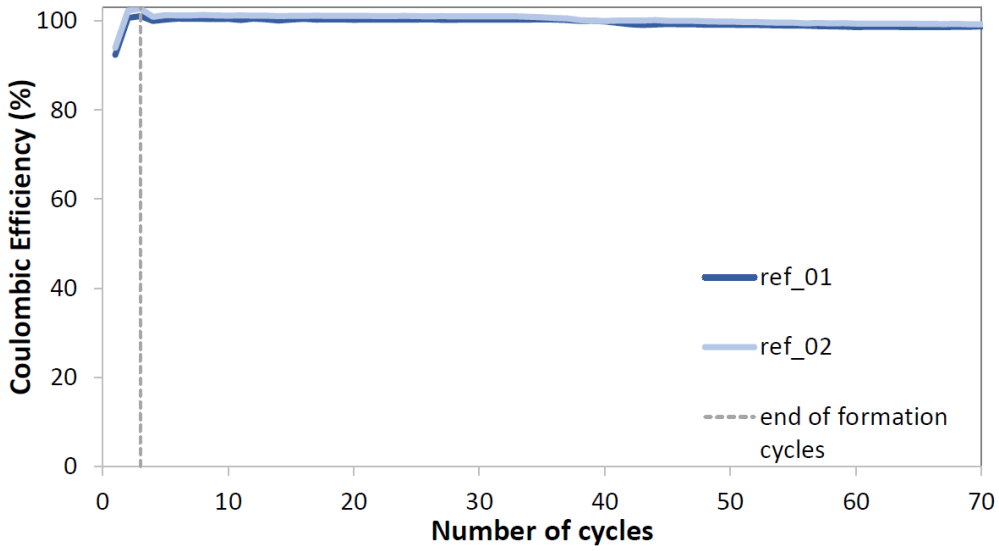

FIGURE 4.6: Coulombic efficiency per cycle for the reference cells. Load of active material: 0.38 mg/cm^2 (ref_01) and 0.42 mg/cm^2 (ref_02).

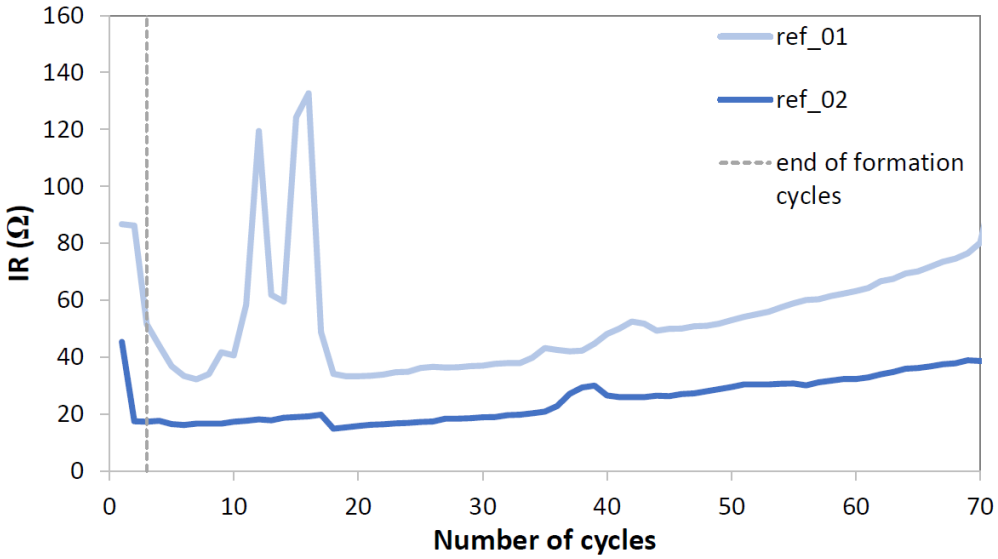

FIGURE 4.7: Internal resistance (IR) measurements for the reference cells. Load of active material: 0.38 mg/cm^2 (ref_01) and 0.42 mg/cm^2 (ref_02).

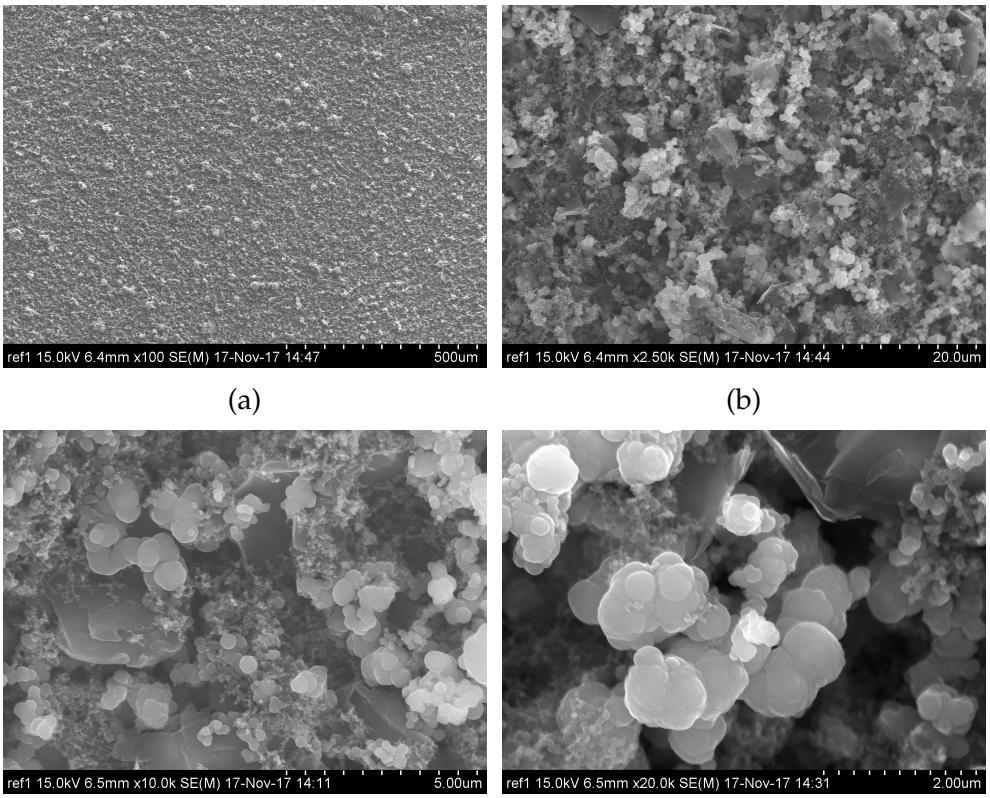

FIGURE 4.8: SEM micrographs of a reference Si electrode with scale bar lengths of a) 500 μm, b) 20 μm, c) 5 μm and d) 2 μm.

4.2.2 Electrochemical Prelithiation

Electrochemically prelithiated cells were made for both standard cycling and limited capacity cycling. The cells EP_04 – EP_06 were cycled on the standard cycling program and their data will be presented in this section. The cells EP_07 – EP_10 were cycled on the limited capacity programs, and their cycling data will be presented in section 4.3.

As the EP_06 cell showed the highest degree of prelithiation, it was used to plot the graphs in this section. The data from the two other EP cells showed similar results.

Figure 4.9 shows the voltage-capacity relation for the ten first cycles in the EP_06 cell. The cell voltage decreases until the cut-off at 0.05 V (vs. Li^+/Li) during lithiation, and increases until the cut-off at 1 V (vs. Li^+/Li) during delithiation. It can be seen that cycle one (the green curve) has shifted to the left and its peak cell capacity is close to zero. This indicates that a high degree of prelithiation was obtained. The capacity is not actually negative during the first cycle, but has shifted strongly to "negative" capacity because more Li-ions are extracted during delithiation than inserted during lithiation. Only the very end of the first cycle lithiation/discharge curve is plotted, as the remaining insertion of Li-ions was done during prelithiation and therefore happened before this measurement started.

Similarly to the reference cell, cycle two has the highest cell capacity. However, already from cycle three the capacity decreases slowly each cycle, which is different from the reference cells. These small changes in the voltage-cycles can correspondingly be seen in the discharge capacity curve in Figure 4.10, which has a smaller drop in the first cycles discharge capacity than seen for the reference cells. This indicates that the EP cells can obtain a longer cycle life than the reference cells.

The differential capacity (dQ/dV) plot for the two first cycles in the EP_06 cell is shown in Figure 4.11. Again it can be seen that the cell voltage decreases during lithiation and increases during delithiation. The peaks correspond to phase transitions occurring on the Si electrode, and was not possible to detect by studying the voltage-capacity curves (Figure 4.9) without differentiating them. The areas under the curves are similar in size as confirmed by the high CE (Figure 4.12), which is expected from rechargeable cells.

The calculated initial CE and HC efficiencies for the two reference cells are shown in Table 4.5. All the EP cells show an initial CE well above 100 %, confirming that prelithiation was successful. The high initial CE corresponds well with the calculated degree of prelithiation showed in Table 4.2. Figure 4.12 shows the CE per cycle for the EP cells cycled on the standard cycling program. The CE is stable at $\sim$ 100 %, which corresponds well with the results in the voltage-cycle and discharge capacity figures. The HC efficiency is > 90 % for all the EP cells, indicating that the charge/discharge ratio of the HCs are high, and hence they have a good rechargeability.

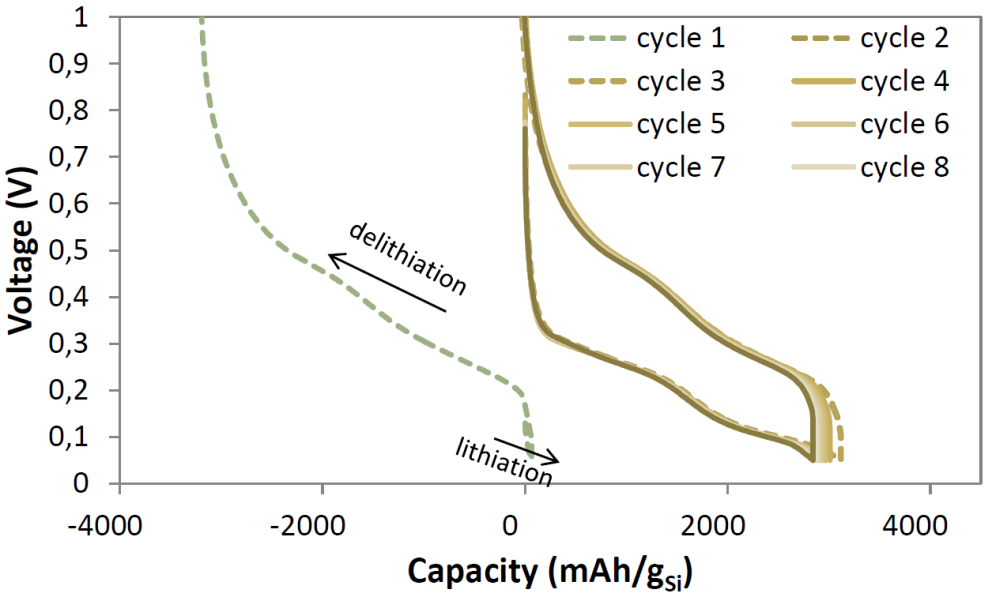

FIGURE 4.9: Voltage-capacity curves for the ten first cycles in the EP_06 cell. Load of active material: 0.38 mg/cm^2.

TABLE 4.5: Initial Coulombic Efficiency (CE) and HC efficiency for the EP cells.

Cell	CE (%)	HC efficiency (%)
EP_04	328	98.7
EP_05	4486	97.8
EP_06	4956	96.7
EP_07	5383	94.9
EP_08	4664	90.4
EP_09	3536	96.9
EP_10	5008	96.6

The evolution of the discharge capacity during cycling of the EP cells cycled on the standard cycling program is plotted in Figure 4.10. A smaller decrease in the discharge capacity compared to the reference cell is seen during the formation cycles. After this point the discharge capacity decreases slowly, and from cycle 2 to 10 the discharge capacity decayed with 5 % in the EP_06 cell. It can also be seen that after $\sim$ 50 cycles the discharge capacity falls below 80 % of post-formation discharge capacity. This corresponds well with the CE just reported. The discharge capacity is high and the EP_06 cell has a reversible capacity of $\sim$ 2,700 mAh/g$_{Si}$ for cycles 4 – 48. The small changes in voltage-cycles and discharge capacity confirms that the cells are rechargeable.

The same trend is seen in the IR plot in Figure 4.13. Some variations in IR and between the EP cells are seen, but the general trend is that after the formations cycles it slowly increases each cycle. Some variations in IR is to be

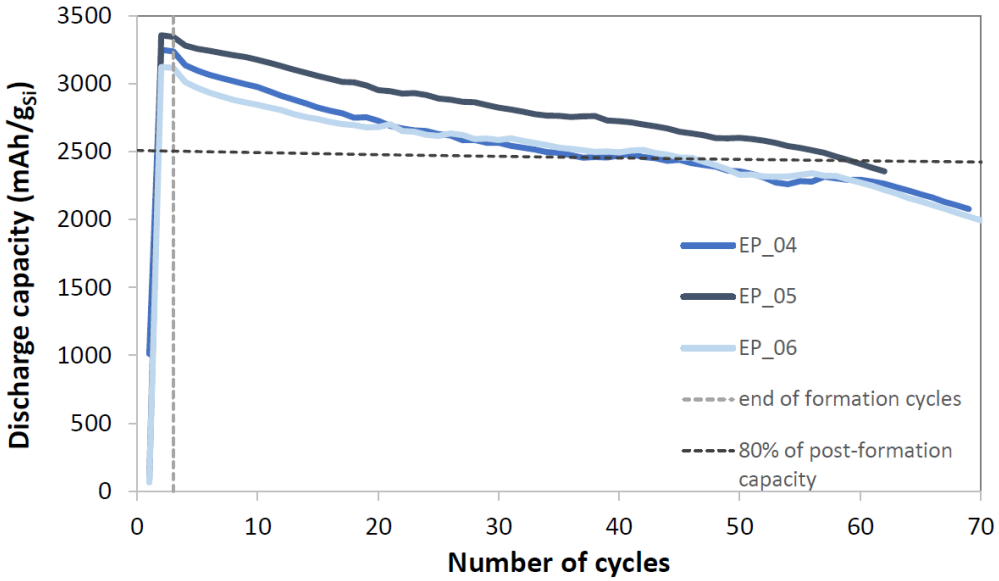

FIGURE 4.10: Discharge capacity and cycle life plot for the EP cells cycled on the standard cycling program. Load of active material: 0.38 mg/cm^2 (EP_04), 0.32 mg/cm^2 (EP_05), and 0.38 mg/cm^2 (EP_06).

expected and was also seen for the reference cells. The slowly increasing IR corresponds well with the slowly decreasing discharge capacity.

An EP Si electrode was studied in SEM and micrographs are shown in Figure 4.14. The micrographs show no significant change in the particles compared to the reference electrode, other than being slightly more merged. The additional particles that have merged are likely prelithiated particles. These particles should have experienced a volume change up to $\sim$ 300 %, and as they have a restricted volume to expand in it is natural to expect them to merge. The C also seem less visible compared to the reference electrode, which can be a result of the Si particles expanding around the C chunks during prelithiation.

At lower SEM magnification the EP electrode surface looked rougher than what was seen for the reference electrode. This was also observed for the MP electrode as later will be demonstrated in Figure 4.20a. Compared to the reference electrode, the prelithiated electrode has been exposed to more stress, and the rough surface is seen as a sign of this stress.

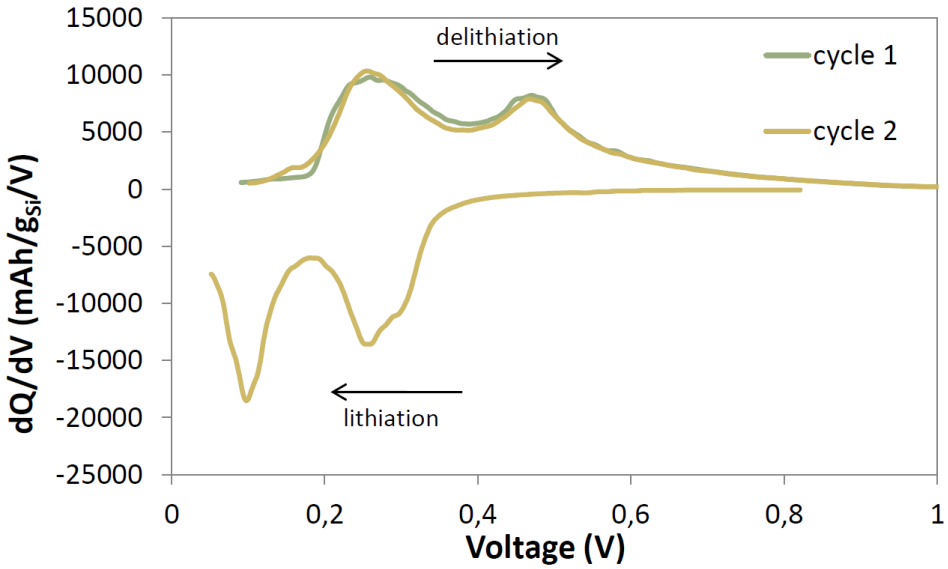

FIGURE 4.11: Differential capacity (dQ/dV) plot for the EP_06 cell. Load of active material: 0.38 mg/cm^2.

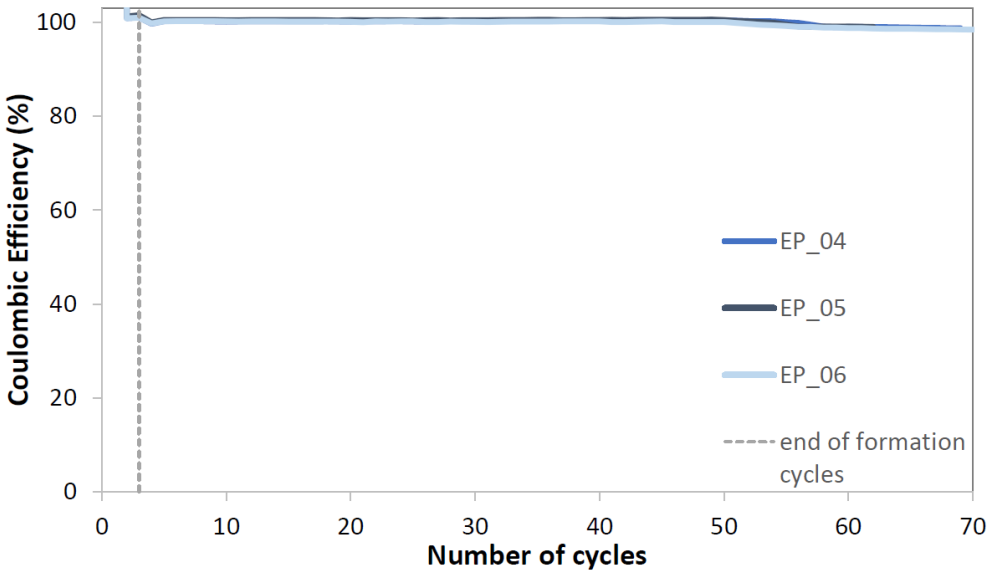

FIGURE 4.12: Coulombic efficiency for the EP cells cycled on the standard cycling program. Load of active material: 0.38 mg/cm^2 (EP_04), 0.32 mg/cm^2 (EP_05), and 0.38 mg/cm^2 (EP_06).

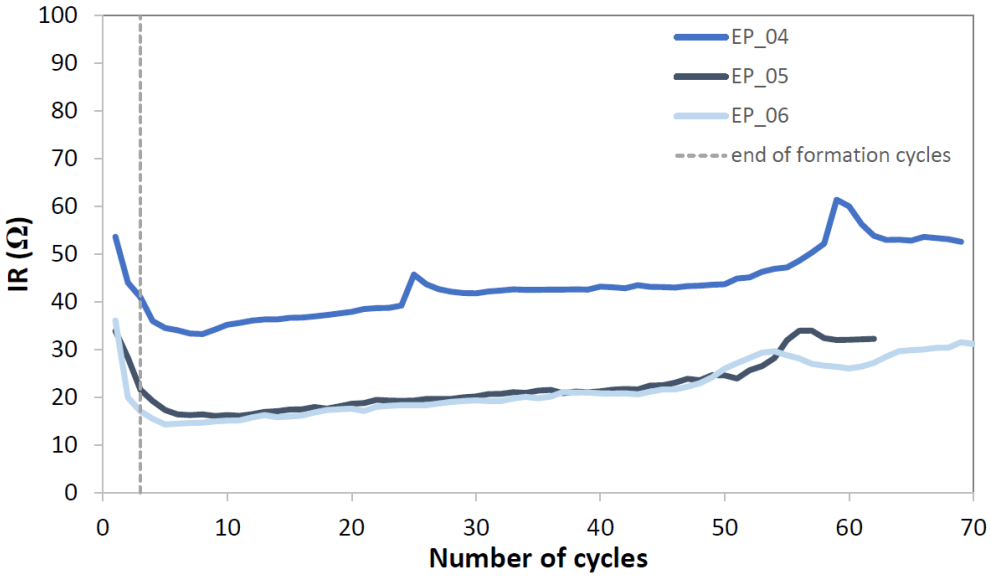

FIGURE 4.13: Internal resistance (IR) measurements for the EP cells cycled on the standard cycling program. Load of active material: 0.38 mg/cm^2 (EP_04), 0.32 mg/cm^2 (EP_05), and 0.38 mg/cm^2 (EP_06).

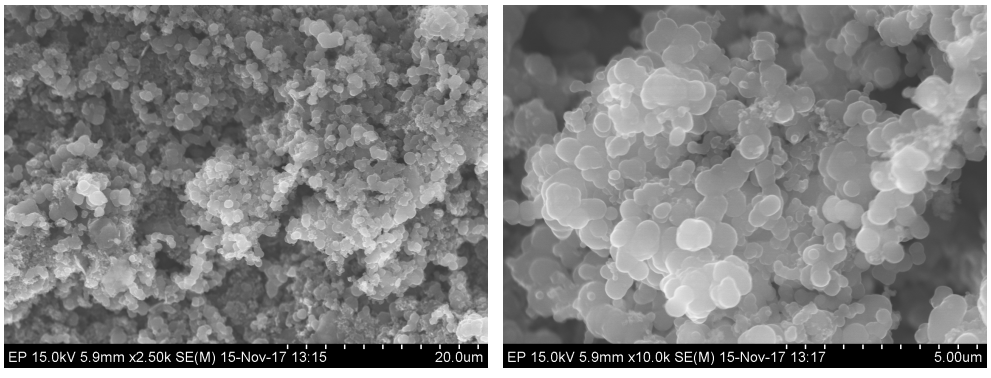

(a) (b)

FIGURE 4.14: SEM micrographs of electrochemically prelithiated Si electrodes with scale bar lengths of a) 20 μm, and b) 5 μm.

4.2.3 Mechanical Prelithiation

Mechanically prelithiated cells were made for both standard cycling and limited capacity cycling. The cells MP_04 – MP_09 and MP_11 – MP_13 were cycled on the standard program and their cycling data will be presented in this section. The cells MP_10 and MP_14 – MP_17 were cycled on the limited capacity programs, and their cycling data will be presented in section 4.3. The graphs in this section are plotted with the cycling data from the MP_07 (3 min MP), MP_08 (9 min MP), and MP_09 (27 min) cells.

Figure 4.15 shows the ten first voltage-capacity cycles for MP cells prelithiated for 3 min, 9 min and 27 min, respectively. It can be seen that the cell voltage decreases until the cut-off voltage of 0.05 V (Li^+/Li) during lithiation, and increases until the cut-off voltage of 1 V (Li^+/Li) during delithiation. No significant change in the shape of each voltage-cycle can be seen compared to the reference cell. However, in all the cases the first cycle graph has shifted to the left, indicating that prelithiation was successful. Again, the cell capacity in the first cycle is not actually negative, but shows "negative" values because more Li-ions are extracted during delithiation than inserted during lithiation. Only the end of the first cycle lithiation/discharge capacity curve is plotted, as the remaining insertion of Li-ions was done during prelithiation and therefore not recorded in this measurement.

The degree of prelithiation can be seen as a function of how close to the y-axis the first cycle cell capacity has shifted in the voltage-capacity plot (Figure 4.15). How far it has shifted increases with prelithiation time, i.e. the degree of prelithiation increases with prelithiation time. This corresponds well with the degree of prelithiation results earlier seen in Figure 4.1.

For the 3 and 9 min MP cells in Figure 4.15a and 4.15b, the first cycle voltage-capacity curves have shifted almost the same distance, indicating that the degree of prelithiation is close to similar. This corresponds well with the calculated degree of prelithiation from Table 4.1 of 27 and 34 %, respectively. In Figure 4.15c the voltage-capacity cycles for the 27 min MP cell are plotted. The first cycle has shifted significantly to the left, indicating an higher degree of prelithiation. This corresponds well with the the cell's calculated degree of prelithiation of 91 %.

Similar to the reference cell, the voltage-capacity plots show that cycle two has the highest cell capacity. It can be seen that for the 3 min MP cell the difference between first and second cycle cell capacity is the greatest, for the 9 min MP cell the difference is reduced, and for the 27 min MP cell there is almost no difference at all. A small cell capacity decay is an indicator of good reversibility.

The areas under the dQ/dV curves are confirmed by the high CEs (Figure 4.18) to be of similar size, indicating that the cells have a high rechargeability. However during the first cycle delithiation, an additional sharp peak emerges, as shown in Figure 4.16. The peak is seen between 0.4 and 0.5 V (vs. Li $+$/Li) for all three of the MP cells, and after the first cycle it disappears. It

TABLE 4.6: Initial Coulombic efficiency (CE) and HC efficiency for the MP cells.

Time of MP (min)	Cell Label	CE (%)	HC efficiency (%)
3	MP_04	117	99.9
	MP_07	124	97.5
9	MP_05	188	99.2
	MP_08	139	98.0
	MP_14	139	99.0
	MP_16	137	96.2
27	MP_06	849	98.7
	MP_09	1069	97.6
	MP_10	496	98.3
	MP_17	282	97.2
81	MP_15	1819	94.7
243	MP_12	4786	91.0
1027	MP_13	11 470	89.7

can be seen that the peak increases with time of MP. This peak is not visible in the dQ/dV plots for the reference and EP cells, and is related to a crystallisation step occurring during the transformation from SiNPs to the fully lithiated $Li_{3.75}Si$ [36].

The calculated initial CE and HC efficiencies for the two reference cells are shown in Table 4.6. All cells have an initial CE well above 100 %, confirming that prelithiation was successful. The initial CE is also seen to increase with MP time, while the HC efficiency is seen to decrease with MP time. Even though the initial HC efficiency is seen to decrease with MP time, all cells obtained a value of 90 to 100 %.

Figure 4.18 shows CE per cycle for the MP cells cycled on the standard cycling program. The CE is stable at $\sim$ 100 % after the formation cycles in all the cells, which corresponds well with the results in the voltage-cycle and discharge capacity figures.

The discharge capacity curves for the MP cells cycled on the standard cycling program are plotted in Figure 4.17. Unlike the reference cells, the discharge capacity is nearly flat in the three first cycles (the formation cycles). After the formation cycles the discharge capacity decreases slowly for all the MP cells, and remarkably slowly for the 243 min MP cell. For the 3 min MP cell in the discharge capacity decayed with 8 % from cycle 2 to 10, for the 9 min MP cell it decayed 7 % and for the 27 min MP cells it decayed 6 %. The 243 min and 1027 min MP cells both showed a decay of only 4 % from cycle 2 to 10. It can also be seen that all cells maintain 80 % of post-formation discharge capacity for $\sim$ 50 cycles, similar to the reference and EP cells.

The stable discharge capacity curve corresponds well with the stable CE seen in Figure 4.18 and the IR shown in Figure 4.19. Again some variation is seen in IR, but the general trend is that IR gradually increases cycle by cycle. Some degree of variation is expected, and was also seen for both the reference and the EP cells.

SEM measurements were performed on two MP electrodes: 27 min and 81 min of prelithiation. According to earlier results, there is a difference in the degree of prelithiation between these two MP times, and they were therefore chosen for further analysis with SEM.

Micrographs of the electrodes prelithiated for 27 and 81 min are shown in Figure 4.20 and 4.21, respectively. To obtain clear micrographs of the nanoparticles, two different detectors were used: mixed detector (M) and upper detector (U). Unfortunately, this complicates the comparing of the micrographs to those of the reference electrode, and no more micrographs were taken due to the time limitation of this study.

By comparing with caution, no significant change in the nanoparticles was seen compared to the EP and reference electrodes. Similar to the EP electrode, the nanoparticles seem to have merged more. With the great expansion of the particle volume and the limited space for them to expand in, merging is a natural result. Similar to the EP electrode, C seem less visible, which can come from the Si particles expanding around the carbon chunks.

On both prelithiated electrodes, a rough surface was seen with morphology features that looked like "hollow towers" of SiNPs. The rough surface can be seen in Figure 4.20a, 4.21a and the "hollow tower" of SiNPs in Figure 4.21c. During prelithiation the electrode is exposed to great stress, especially the MP electrode (as they are short-circuited with the Li-foil). This stress can cause damage, such as cracking, on both individual particles and on the surface as a whole. The rough surface is believed to be a result of this stress.

When studying the prelithiated electrodes by eye, dark spots were observed on the electrodes, especially on the MP electrodes. In SEM these dark spots looked smoother than the rest of the electrode. The micrographs in Figure 4.21a and 4.21b are taken from this area. When pealing the Li-foil off of the Si electrode, these same areas looked dryer than the rest of the electrode. It is therefore believed that these areas were less prelithiated than the rest of the electrode due to shortage of electrolyte. In SEM it was easier to detect C in the "dark spots" compared to the rest of the electrode. The "dark spots" thus looks more like the reference electrode than the rest of the prelithiated electrode. These spots can have prevented the electrodes from becoming fully prelithiated.

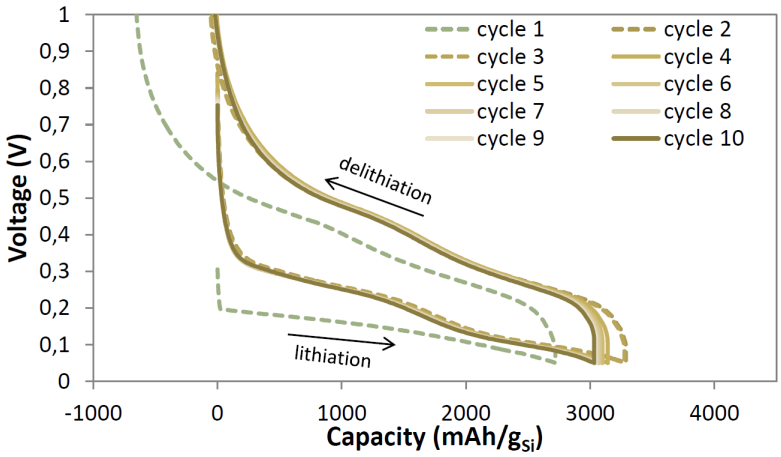

(a)

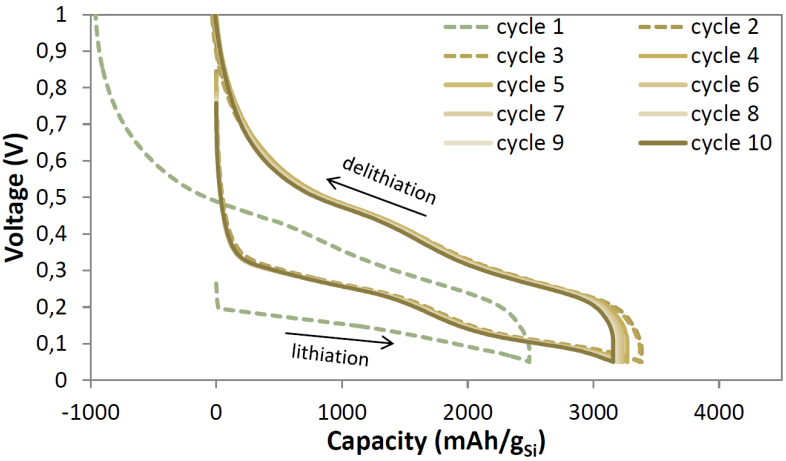

(b)

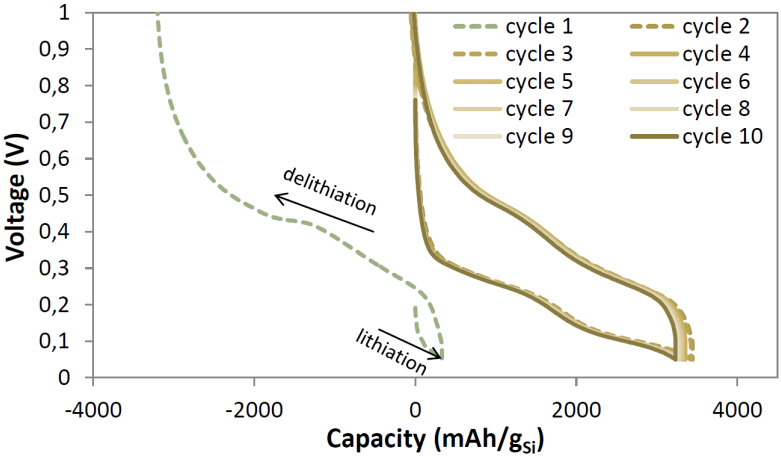

(c)

FIGURE 4.15: Voltage-capacity cycles for the two first cycles for mechanically prelithiated cells. Prelithiation time of a) 3 min (0.42 mg/cm^2) , b) 9 min (0.42 mg/cm^2), and c) 27 min (0.34 mg/cm^2).

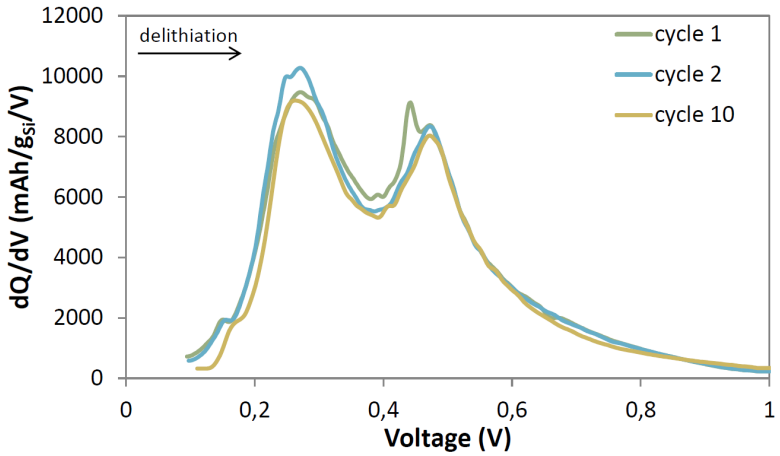

(a)

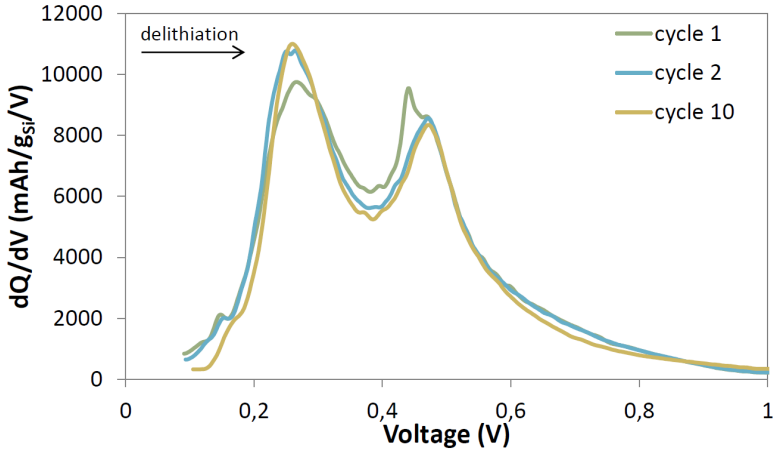

(b)

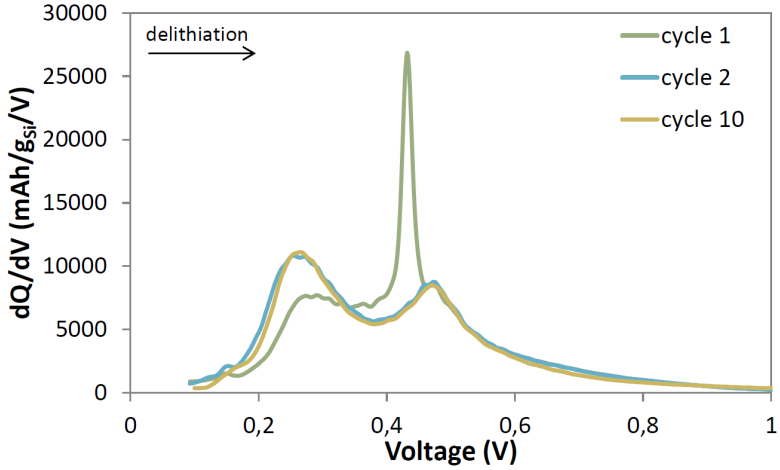

(c)

FIGURE 4.16: dQ/dV plots during charge of mechanically prelithiated cells. Prelithiation time of (a) 3 min (0.42 mg/cm^2), (b) 9 min (0.42 mg/cm^2), and (c) 27 min (0.34 mg/cm^2).

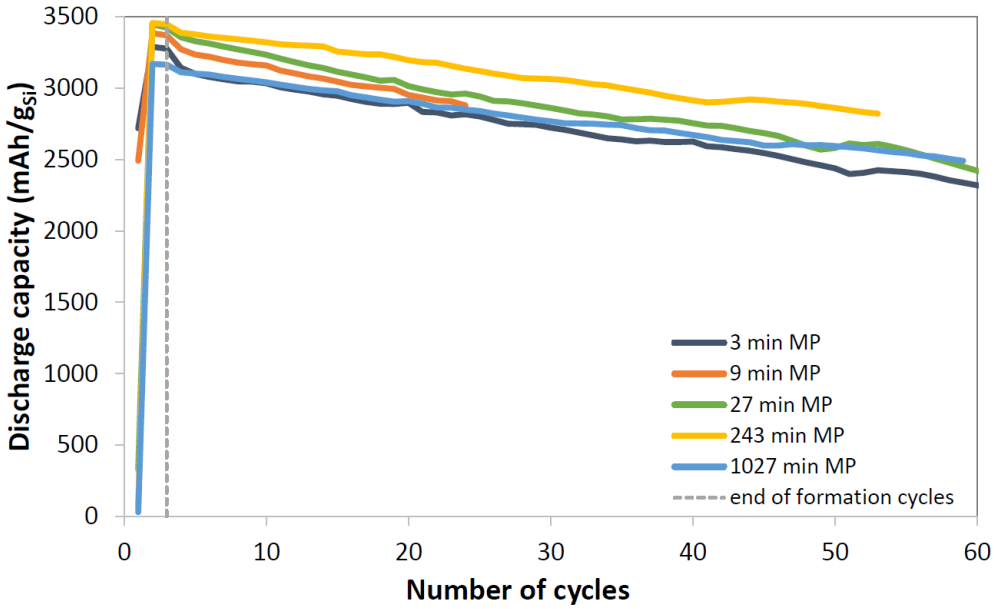

FIGURE 4.17: Discharge capacity and cycle life plot for cells with different times of MP cycled on the standard cycling program. Load of active material: 0.42 (3 min), 0.42 mg/cm^2 (9 min), 0.34 mg/cm^2 (27 min), 0.40 mg/cm^2 (243 min), and 0.31 mg/cm^2 (1027 min).

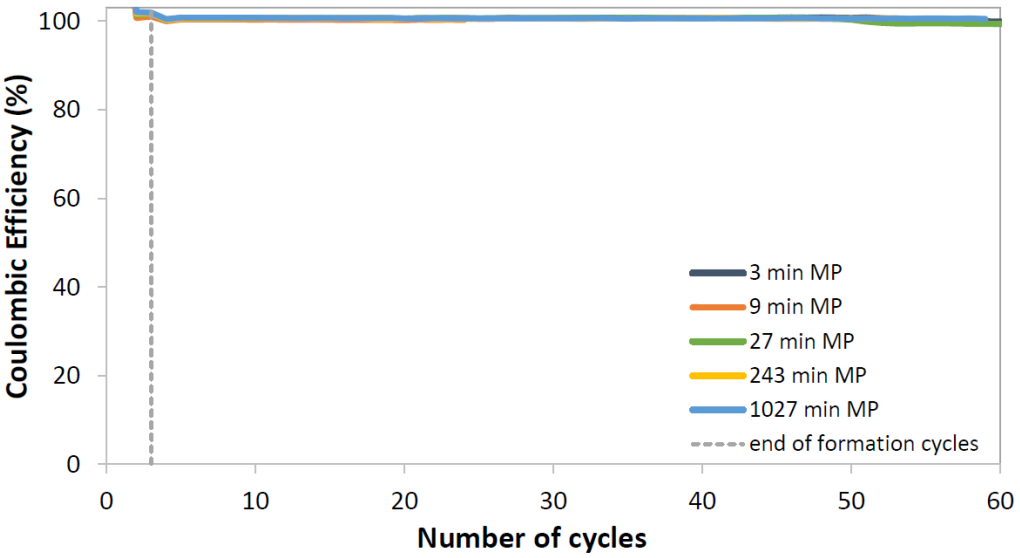

FIGURE 4.18: Coulombic efficiency for MP cells cycled on the standard cycling program. Load of active material: 0.42 (3 min), 0.42 mg/cm^2 (9 min), 0.34 mg/cm^2 (27 min), 0.40 mg/cm^2 (243 min), and 0.31 mg/cm^2 (1027 min).

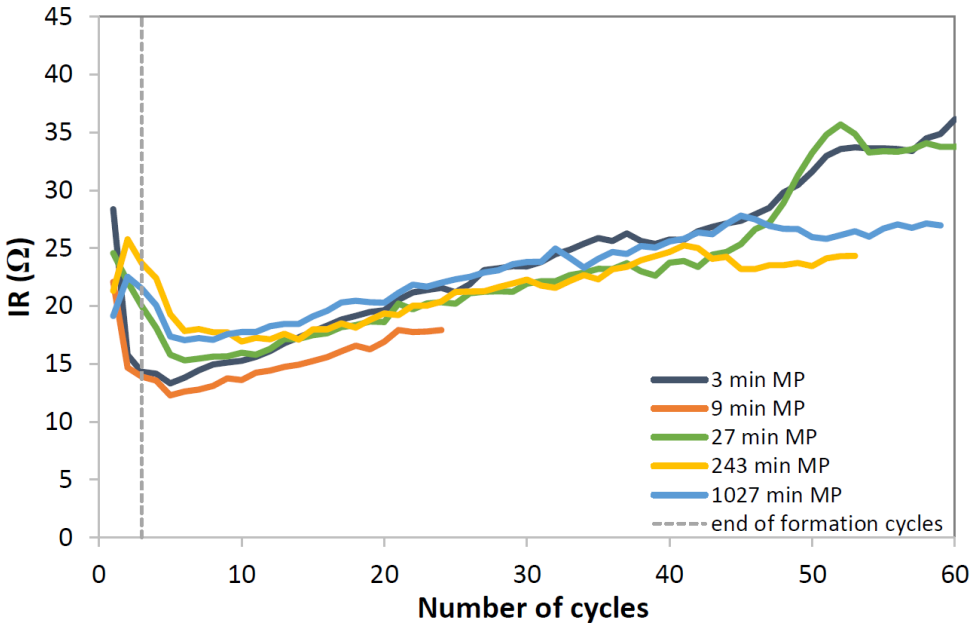

FIGURE 4.19: Internal resistance (IR) measurements for the cells prelithiated with different times of MP cycled on the standard cycling program. Load of active material: 0.42 (3 min), 0.42 mg/cm^2 (9 min), 0.34 mg/cm^2 (27 min), 0.40 mg/cm^2 (243 min), and 0.31 mg/cm^2 (1027 min).

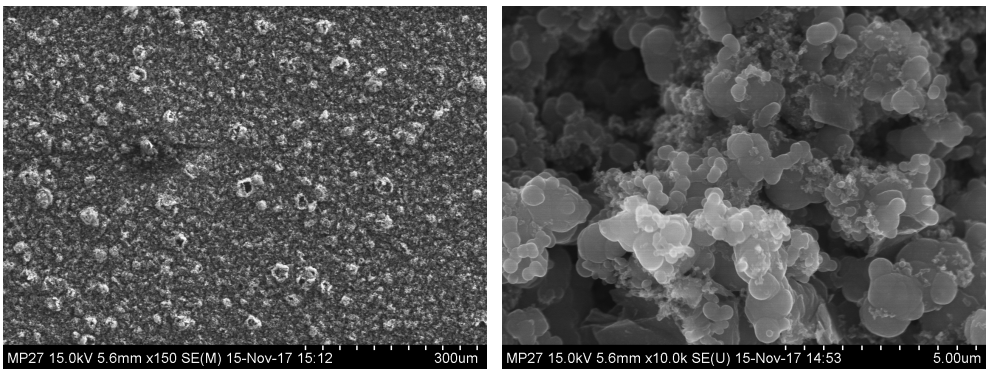

(a) (b)

FIGURE 4.20: SEM micrographs of a 27 min mechanically prelithiated Si electrode, where a) shows a "hollow towers" region, and b) shows a "non-tower" region.

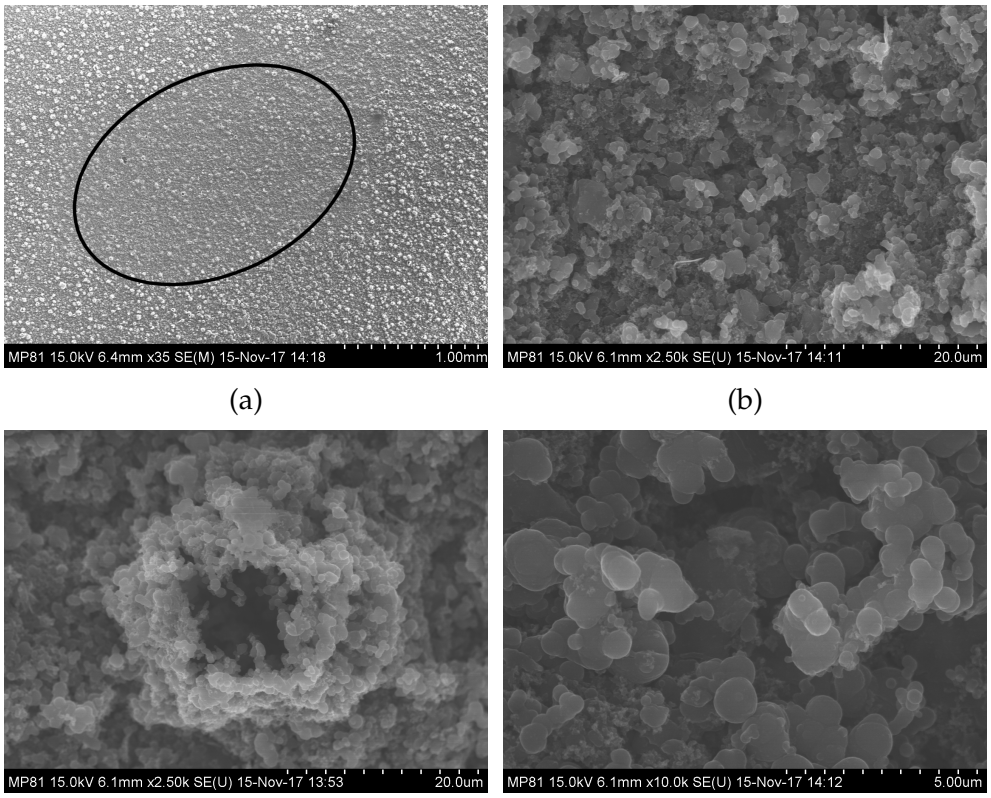

FIGURE 4.21: SEM micrographs of a 81 min mechanically prelithiated Si electrode. a) The black circle shows where a darker area was seen by the eye after prelithiation, and in the SEM a "smoother" area was seen. b) Inside the encircled area. c) Outside the encircled area: one of the SiNP "hollow towers" which was seen on the two MP electrodes (see Figure 4.20a) and the EP electrode. d) Outside the encircled area.

4.2.4 Summary of Performance

Table 4.7 shows a summary of the the cell performance for the reference cells, the EP cells, and the MP cells cycled on the standard cycling program. It shows reversible capacity which was calculated based on discharge capacity from cycle 4 to the cycle where the discharge capacity was reduced with > 20 %. Cycle life is here the cycle number where the discharge capacity dropped below this limit. It can be seen that the cells have a high reversible capacity, however only for $\sim$ 50 cycles. Only one cell reaches a higher cycle life of $\sim$ 60 cycles, and that was the 1027 min MP cell. However, by the end of this thesis work, two MP cells were still cycling (as shown in Table 4.8), and the 243 min MP cell (MP_12) is showing promising results and will surpass the other cells in term of cycle life. Nevertheless, they are not expected to surpass the other cells by much.

Figure 4.22 graphically shows the discharge capacity for a reference cell, a EP cell and a MP cell. In addition to the different prelithiation methods, variation can come as a result of different loading of active material (Si) on the electrodes and the assembling process. The graphs show that the ICL during the initial cycles seem bigger for the reference cell than the prelithiated cells, however after about 20 – 25 cycles the prelithiated cells have reached the same discharge capacity as the reference cell. All cells reach the 80 % of post-formation discharge capacity limit approximately at the same time (after ca. 50 cycles). It can also be seen that after the 80 % limit, the prelithiated cells seem to perform better, and if the 80 % limit had been lower, the prelithiated cells would have reached a higher cycle life than the reference cell. However, no significant improvement is expected.

TABLE 4.7: Summary of the cell performance for the reference cells, the MP cells and the EP cells cycled on the standard cycling program.

Cell	Reversible Capacity (mAh/g_{Si})	Cycle Life (number of cycles)
ref_01	2959	49
ref_02	3011	51
MP_04	2544	52
MP_05	2247	51
MP_06	2072	34
MP_07	2862	47
MP_09	3037	46
MP_13	2830	59
EP_04	2861	34
EP_05	2983	47
EP_06	2706	48

TABLE 4.8: The two MP cells still cycling, showing promising capacity retention.

Cell	Discharge Capacity (mAh/g_{Si})	Cycles (number of cycles)	Capacity Retention (%)
MP_08	2879	24	88
MP_12	2821	53	83

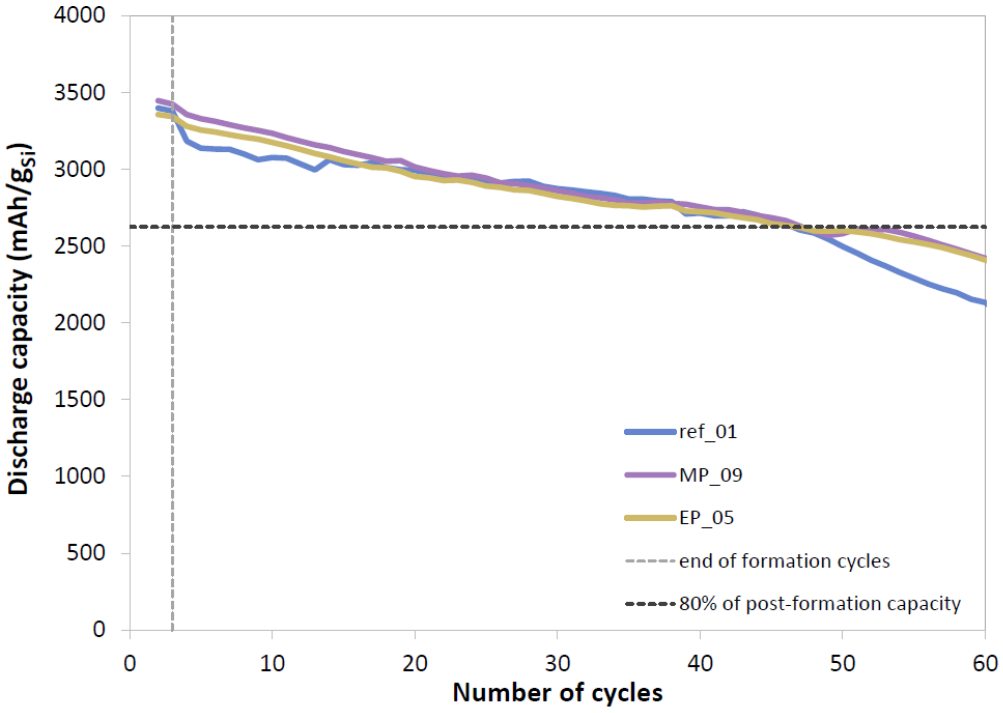

FIGURE 4.22: The discharge capacity of a reference cell, a MP cell and an EP cell cycled on the standard cycling program. Mass of active material: 0.38 mg/cm^2 (ref_01), 0.34 mg/cm^2 (MP_09), and 0.32 mg/cm^2 (EP_05).

4.3 Limited Capacity Cycling

To study prelithiated cell's performance over extended cycling, both EP and MP cells were cycled on a limited capacity cycling program. Two different programs were used, one limiting the lithiation step, i.e how many Li-ions are inserted into the Si electrode during discharge, and the other limiting the delithiation step, i.e how many Li-ions are extracted from the Si electrode during charge. Both programs were limited by a capacity of 372 mAh/g_{Si}, similar to the theoretical capacity of the graphite anode.

The discharge capacity for the cells cycled on the limited delithiation program is plotted in Figure 4.23 and on the limited lithiation program in Figure 4.24. The results show that the discharge capacity is stable over the 500 cycles, which is much better than what the cells performed on the standard cycling program.

A summary of all the LC cells' performances is shown in Table 4.9. The table shows the reversible capacity for each cell and the number of cycles they had cycled when data was extracted for this thesis. The reversible capacity is calculated based on the discharge capacity from cycle four (after the formation cycles) and on. All cells retained a reversible capacity close to 372 mAh/g_{Si} for all 500 cycles of the cycling program.

Figure 4.25 and 4.26 show the IR measured in the LC cells. Only small variations are see, which was also observed for the cells cycled on the standard cycling program. Since the cell's are cycled on limited capacity programs, a change in IR will not necessarily correspond to what is seen in the discharge capacity curve. The IR can increase significantly before it is visible in the discharge capacity plot as the buffer between 372 and 3,579 mAh/g_{Si} is large. However, an IR decrease of significant magnitude will naturally reduce the cycle life. The results in Figure 4.25 and 4.26 show that the IR for the LC cells only have smaller variations within 10 – 25 ohms, which is important to ensure long cycle life.

TABLE 4.9: Summary of the LC cells' performance.

Cycling program	**Cell**	**Reversible Capacity (mAh/g$_{Si}$)**	**Cycles**
LC delith.	MP_10	370	500
	MP_14	369	500
	MP_15	369	500
	EP_07	369	500
	EP_08	369	500
LC lith.	MP_16	373	468
	MP_17	373	477
	EP_09	373	500
	EP_10	373	417

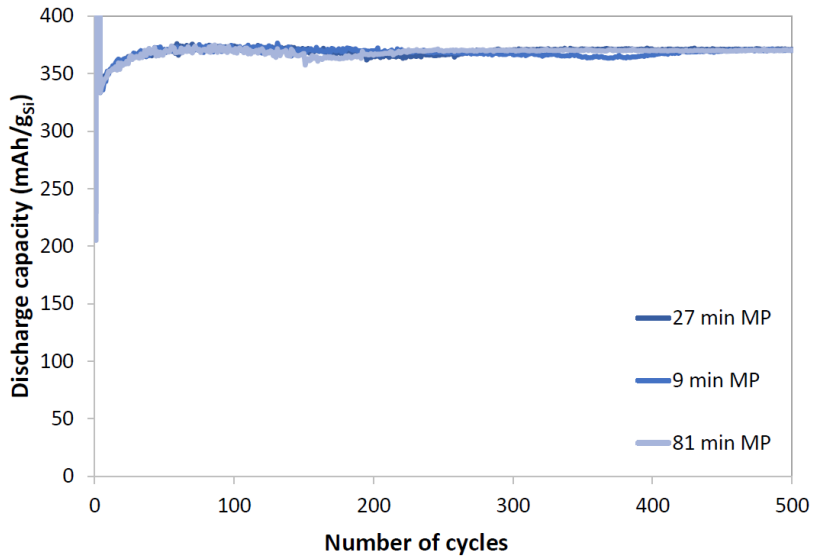

(a)

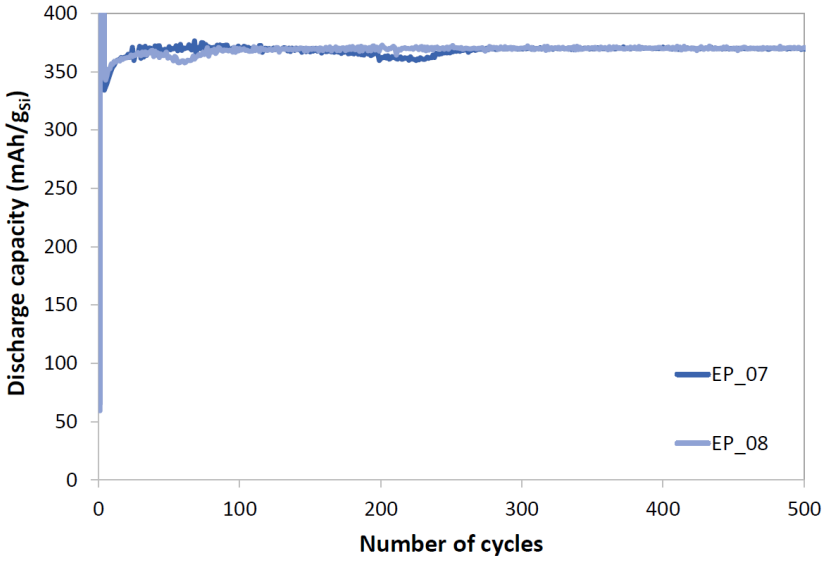

(b)

FIGURE 4.23: Discharge capacity for cells cycled on limited delithiation capacity for a) the MP cells, and b) the EP cells. Load of active material: 0.36 mg/cm^2 (27 min MP), 0.42 mg/cm^2 (9 min MP), 0.40 mg/cm^2 (81 min MP), 0.42 mg/cm^2 (EP_07), and 0.42 mg/cm^2 (EP_08).

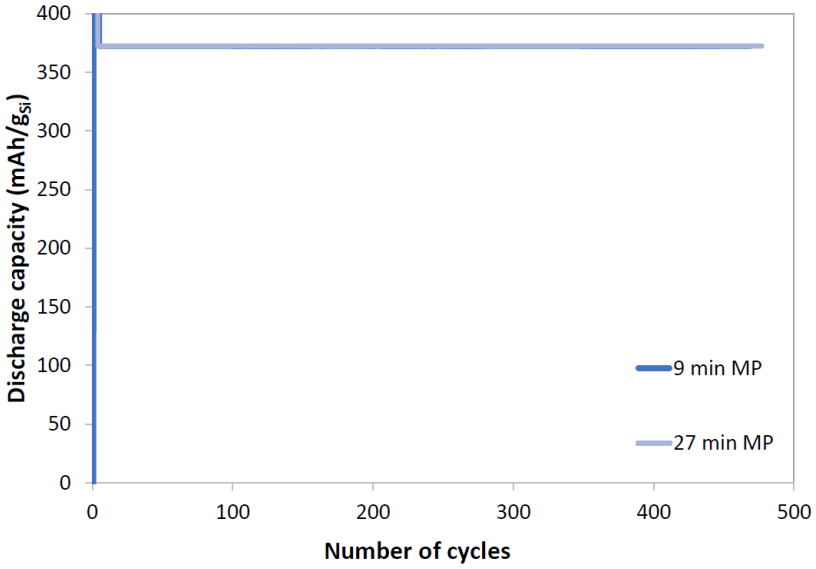

(a)

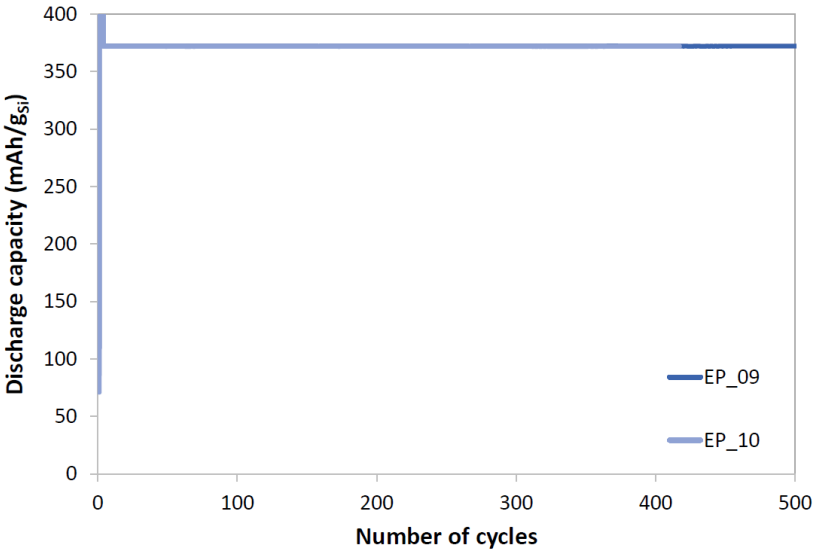

(b)

FIGURE 4.24: Discharge capacity for cells cycled on limited lithiation capacity for a) the MP cells, and b) the EP cells. Load of active material: 0.42 mg/cm^2 (9 min MP), 0.39 mg/cm^2 (27 min MP), 0.33 mg/cm^2 (EP_09), and 0.45 mg/cm^2 (EP_10).

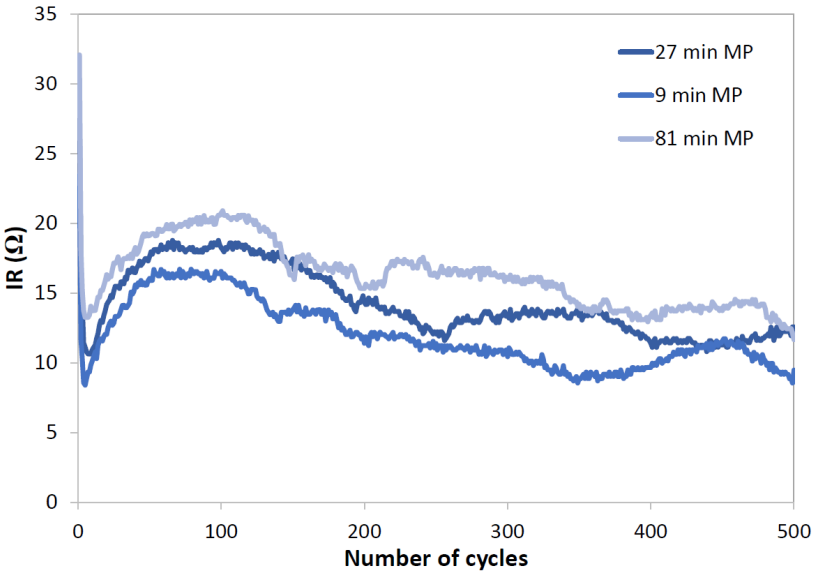

(a)

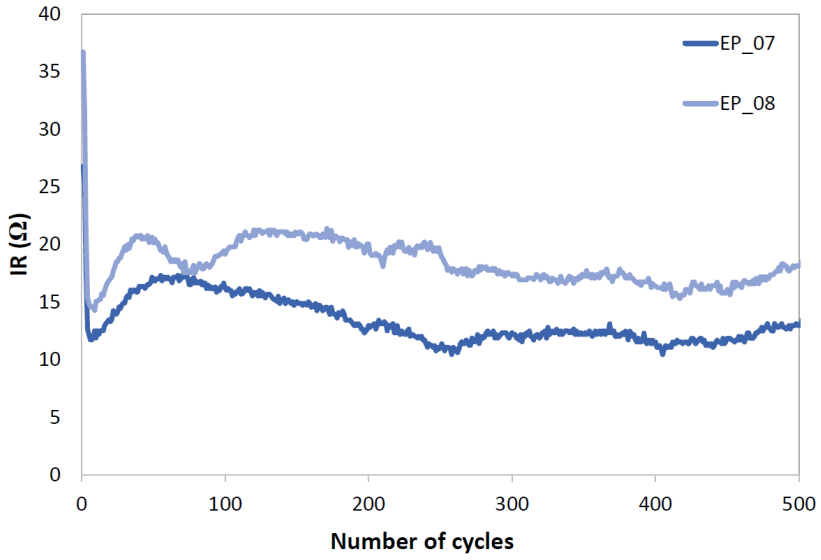

(b)

FIGURE 4.25: Internal resistance for the cells cycled on the limited delithiation cycling program: a) the MP cells, and b) the EP cells. Load of active material: 0.36 mg/cm^2 (27 min MP), 0.42 mg/cm^2 (9 min MP), 0.40 mg/cm^2 (81 min MP), 0.42 mg/cm^2 (EP_07), and 0.42 mg/cm^2 (EP_08).

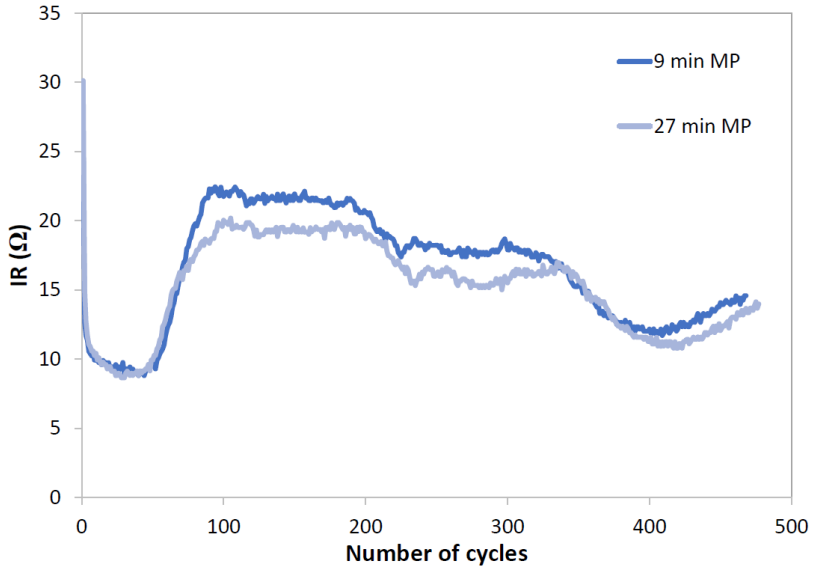

(a)

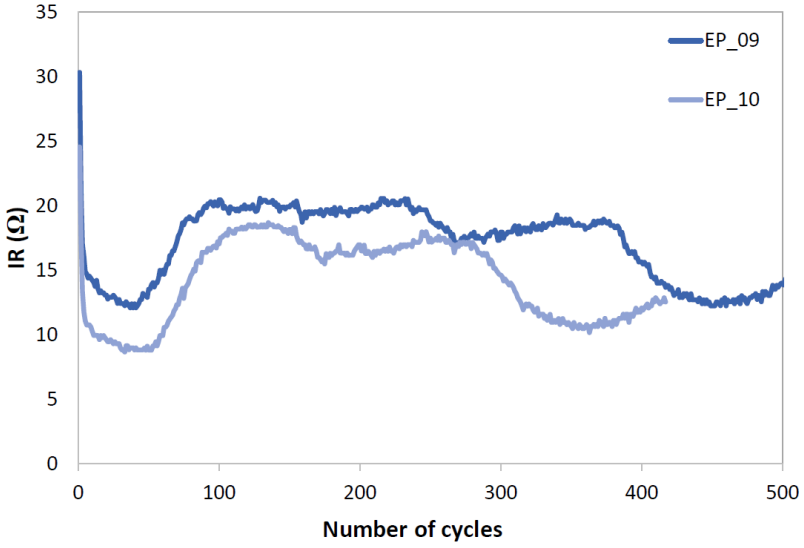

(b)

FIGURE 4.26: Internal resistance for the cells cycled on the limited lithiation cycling program: a) the MP cells, and b) the EP cells. Load of active material: 0.42 mg/cm^2 (9 min MP), 0.39 mg/cm^2 (27 min MP), 0.33 mg/cm^2 (EP_09), and 0.45 mg/cm^2 (EP_10).

5 Discussion

5.1 Prelithiation over time

5.1.1 Degree of Prelithiation

A systematic study of the amount of Li preloaded into the Si electrodes as a function of prelithiation time was done. By theory lithiation is a process controlled by diffusion where Li ions are inserted into the SiNPs from the surface to the core. Lithiation of the entire Si electrode is a similar process. In other words, the degree of prelithiation is expected to increase quickly during the first minutes of prelithiation. This was seen in our MP results (Figure 4.1), where the increase is steep at first, before it flattens out completely. The prelithiation process is fast because it resembles the short-circuiting of a galvanic cell. According to Gibbs free energy (ΔG = -36 kJ/mol), the chemical reaction is highly spontaneous and drives the prelithiation process to take place quickly and completely. However, a degree of prelithiation of 100 %[1] was not reached for any of the cells, and the data points collected seemed to follow an asymptotic increase. By non-linear least squares fitting, the trendline for the MP data in Figure 4.1 was found. It shows that the insertion of Li ions is fast until a certain degree of prelithiation, and that it is possible to obtain a close-to-fully prelithiated (> 90 %) Si electrode in 60 min. However, the measured degree of prelithiation is not consistent, and a degree of prelithiation of both 70 and 90 % was reached in just 30 min (Table 4.1). The remaining prelithiation seems to be a slow process, and even when increasing the prelithiation time to $\sim$ 17 hours a degree of 100 % was not reached. This result is in accordance with what is expected from diffusion processes, which typically are very slow when close to equilibrium.

When studying the degree of prelithiation for the EP cells (Table 4.2) the same problem was seen, even though these cells were prelithiated for ca. 20 hours. This observation reinforces the theory that the remaining prelithiation is a slow process and that a degree of prelithiation of 100 % is hard to reach. There are many internal mechanisms that can prevent the electrodes from reaching this level, e.g. kinetic limitations/diffusion and physical barriers, in that some Si particles may be isolated or stuck deep in the electrode structure preventing the Li ions from reaching them. The EP cells were also limited by the voltage range of 0.05 – 1 V (vs. Li^+/Li), which may have prevented a complete prelithiation (see cycling program specifications in Appendix B.1).

[1] The fully lithiated state is here defined as the $Li_{3.75}Si$ state.

By visual inspection and SEM measurements (Figures 4.14 and 4.21), what are assumed to be less lithiated spots on the electrodes were detected. Less lithiated spots, e.g. due to shortage of electrolyte or insufficient contact between the Si electrode surface and the Li foil, will naturally reduce the degree of prelithiation that the Si electrode manages to reach. This defect is possible to control and can be avoided by adding more electrolyte and pressure. However, leakage of the electrolyte must be avoided and a setup where this is prevented is important if a higher degree of prelithiation is wanted.

5.1.2 Potential Sources of Error in the Determination of the Calculation of the Degree of Prelithiation

For the calculations of the degree of prelithiation in Tables 4.1 and 4.2, each prelithiated cell was compared to the average discharge capacity of the reference cells. This discharge capacity was assumed to be the maximum capacity that the prelithiated cells would have also reached if not prelithiated. The difference between the two values was then used to calculate the degree of prelithiation. However, when cycling cells, variations are unavoidable. Despite studying duplicate cells, variations are seen in both initial discharge capacity, nominal voltage, and cycle life. Even for cells with the same loading of active material (i.e. load of Si), variation is seen. Some variation is believed to come from the coin cell assembly process, and the exact variation is hard to predict.

The measured discharge capacities can not necessarily be assumed to directly describe the the amount of Li inserted into the Si electrodes. The discharge capacity is rather a measurement of the number of electrons that pass through the cell between the start and end voltage. How much is used to prelithiate the Si electrode and how much is used to form the SEI layer are, however, uncertain. It can be assumed that the amount used to form the SEI layer is similar for all cells, but when it comes to the prelithiated cells, this value might be different.

5.1.3 Washing of the Prelithiated Electrodes

Even though all cells were washed with DMC before cell assembly, with the intention to remove any SEI that formed during prelithiation, washing might not have completely succeeded. While the surfaces of the electrodes were thoroughly washed, it is undetermined whether there was remaining SEI inside the electrode structure or not. This concern is especially raised for the EP cells. The EP process includes a full charge/discharge cycle in the Arbin, allowing the SEI to fully form. If there is SEI left in the EP electrodes, fewer Li ions are required to form the remaining SEI layer in the reassembled cells. The fraction of the discharge capacity used to form the SEI layer will thus be different from that in the reference cells.

In the study done by Liu et al. [26], a thin coating layer of organic content was observed on the mechanically prelithiated SiNWs. They believed that this formation occurred due to decomposition of the electrolyte on the SiNWs' surface during prelithiation, a process that resembles the SEI formation seen during cell cycling. If a similar layer was formed on the SiNPs during MP in our study, it might not have been completely washed away after prelithiation, and can thus have affected the amount of charge used to form the SEI layer.

To summarise, this effect means that even though all cells measured a first cycle discharge capacity > 0 mAh/g_{Si}, the electrodes may have been fully prelithiated and the measured values depicted the capacity used to form the SEI layer.

5.1.4 Mass Change and Prelithiation Time

Mass measurements were taken before and after prelithiation to study correlation between the mass change and prelithiation time. Comparison of the mass measurements was expected to be another method of studying the degree of prelithiation as change in mass should increase with prelithiation time. The results show that the correlation is positive and approximately linear the first $\sim$ 80 min of MP, but the variation is also large and increases with prelithiation time (Figure 4.2b).

For the EP electrodes, the increase of the electrode material mass ranged from 50 to 90 %, while for the MP electrodes it ranged from 10 to 130 %. By theoretical calculation, a fully lithiated electrode (when assuming $Li_{3.75}Si$ as the fully lithiated state) would experience a mass increase of 56 %. For the EP electrodes, all except one obtained a close to fully degree of prelithiation, and for all except one, mass changes above expected values were observed (Table 4.3). No correlation between the lowest degree of prelithiation and the lowest mass change was seen.

In Table 5.1 the degree of prelithiation (from Table 4.1) and the mass change (from Figure 4.2) for the MP cells are compared. Overall, the mass increases with the increasing degree of prelithiation, but the variations are large and an obvious correlation between the two is not seen.

The scale used to measure the prelithiated electrodes in this study is believed to have influenced the results. The prelithiated electrodes were weighed on a scale inside the glove box, and the mass displayed by this scale was varying due to vibrations applied by the vacuum pump and changes in glove box pressure with the smallest movement of the operator's arms. Remaining DMC on the electrodes could have also influenced the measured masses. Precipitated salt from the electrolyte, dust collected when drying, or leftover SEI/organic layer (as discussed above) could also have influenced the mass of the electrodes. A substantial variation in the mass measured after prelithiation was observed for both the EP and MP cells.

TABLE 5.1: Combined degree of prelithiation and mass change results for MP cells. Degree of prelithiation data collected from Table 4.1 and mass change data from Figure 4.2.

Degree of Prelithiation (%)	Mass Change (%)
30	26
30	12
33	24
63	19
68	31
92	24
95	63
98	68
99	56

5.2 Electrochemical Cycling

According to theory, prelithiated cells are expected to have a reduced initial irreversible capacity loss (ICL), but otherwise the same electrochemical signature as non-prelithiated cells. Our results point in the same direction. The cycling data, i.e. discharge curves, voltage curves, dQ/dV curves and IR curves, for the prelithiated cells follow the same trends as those of the reference cells. Similar observations were done by Liu et al. [26] when prelithiating SiNWs. Variations in the electrochemical cycling are seen, however this is also seen between the reference cells and between duplicates of the prelithiated cells. Even though an extensive effort is made to reduce the number of influencing variables, some variations are common in cell cycling, and are often not easy to explain as there are many possible reasons/explanations for their occurrence, e.g. cell assembly, load of active material, internal chemistry, or defects in cell components.

The similar electrochemical cycling and the retention of capacity, can be explained by the survival of the nanostructure of the SiNPs after prelithiation, which is confirmed by the SEM study (Figures 4.14, 4.20, and 4.21). The same observation was made by Liu et al. [26]. Even though a macroscopically rougher surface is observed for the prelithiated electrodes than the non-prelithiated electrodes, the nanostructure of the SiNPs themselves is maintained, and this seems to have a greater impact on the overall performance than the rough surface of the electrodes.

5.2.1 Variation in Mass Loading

Some of the variation can potentially be explained by variation in mass loading. Small differences were seen in the mass loading for the cells cycled in this study, from about 0.30 mg_{Si}/cm^2 to 0.45 mg_{Si}/cm^2. Higher loading of active material generally results in thicker electrodes, and the particles are more distant from the current collector. This reduces the cycling stability and cycle life [23]. However no significant variation in the cycle life due to the loading of active material was seen in our results. For example, the EP cell with the lowest loading maintained a reversible capacity for 47 cycles, while the two EP cells with the highest loading (both had the same loading of 0.38 mg_{Si}/cm^2) maintained a reversible capacity for 34 and 48 cycles. The cycle life was here calculated as the number of cycles the cells managed to retain a discharge capacity of at least 80 % of the post-formation capacity. All cells except one had a cycle life of ~ 50 cycles as seen in Table 4.7, and a consistent correlation between the variation in mass loading and cycle life was not seen.

5.2.2 Coulombic Efficiency and HC Efficiency

Two different efficiencies were calculated in this study: CE and HC. The CE describes the efficiency of the lithiation/delithiation process of the Si electrode in the cell. The HC efficiency describes the charge/discharge efficiency of the HC, and hence gives information about the HC's working principle. The initial CE and HC efficiencies were calculated for all cells and are found in Tables 4.4, 4.5, and 4.6 for the reference, EP, and MP cells, respectively.

Both calculations were based on measured charge and discharge capacities, which are measurements of the number of electrons flowing in and out of the cell between the start and stop voltages. The number of electrons flowing could potentially include parasitic redox reactions involving ions other than the Li ions, e.g. from salts, water, or other components from the electrolyte. The complexities of each calculation are discussed next.

Coulombic Efficiency

CE was defined earlier as the ratio between the amount of charge delivered during discharge to the amount of charge consumed in the previous charging (Section 2.6.1, equation 2.12). This definition is valid for a full cell (FC), but also for the HCs in this study, as a cycle is defined as the spontaneous lithiation step, followed by the non-spontaneous delithiation step. However, for our HCs with Si as negative electrode, the "charge" and "discharge" notation is reversed compared to the case of a FC. Thus, the CE reported here was calculated by dividing the HC charge capacity by the *preceding* discharge capacity measurement.

The greatest difference in CE was seen between the initial CE for the reference cells and the prelithiated cells. While the reference cells obtained values of 94 – 99 % (Table 4.4), the prelithiated cells obtained initial CEs well above this, reaching as high as 11,000 % for the MP cell with the highest degree of prelithiation (Tables 4.5, and 4.6). This result is directly connected to prelithiation and the choice of cycling program. As all the prelithiated electrodes were partly or close to fully prelithiated, only a small portion of the lithiation capacity was left before the cells reached the cut-off voltage of 50 mV (vs. Li^+/Li) during the first cycle discharge. The more Li already in the electrode, the less lithiation capacity was left before reaching the cut-off voltage, and the higher the initial CE was obtained. This trend illustrates the limited usefulness of CE as a measure of first cycle reversibility in prelithiated cells.

In Table 4.6 it can be seen that the initial CE increases with MP time. This is confirmed by the earlier discussion that the degree of prelithiation also increases with MP time. After the first cycle, the CE stabilises to a level of about 100 % in both the reference and prelithiated cells, and no significant difference is seen between the prelithiation methods.

Theoretically, it is not possible to obtain CEs > 100 %, as one can not take out more Li ions of the Si electrode than are put in. Only with prelithiation, where the Si electrode already is pre-alloyed with Li, is an initial CE > 100 % expected. After the first cycle, all the Li ions are assumed extracted during delithiation, and the CE should ideally be stable just below 100 % in the cycles hereafter [23]. However, in our study, CE values above 100 % were consistently observed in later cycles.

There can be many reasons for obtaining CE values above this level in later cycles. Li ions could be stuck in the Si electrode from prelithiation and/or lithiation in previous cycles, which then can be extracted in the later cycles. This would lead to higher charge capacities, and potentially CEs > 100 %. Another factor that could have affected the CEs is the voltage range of the cycling programs. Since the cycling programs are limited by the voltage range of 0.05 – 1 V (vs. Li^+/Li), the lithiation and delithiation are not allowed to completely fill and empty the Si electrodes with Li. This could affect the measured discharge and charge capacities in the current or later cycles, and hence the CE.

Since the CEs were consistently higher than 100 % in the later cycles in all cells, another possibility is that the high values could be a result of a systematic measurement error in the Arbin tester. However, we have little reason to believe that this is the case, as the other cycling results were as expected and no error has been reported by the other lab users. It was also not considered to be a result of prelithiation, as CEs > 100 % were obtained for both the reference cells and the prelithiated cells.

For Si anodes, an initial CE in the range of 65 – 85 % is expected, which is far below that seen for graphite anodes of 90 –99.7 %. In later cycles, CE is expected to reach 98 – 99.7 %, however an even higher CE of > 99.8 – 99.9 % is needed for battery applications [23]. Compared to these expected values, the

cells in our study obtained initial CEs well above the range expected for the Si anode. Our later cycles CEs were also consistently higher than expected.

Even though both initial and later cycle CEs showed high values, which normally would indicate well performing cells with long cycle life, the cycle life was not significantly improved for either of the cells in this study. This will be further discussed later. While the high initial CE gave an indication of the degree of prelithiation obtained, it could not be used to conclude whether the prelithiation process reduced the ICL or not, as no reasonable comparison between the reference and prelithiated cells could be made.

HC Efficiency

The HC efficiency is defined as the ratio of charge flowing out of the HC to the charge flowing into the HC. It is calculated by dividing the HC charge capacity by the *following* discharge capacity measurement, rather than the preceding measurement as in CE. This value describes the cell's rechargeability as a whole, rather than being used to interpret the rechargeability of the Si electrode.

The two reference cells had initial HC efficiencies of 97 and 99 %. For the EP cells the initial HC efficiency varied from 90 to 99 %, and for the MP cells it varied from 90 to 100 %. Obtaining values below 100 % was expected due to an increase in entropy. As the discharge (lithiation) step is spontaneous and the charge (delithiation) step is not, an increase in entropy is expected each cycle, and thus, the charge (delithiation) process requires more energy to return the Si to its original state than was usefully extracted by the spontaneous discharge (lithiation) process. High HC efficiencies are wanted to ensure good rechargeability through minimising energy loss due to entropy.

Studying the HC efficiency for the MP cells (Table 4.6), it can be seen that the HC efficiency decreases with increasing MP time. This means that some of the charge into the cell in the first HC cycle was not extracted in the following cycle. This behaviour is the opposite of the initial CE, where an increase was seen with the increasing MP time. The loss of charge extracted can again be explained by the additional energy required to overcome the increasing entropy from cycling between the spontaneous and non-spontaneous processes.

Conversely HC efficiency can be looked upon in terms of the flow of Li ions. The decreasing HC efficiency means that a smaller amount of Li ions was inserted into the Si electrode than what was extracted. With longer MP times, more Li ions are inserted into the Si electrode with no voltage cut-off limiting the insertion. During electrochemical cycling, the delithiation and lithiation are limited by the voltage range of 0.05 – 1 V (vs. Li^+/Li). This voltage range can prevent complete lithiation and delithiation, compared to the unlimited process. During the first delithiation, the amount of Li extracted from the Si electrode is cut off by the 1 V (vs. Li^+/Li) limit, and this happens no matter

how much Li remains in the Si electrode. Between lithiation and delithiation, the Li can evenly distribute itself in the Si electrode structure (i.e. through diffusion). During the following lithiation, the remaining Li in the Si electrode (Li_xSi with x < 3.75), limits how many more Li ions are able to be inserted during the voltage window. The higher the degree of prelithiation, the more Li will be left in the Si electrode after delithiation (i.e. the higher the x in Li_xSi is), and the lower the HC efficiency becomes.

The decreasing HC efficiency also points in the direction that excessive prelithiation can be damaging on some level, as reported by Domi et al. [9]. With increasing prelithiation time, the Si electrodes (and SiNPs) are believed to be exposed to an increasing amount of stress. The MP method is essentially short-circuiting the Si electrode and the Li foil, a process that is expected to expose the SiNPs to more stress than in the EP process. The increased amount of stress applied to the electrodes and SiNPs can be damaging on such a level that cracking and eventually material pulverisation is induced more quickly.

However, the reduced HC efficiencies seem to have no influence on the cycle life of the cells, as the cells with long MP times perform as well as the rest of the cells. Two of the cells with the lowest HC efficiencies even reached longer cycle lives than the rest of the tested cells. Following the mechanism described above, the remaining Li in the Si electrode could be stored over many cycles, possibly being released/delithiated in later cycles and improving the cycle life of the cells.

5.2.3 Voltage-Capacity Cycles

No significant difference in the shape of the voltage-capacity cycles for the reference, EP, and MP cells was seen (Figures 4.3, 4.9, and 4.15). However, for the prelithiated cells the first cycle shifted strongly to the left. This is a result of the cycling process beginning with discharge (lithiation), and the prelithiated electrodes already being partly or fully alloyed with Li. Small lithiation capacities were measured, resulting in the first cycle graphs shifting to the left.

The voltage-capacity cycles could be used to discuss the ICL by studying how the cell capacity changes each cycle. For the reference cell (Figure 4.3) cycle one reaches the highest capacity, cycle two and three are both considerably reduced, and thereafter the cell capacity decreases slowly. The same is shown graphically in Figure 4.4, where the sharp drop seen in the discharge capacity in the formation cycles describes the reduction seen for the three first cycles in the voltage-capacity plot. This decrease can be a result of ICL, and is ideally reduced for a more stable cycling and possibly longer cycle life.

Figures 4.9 and 4.15 show the voltage-capacity cycles for the EP and MP cells. In both cases the first cycle has shifted to the left, confirming that prelithiation has occurred. This shift, however, complicates the comparison of the first cycle capacity to the second cycle capacity, and the ICL between first and

second cycle is not as easily observed as for the reference cell. What can be calculated is the discharge decay from the corresponding discharge capacity plots (Figures 4.10 and 4.17), which will be discussed later.

5.2.4 Differential Capacity

The biggest difference in the electrochemical cycling data was seen in the dQ/dV plot for the MP cells (Figure 4.16). As the MP time increased, a peak at $\sim$ 0.43 V (vs. Li^+/Li), which was not observed for the reference cells nor the EP cells, became more distinct. A peak in the dQ/dV plot represents a phase transition, which indicates that an additional phase transition occurs in the MP cells compared to the reference and EP cells. This peak is likely to be related to the crystalline phase of the fully lithiated silicon (c-$Li_{15}Si_4$). The effect of crystallinity on initial electrochemical cycling is a widely studied subject, and it is well known that during the first lithiation of c-Si there is a two-phase region due to the conversion of c-Si to partly lithiated a-Si. Obrovac et al. [35] reported that the two-phase region remains until $\sim$ 50 mV, while below this voltage limit the lithiated a-Si suddenly crystallises into $Li_{15}Si_4$. Research done by Ogata et al. [36] relates a peak found at 0.43 V (vs. Li^+/Li), similar to our results (see Figure 5.1), to the delithiation of the c-$Li_{15}Si_4$-phase. The research also shows that the phase is avoided when the cycling is limited by a voltage cut-off of 50 mV (vs. Li^+/Li) or higher. In our experiments all galvanostatic cycling, including the EP process, was limited by a cut-off voltage of 50 mV (vs. Li^+/Li) to avoid this crystallisation from occurring. However, the MP process was not controlled by a cut-off voltage, and the Si electrodes were practically short-circuited before assembled into coin cells. Short-circuiting the electrodes eventually allows the voltage to reach 0 V (vs. Li^+/Li). The longer the prelithiation time the lower the voltage is allowed to be pushed and the longer the voltage stays below 50 mV (vs. Li^+/Li). This is believed to be the reason why the peak is increasing with prelithiation time. The occurrence of a crystalline phase on lattice level could induce damage to the Si electrode on particle level and/or electrode level.

5.2.5 Cell Failure

As seen from the complete list of the cells produced in this study (Appendix C), a total of five cells completely failed during cycling.[2] There are many mechanisms that can cause cell failure, and for that reason it was important to test multiple cells. As cell failure was seen for both reference and prelithiated cells, the cause of the failure was not considered to be related to the prelithiation process.

[2]Four of the cells reached an "unsafe voltage" level and had to be removed from cycling, and one short-circuited.

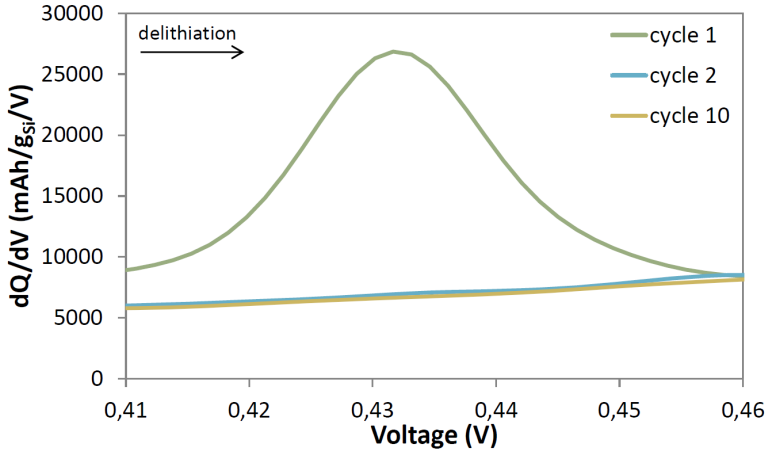

FIGURE 5.1: A subset of Figure 4.16c, showing the dQ/dV peak occurring close to 0.43 V.

5.2.6 Performance

With prelithiation the performance in terms of cycle life is by some researchers expected to increase due to the suppression of the volume change of Si. Cui et al. [7] showed that a slow and shallow lithiation should improve the cyclability. Electrodes prelithiated for shorter times will experience a shallower lithiation, thus shorter prelithiation times are expected to retain capacity better than longer prelithiation times. In other words, in terms of cyclability, the cells cycled with shorter MP times, should perform best. In a paper by Domi et al. [9] it was pointed out that excess prelithiation could in fact reduce battery performance.

Neither of these results were confirmed in this study (Table 4.7). As earlier discussed, all cells showed similar electrochemical cycling properties, indicating that the cycle life should, if not become better, at least be similar to the reference cells'. This is what was observed and all cells, even the reference cells, maintained 80 % discharge capacity retention for $\sim$ 50 cycles. The same result was observed by Domi et al. [9], who saw that when prelithiated Li was extracted from the Li-Si alloy during the first cycle, the cell exhibited as poor a cycle performance as the non-prelithiated Si cell. Even though the cells in our study were exposed to different amounts of stress, and limited with and without a voltage range, no significant difference was seen in the cycle life.

When comparing the performance of a reference, an EP, and a MP cell in Figure 4.22, the only notable difference between the prelithiated and non-prelithiated cells was seen in the first few cycles. A subset of the figure is plotted in Figure 5.2. It can be seen that the two prelithiated cells follow a more gradual capacity decay, while the reference cell decreases more abruptly before it flattens out. From cycle 2 to 10, the discharge capacity was reduced by 5, 6, and 9 % for the EP, MP and reference cell, respectively. This trend indicates that the ICL is bigger for the reference cell than for the prelithiated

cells in the first cycles, which is likely to be a result of the suppressed volume change of Si as expected by Domi et al. [9]. This volume change seems sufficient to decrease the discharge capacity decay for the first few cycles, but after $\sim$ 25 cycles, the overall cycle life was the same for both the prelithiated and reference cells.

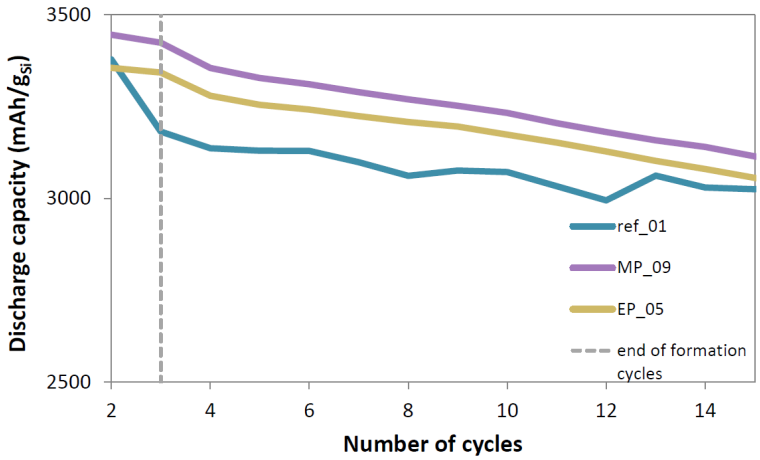

FIGURE 5.2: A subset of Figure 4.22, showing the discharge capacity for the first cycles for a reference cell, EP cell and MP cell.

By further investigation of the performance of the MP cells, it can be seen that the discharge capacity decay in cycles 2 through 10 decreases with the increasing MP time (see Table 5.2). It was discussed earlier that the degree of prelithiation increases with the MP time. Furthermore, with an increasing degree of prelithiation the volume change correspondingly increases. It is thus seen that with the increasing volume change the discharge capacity decay in the first few cycles is reduced. This can be related to a smaller loss of irreversible capacity, and the longer the prelithiation time, the smaller the loss. However, only the MP cell prelithiated for 243 min showed superior cycle life, and otherwise the increased volume change did not seem to influence the decay in the first few cycles, nor the total cycle life much. The MP cells prelithiated for > 200 min and the EP cells prelithiated for $\sim$ 20 hours all obtained the same discharge capacity decay of 4 to 5 %, indicating that increasing the prelithiation time had no further effect on reducing the decay.

Even though the discharge capacity decay in the first few cycles was reduced with prelithiation time, the overall cycle life was not significantly improved compared to the reference cells. However, it is a good sign that the prelithiated cells performed as well as the reference cells, and it indicates that neither of the prelithiation processes were significantly damaging for the cycling of the cells.

TABLE 5.2: Discharge capacity decay for cycle 2 - 10 for MP.

MP time (min)	Discharge capacity decay cycle 2 – 10 (%)
3	8
9	7
27	6
243	4
1027	4

5.3 Limited Capacity Cycling

Even though the cells cycled on the standard cycling program showed poor cycle life, with the huge specific capacity of Si, the electrodes have many times the capacity of the graphite anode and many Li-free cathodes [26]. Prelithiated cells were therefore cycled with limited capacity to study how many cycles they managed to maintain a stable capacity under less harsh conditions.

The cells were tested on two different limited capacity cycling programs, one limiting the lithiation process and the other limiting the delithiation process. The results in Table 4.9 show a significant improvement compared to the standard cycled cells, and no significant difference between the two methods. The excess Si capacity is so large that within the 500 cycles the cells were cycled, both methods perform equally well. These results indicate that when the capacity is limited, the prelithiated cells perform just as well as the graphite anodes. Similar improvements of the cycle life were seen by Chakrapani et al. [4] when limiting the capacity during cycling of SiNW-based cells.

Limited capacity cycling is believed to be less stressful for the SiNPs on the electrodes, resulting in the greatly improved cycle life. Limiting the charge/discharge drawn from the cells, the lithiation and delithiation is certainly more shallow, as only a fraction of the silicon's specific capacity is used. This is in accordance with the study by Cui et al. [7] who stated that a slow and shallow lithiation improves cyclability. The excess amount of Li on the counter electrode and excess specific capacity of Si ensure a stable discharge capacity and long cycle life.

When cycling with limited capacity, a direct correlation between change in IR and change in discharge capacity is not necessarily seen. The full potential of the cell is not used, i.e. there is excess Li ions and room for Li ions to be lost without it showing on the cell's discharge capacity. In other words, degradation of the cell can happen without it affecting the discharge capacity of the cell. The discharge capacity is a measure of the amount of electrons flowing into/out of the cell, but not of how many electrons were actually used

for lithiation or how many were lost to parasitic reactions. That is why IR measurements, especially in limited capacity cycling, are important to understand the "state of health" of the cell. With an increasing IR, the flow of ions through the system is impeded. Our IR measurements (Figures 4.25 and 4.26) show minimal variation for all 500 cycles, indicating that the cells could have continued cycling for more than 500 cycles without reduced capacity.

5.4 Evaluation of the Prelithiation and Galvanostatic Cycling Methods

5.4.1 Electrochemical Prelithiation

The intention of the EP method was to develop a simple prelithiation method that resembles something that is/could be done in industry. After one round of discharge/charge identical to the first cycle in the standard cycling program, the cells were lithiated and disassembled. The intention of the disassembling was to wash away the SEI layer, so that the new cells would have a starting point as similar as possible to the reference and MP cells. The intention was also to let the SEI layer reform when the SiNPs were at their expanded state in the prelithiated cells. However, the electrodes were only washed on the surface, and how much or little SEI was left deeper in the electrode structure is unknown. The SEM micrographs did not show signs of remaining SEI, however this was also a surface measurement. If some SEI was left in the prelithiated Si electrodes, it will have affected the measured discharge capacity and mass measurements.

The disassembly process can also be quite a damaging process on the electrodes, as they easily can be scratched, cracked or ripped in the process.

On the positive side the EP results showed successful prelithiation, and it was a more controlled method than MP, which made it interesting to compare the two. The EP process was controlled by a voltage range of 0.05 - 1 V (vs. Li^+/Li) and a constant lithiation rate of C/20, neither of which were controlled in the MP process. It is also a simple method to reproduce and test in other labs.

5.4.2 Mechanical Prelithiation

The MP method was inspired by Liu et al.[26] who prelithiated a SiNW electrode by sandwiching a piece of the electrode with electrolyte to a piece of Li foil between two glass plates. Similarly, in this study, a SiNP-based electrode with electrolyte was sandwiched together with a piece of Li foil between two glass dishes. With the glass dishes, the intention was that more or less weight easily could be added in future experiments aimed at studying the effect of pressure.

In the experiment by Liu et al. [26], the glass plates had been squeezed together using paper clips, so by using a measurable weight in this study, more information about the pressure added could be found.

The MP process can be quite damaging on the electrodes, and without the separator between the Si electrode and the Li foil, they are practically short-circuited. The Li foil was scraped with a scalpel, resulting in a rough surface possibly with small pieces of Li only partly attached to the Li foil. The rough Li surface, and the run-off of electrolyte, are believed to result in pieces of the Si electrode not becoming completely prelithiated. The handling of the electrodes during and after MP could also be a damaging process, easily resulting in scratching of the surfaces. An example of an electrode after MP is shown in Figure 5.3. Traces of the handling can be seen in form of scratches and colour variations.

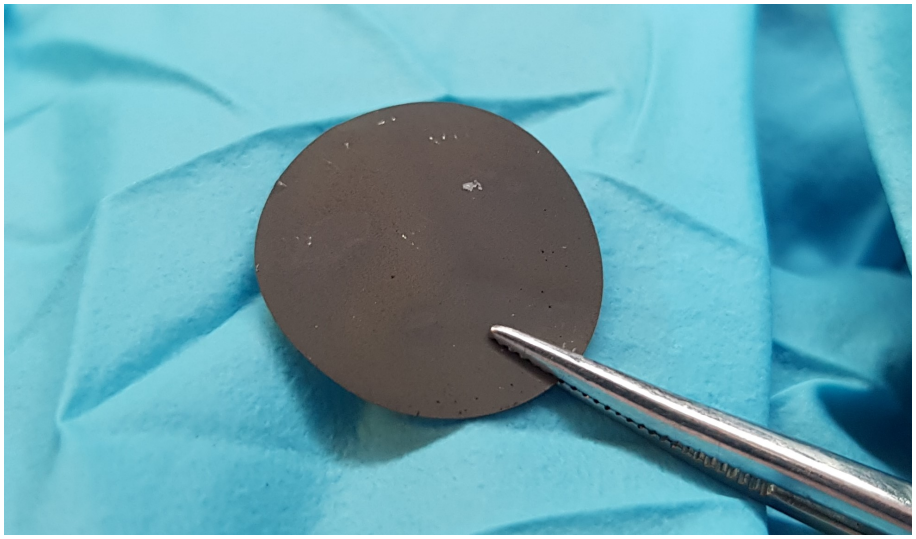

FIGURE 5.3: A Si electrode after MP showing traces of rough handling.

On the positive side the method functioned well as a proof of concept and proved to successfully prelithiate the Si electrodes. Different degrees of lithiation were obtained by increasing or decreasing the prelithiation time, and the MP electrodes were well suited for coin cell assembly. The method was in many ways different from the EP method, especially in the degree of prelithiation not being controlled by neither voltage range nor constant C-rate. It was an interesting method to study and by comparing the MP cells' cycling data to the EP cells' cycling data, much was learned about the prelithiation process and the differences between the methods. Even without the controlling parameters used in the EP process, and with the handling of the electrodes as discussed above, the MP cells were shown to perform as well as both the EP cells and the reference cells.

5.4.3 Galvanostatic Cycling

Starting the cell cycling with discharge was a conscious choice and the intention was to obtain a measurement of how much Li was inserted into the Si electrode after prelithiation, i.e. to calculate the degree of prelithiation. Starting the cell cycling with discharge, i.e. lithiation, is also the same cycling a FC goes through, and the calculated CE would then be similar to those calculated for FCs.

The degree of prelithiation was calculated from the measured discharge capacities and compared to the expected maximum discharge capacity calculated from the reference cells. The low discharge capacities measured indicated that the choice of method was good for this purpose. However, as earlier discussed, the measured discharge capacity values might not be completely suited for this kind of calculation, as it is a measurement of the number of electrons flowing in/out of the cell and not the number of Li ions.

Another drawback with the choice of method was that it complicated the calculation of ICL. Comparing measured discharge and charge capacity in the first cycle gave CEs far in excess of 100 % for the prelithiated cells, which give little information about the ICL or "real" CE. Reduced ICL is supposed to be the main advantage with prelithiation, and a better way to properly measure it should be developed.

On the positive side, all the cells cycled on the same program, which made it easy to compare the effect of the prelithiation methods. The limited capacity programs were designed with the same formation cycles, so that the only difference was the way the cells were limited. Again, this was an important choice to be able to compare the methods. The galvanostatic cycling programs are also easy to reproduce, and new adjustments can simply be made for further work.

6 Conclusion

The main goal of this study was to investigate prelithiation as a promising solution to enable the use of silicon as anode material in lithium-ion batteries (LIBs), and provide a simple method for prelithiation of silicon nanoparticles (SiNPs) in the lab. With room for improvement and further work, this goal can be considered as met.

Two prelithiation methods were developed and compared to each other: electrochemical and mechanical prelithiation. Both methods successfully prelithiated the SiNPs, and a degree of prelithiation close to 100 % was reached with both methods. This result is very promising for use in practical applications, where the prelithiated Si electrodes can be paired with Li-free cathodes and thus remove the requirement that LIB cathodes must contain Li in their synthesised state.

Prelithiation has also been considered a promising method to reduce the initial irreversible capacity loss (ICL) seen during cycling of Si Li-ion cells, and the results in this study point in the same direction. However, despite the initial ICL being reduced, electrochemical cycling shows that the prelithiated cells have similar cycling properties as the reference cells, and fade in less than 100 cycles. With prelithiation having little or no negative effect on the cycling of the Si electrodes, it can without large adjustments be used in combination with other enhancement solutions, to possibly improve cycle life of the Si Li-ion cells.

The study has also shown that mechanical prelithiation can potentially be regulated by time and mass measurements, and with further work and optimisation of the method, this is believed to be achievable. With a controllable prelithiation method, a certain degree of prelithiation can be obtained by changing the control parameters. This is especially important when wanting to use prelithiation in combination with other solutions.

Prelithiation has also been seen to be an exhausting process on the Si electrodes, and excess prelithiation might do more harm than good for the overall cyclability of the cells. However, cycling with limited capacity greatly improved the cycle life for all cells. When limiting the capacity to 372 mAh/g_{Si}, similar to the theoretical capacity of graphite, no significant discharge capacity decay was seen after 500 cycles; hence preforming as well as the graphite Li-ion batteries. It was seen that when the capacity was limited, the excess prelithiation seemed to have little or no negative effect on the cycling up to 500 cycles. These promising results are motivating for cycling the cells with higher limited capacities in further work.

The overall conclusion after this study is that prelithiation is still considered a promising solution on the way to use silicon as anode material for the next-generation LIBs. However, a better understanding and more controllable prelithiation process is needed. It is believed that the right degree of prelithiation and the right rate of stress applied to the Si electrodes, will reduce the ICL and potentially prolong cycle life. However, where or what that exact limit is, is yet to be explored. With a better understanding of the process at microscopic level, a more controlled and targeted prelithiation method can be developed.

7 Further Work

The main focus of this study was to investigate the mechanism of mechanical and electrochemical prelithiation compared to a set of reference cells. Further work should be done on optimising the methods, especially if a higher degree of control over the methods is wanted. Further work should also include testing of prelithiated Si electrodes in FCs. Here are some suggestions for further work:

- To avoid electrolyte shortage in the MP method, more electrolyte should be added, and the setup should be so that electrolyte runoff is avoided, e.g. the Si electrode could be placed in the bottom of an empty coin cell.
- MP experiments with the same and other prelithiation times should be done to further investigate the correlation between the degree of prelithiation and prelithiation time. With more information about the correlation between the two, the MP method will ideally be finely and predictably controlled by prelithiation time.
- An improved method for recording the mass change of the electrode material after prelithiation should be developed.
- Prelithiated Si electrodes should be tested in FCs. They should especially be tested in FCs with Li-free cathodes, as prelithiation is regarded a method to remove the requirement that the LIB cathode must contain Li in its original state [26].
- Limited capacity cycling: the capacity should be tested using values other than the 372 mAh/g_{Si} chosen in this study. Obtaining long cycle life for any limited capacity above this level will be an improvement compared to the graphite-anode.
- Carbon coating of the prelithiated SiNPs: coating of the prelithiated SiNPs can be another method for producing core- or yolk-shell particles. Yolk-shell particles have been reported as a promising solution for the next-generation LIBs [25].

Bibliography

[1] Maziar Ashuri, Qianran He, and Leon L. Shaw. "Silicon as a potential anode material for Li-ion batteries: where size, geometry and structure matter". In: *Nanoscale* 8 (1 2016), pp. 74–103. DOI: 10.1039/C5NR05116A.

[2] Allen J. Bard, György Inzelt, and Fritz Scholz. *Electrochemical Dictonary*. 2nd. Springer-Verlag Berlin Heidelberg, 2012. DOI: 10.1007/978-3-642-29551-5.

[3] L. Y. Beaulieu et al. "Colossal Reversible Volume Changes in Lithium Alloys". In: *Electrochemical and Solid-State Letters* 4 (9 2001), pp. 137–140. DOI: 10.1149/1.1388178.

[4] Vidhya Chakrapani et al. "Silicon nanowire anode: Improved battery life with capacity-limited cycling". In: *Journal of Power Sources* 205 (2012), pp. 433–438. DOI: 10.1016/j.jpowsour.2012.01.061.

[5] Candace K. Chan et al. "High-performance lithium battery anodes using silicon nanowires". In: *Nature Nanotechnology* 3 (2007), pp. 31–38. DOI: 10.1038/nnano.2007.411.

[6] Shu-Lei Chou et al. "Enhanced reversible lithium storage in a nanosize silicon/graphene composite". In: *Electrochemistry Communications* 12 (2 2010), pp. 303–306. DOI: https://doi.org/10.1016/j.elecom.2009.12.024.

[7] Li-Feng Cui et al. "Crystalline-Amorphous Core-Shell Silicon Nanowires for High Capacity and High Current Battery Electrodes". In: *Nano Letters* 9 (1 2009), pp. 491–495. DOI: 10.1021/nl8036323.

[8] R. M. Dell and D. A. J. Rand. *Understanding Batteries*. Cambridge, UK: Royal Society of Chemistry, 2001.

[9] Yasuhiro Domi et al. "Effect of Mechanical Pre-Lithiation on Electrochemical Performance of Silicon Negative Electrode for Lithium-Ion Batteries". In: *Journal of The Electrochemical Society* 164 (7 2017), pp. 1651–1654. DOI: 10.1149/2.1361707jes.

[10] Bruce Dunn, Haresh Kamath, and Jean-Marie Tarascon. "Electrical Energy Storage for the Grid: A Battery of Choices". In: *Science* 334 (2011), pp. 928–935.

[11] Norsk elbilforening. *Personbilsalget 2016*. Access: 2017-11-10. 2017. URL: https://elbil.no/elbilstatistikk/elbilsalg/.

[12] Michael W. Forney et al. "Prelithiation of Silicon-Carbon Nanotube Anodes for Lithium Ion Batteries by Stabilized Lithium Metal Powder (SLMP)". In: *Nano Letters* 13 (9 2013), pp. 4158–4163.

[13] The Guardian. *Carmakers' electric dreams depend on supplies of rare minerals*. Accessed: 2017-11-28. 2017. URL: https://www.theguardian.

com/environment/2017/jul/29/electric-cars-battery-manufacturing-cobalt-mining.

[14] IEA. "CO2 Emissions from Fuel Combustion - Highlights". In: (). Accessed: 2017-10-10. URL: https://www.iea.org/publications/freepublications/publication/CO2EmissionsfromFuelCombustionHighl pdf.

[15] IEA. "Global EV Outlook 2017". In: (2017). Accessed: 2017-10-10. URL: https://www.iea.org/publications/freepublications/publication/GlobalEVOutlook2017.pdf.

[16] LiCo Energy Metals Inc. *The importance of cobalt*. Accessed: 2017-11-28. URL: https://licoenergymetals.com/cobalt/#prettyPhoto.

[17] Arbin Instruments. *Battery: Cell testing - General Specifications*. Dec. 2017.

[18] Uday Kasavajjula, Chunsheng Wang, and A. John Appleby. "Nano- and bulk-silicon-based insertion anodes for lithium-ion secondary cells". In: *Journal of Power Sources* 163 (2 2007), pp. 1003–1039. DOI: https://doi.org/10.1016/j.jpowsour.2006.09.084.

[19] Huiqiao Li and Haoshen Zhou. "Enhancing the performances of Li-ion batteries by carbon-coating: present and future". In: *Chemical Communications* 48 (9 2012), pp. 1201–1217. DOI: 10.1039/c1cc14764a.

[20] Jing Li, R. B. Lewis, and J. R. Dahn. "Sodium Carboxymethyl Cellulose - A Potential Binder for Si Negative Electrodes for Li-Ion Batteries". In: *Electrochemical and Solid-State Letters* 10 (2 2007), pp. 17–20. DOI: 10.1149/1.2398725.

[21] Jing Li et al. "Lithium polyacrylate as a binder for tin–cobalt–carbon negative electrodes in lithium-ion batteries". In: *Electrochimica Acta* 55 (8 2010), pp. 2991–2995. DOI: https://doi.org/10.1016/j.electacta.2010.01.011.

[22] Yangxing Li and Brian Fitch. "Effective enhancement of lithium-ion battery performance using SLMP". In: *Electrochemistry Communications* 13 (7 2011), pp. 664–667. DOI: 10.1016/j.elecom.2011.04.003.

[23] Yuzhang Li1 et al. "Growth of conformal graphene cages on micrometre-sized silicon particles as stable battery anodes". In: *Nature Energy* 1 (2016). DOI: 10.1038/NENERGY.2015.29.

[24] David Linden and Thomas B. Reddy. *Handbook Of Batteries*. 3rd. McGraw-Hill, 2002.

[25] Nian Liu et al. "A Yolk-Shell Design for Stabilized and Scalable Li-Ion Battery Alloy Anodes". In: *Nano Letters* 12.6 (2012), pp. 3315–3321. DOI: 10.1021/nl3014814. URL: http://dx.doi.org/10.1021/nl3014814.

[26] Nian Liu et al. "Prelithiated Silicon Nanowires as Anode for Lithium Ion Batteries". In: *ACS Nano* 5 (8 2011), pp. 6487–6493.

[27] Xiao Hua Liu et al. "Size-Dependent Fracture of Silicon Nanoparticles During Lithiation". In: *ACS Nano* 6 (2 2012), pp. 1522–1531.

[28] Xiao Hua Liu et al. "Ultrafast Electrochemical Lithiation of Individual Si Nanowire Anodes". In: *Nano Letters* 11 (6 2011), pp. 2251–2258.

[29] Hardwick Group University of Liverpool. *Peled Model of the Solid Electrolyte Interphase*. Accessed: 2017-15-09. URL: https://www.liverpool.ac.uk/chemistry/research/hardwick-group/research/.

[30] Matthew T. McDowell et al. "The effect of metallic coatings and crystallinity on the volume expansion of silicon during electrochemical lithiation/delithiation". In: *Nano Energy* 1.3 (2012), pp. 401–410. DOI: https://doi.org/10.1016/j.nanoen.2012.03.004.

[31] Exxon Mobil. "2017 Outlook for Energy: A View to 2014". In: (). Accessed: 1027-10-10. URL: http://cdn.exxonmobil.com/~/media/global/files/outlook-for-energy/2017/2017-outlook-for-energy.pdf.

[32] Trygve Mongstad et al. "No Significant Effect of Phosphorous Doping on the Electrochemical Performance of Silicon-Carbon Composite Anodes for Li-ion Batteries". In: *ECS Transactions 2016* 73 (2016). DOI: 10.1149/07301.0275ecst.

[33] Donald A. Neamen. *Semiconductor Physics and Devices: Basic Principles*. 4th. McGraw-Hill, 2012.

[34] Naoki Nitta et al. "Li-ion battery materials: present and future". In: *Materials Today* 18 (5 2015), pp. 252–264.

[35] M. N. Obrovacz and Leif Christensen. "Structural Changes in Silicon Anodes during Lithium Insertion/Extraction". In: *Electrochemical Solid-State Letters* 7 (5 2004), pp. 93–96. DOI: 10.1149/1.1652421.

[36] K. Ogata et al. "Revealing lithium–silicide phase transformations in nano-structured silicon-based lithium ion batteries via in situ NMR spectroscopy". In: *Nature Communications* 5 (2014). DOI: 10.1038/ncomms4217.

[37] Noshin Omar. "European Battery Material Needs for Automative Applications". In: Presentation at the Nordic Battery Conference in Kokkola, Finland, 1.-3. of November 2017.

[38] Francois Ozanam and Michel Rosso. "Silicon as anode material for Li-ion batteries". In: *Material Science and Engineering B* 213 (2016), pp. 2–11.

[39] Jung-Ki Park. *Principles and Applications of Lithium Secondary Batteries*. Weinheim, Germany: Wiley-VCH, 2012.

[40] Matthew B. Pinson and Martin Z. Bazan. "Theory of SEI Formation in Rechargeable Batteries: Capacity Fade, Accelerated Aging and Lifetime Prediction". In: *Journal of Electrochemical Society* 160 (2 2013), pp. 243–250.

[41] Bruno Scrosati. "History of lithium batteries". In: *Solid State Electrochem* 15 (2011), pp. 1623–1630.

[42] *The Commercialization of Lithium Battery Technology*. Vienna, Austria, 2007.

[43] Vijay A. Sethuraman et al. "In Situ Measurements of Stress Evolution in Silicon Thin Films During Electrochemical Lithiation and Delithiation". In: *Journal of Power Sources* 195 (15 2010), pp. 5062–5066. DOI: https://doi.org/10.1016/j.jpowsour.2010.02.013.

[44] Gerard K. Simon and Tarun Goswami. "Improving Anodes for Lithium Ion Batteries". In: *Metallurgical and Materials Transactions A* 42.1 (2011), pp. 231–238. DOI: 10.1007/s11661-010-0438-5.

[45] R. Spotnitz. "Simulation of capacity fade in lithium-ion batteries". In: *Journal of Power Sources* 113.1 (2003), pp. 72–80. DOI: https://doi.org/10.1016/S0378-7753(02)00490-1.

[46] Jeannine R. Szczech and Song Jin. "Nanostructured silicon for high capacity lithium battery anodes". In: *Energy and Environmental Science* 4 (1 2011), pp. 56–72. DOI: 10.1039/C0EE00281J.

[47] J.-M. Tarason and M. Armand. "Issues and challenges facing rechargeable lithium batteries". In: *Nature* 414 (2001), pp. 359–367. DOI: 10.1038/35104644.

[48] Marius Valle. *Teslas Gigafactory blir småtterier sammenlignet med kinesernes kommende batteriproduksjon*. Accessed: 2017-11-28. 2017. URL: https://www.tu.no/artikler/tesla-gigafactory-til-tross-markedet-vil-flomme-over-av-billige-kinesiske-batterier/396817.

[49] Pallavi Verma, Pascal Maire, and Petr Novák. "A review of the features and analyses of the solid electrolyte interphase in Li-ion batteries". In: *Electrochimica Acta* 55 (22 2012), pp. 6332–6341. DOI: https://doi.org/10.1016/j.electacta.2010.05.072.

[50] Bin Wang et al. "High Volumetric Capacity Silicon-Based Lithium Battery Anodes by Nanoscale System Engineering". In: *Nano Letters* 13 (11 2013), pp. 5578–5584.

[51] Hui Wu and Yi Cui. "Designing nanostructured Si anodes for high energy lithium ion batteries". In: *Nano Today* 7 (5 2012), pp. 414–429. DOI: https://doi.org/10.1016/j.nantod.2012.08.004.

[52] Hui Wu et al. "Stable cycling of double-walled silicon nanotube battery anodes through solid–electrolyte interphase control". In: *Nature Nanotechnology* 7 (2012), pp. 310–315. DOI: doi:10.1038/nnano.2012.35.

[53] Wan-Jing Yu et al. "Lithiation of Silicon Nanoparticles Confined in Carbon Nanotubes". In: *ACS Nano* 9 (5 2015), pp. 5063–5071. DOI: 10.1021/acsnano.5b00157.

[54] Sheng Shui Zhang. "A review on electrolyte additives for lithium-ion batteries". In: *Science Direct* 162 (2 2006), pp. 1379–1394. DOI: 10.1016/j.jpowsour.2006.07.074.

[55] Sheng Shui Zhang et al. "Understanding Solid Electrolyte Interface Film Formation on Graphite Electrodes". In: *Electrochemical and Solid-State Letters* 4 (12 2001), pp. 206–208. DOI: 10.1149/1.1414946.

[56] Wei-Jun Zhang. "A review of the electrochemical performance of alloy anodes for lithium-ion batteries". In: *Journal of Power Sources* 196 (1 2010), pp. 13–24. DOI: 10.1016/j.jpowsour.2010.07.020.

[57] Hui Zhao et al. "Toward Practical Application of Functional Conductive Polymer Binder for a High-Energy Lithium-Ion Battery Design". In: *Nano Letters* (2014).

[58] Jie Zhao et al. "Artificial Solid Electrolyte Interphase-Protected LixSi Nanoparticles: An Efficient and Stable Prelithiation Reagent for Lithium-Ion Batteries". In: *Journal of the American Chemical Society* 137 (26 2015), 8372–8375. DOI: 10.1021/jacs.5b04526.

A Best Poster Award at the Nordic Battery Conference 2017

Below the Best Poster Award diploma is printed, and the poster "Mechanical and Electrochemical Pre-lithiation of Silicon Nanoparticles" can be found on the next page.

NordBatt 2017

BEST POSTER AWARD

M.Sc. student Alise Hjellbrekke

The best poster award for her contribution "Mechanical and Electrochemical Pre-lithiation of Silicon Nanoparticles"

On the behalf of the NordBatt2017 scientific committee

Kokkola 3.11.2017

Ulla Lassi, professor

Mechanical and Electrochemical Pre-lithiation of Silicon Nanoparticles

Alise J. Hjellbrekke[1,2], Jan Petter Mæhlen[3], Trygve T. Mongstad[2], Samson Y. Lai[4] and Arne A. Grimenes[1]

[1]Department of Mathematical Science and Technology, Norwegian University of Life Science (NMBU), Ås, Norway
[2]Department of Solar Energy, Institutt For Energiteknikk (IFE), Kjeller, Norway
[3]Department of Energy Systems, Institutt for Energiteknikk (IFE), Kjeller, Norway
[4]Department of Physics, Institutt For Energiteknikk (IFE), Kjeller, Norway

INTRODUCTION

With its high theoretical capacity of 3,572 mAh/g_{Si} for $Li_{15}Si_4$, silicon is one of the most promising anode materials for the next generation Li-ion batteries. However, silicon particles expand greatly during lithiation, which induces many challenges when electrochemically cycled. E.g. silicon anodes suffer from low initial coulombic efficiency.

Pre-lithiation is the process in which silicon nanoparticles get lithiated before being assembled into cells, and is considered a solution to reduce the initial irreversible capacity loss.

The aim of this work is to obtain methods for both electrochemical and mechanical pre-lithiation (called EP and MP) of silicon nanoparticles. Whether the degree of pre-lithiation can be controlled by time of lithiation will be evaluated, as well as the electrochemical cycling performance.

METHODOLOGY

Silicon nanoparticles produced in a free space reactor (FSR) at IFE were used as active material, and Li-foil as counter electrode. Pre-lithiated Si-electrodes were assembled into CR2032 coin cells and cycled in Arbin.

Mechanical Pre-lithiation (MP):

Inspired by Liu et al. [1].

1. Li-foil was scraped until shiny and directly placed onto the Si electrode wetted with 15 µl of electrolyte.
2. Glass dishes were used to sandwich the pieces, and pressure was added by putting on a small weight (132,8 g).
3. After a certain number of minutes passed, the pre-lithiated Si anodes were washed with DMC and left drying overnight, before assembled into coin cells.

Electrochemical Pre-lithiation (EP):

1. Coin cells cycled for one and a half cycle at a rate of C/20 in Arbin. Took the cells out at lithiated state.
2. The cells were disassembled and the lithiated Si electrodes were washed with DMC.
3. Dried overnight before reassembled into new coin cells.

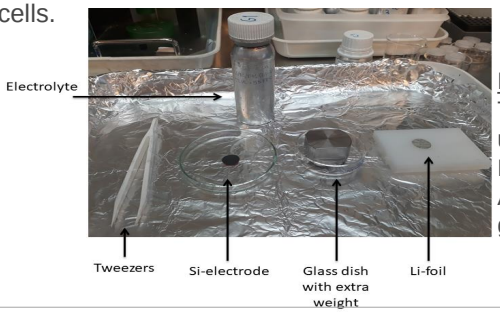

Figure 1: The tools used for MP in an Ar-filled glove box.

ELECTROCHEMICAL PERFORMANCE

Coin cells cycled with:

- 3 formation cycles at C/20 plus 100 cycles at C/10

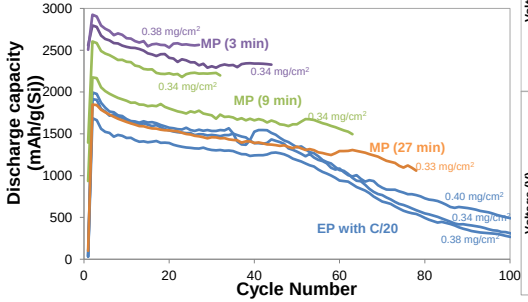

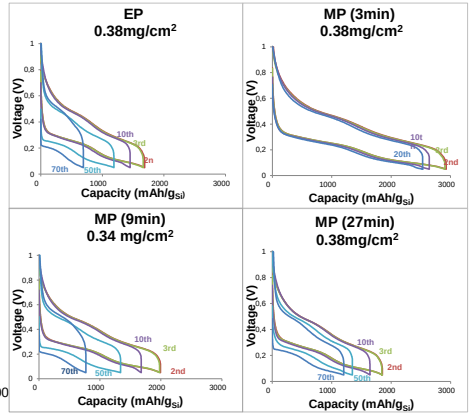

PRE-LITHIATION OVER TIME

Change in electrode mass - MP (%):

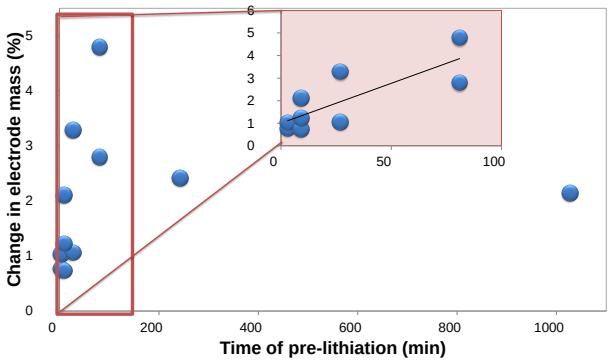

Degree of lithiation (%):

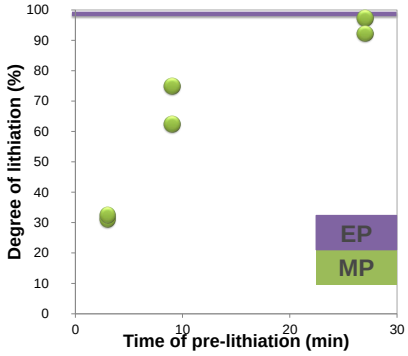

CONCLUSIONS

- Results show that both MP and EP effectively pre-lithiate the electrodes.
- Results show that MP can be measured by mass and 1st cycle discharge capacity, and can be controlled by pre-lithiation time.
- **Work in progress:** comparing the performance of EP, MP and reference cells cycled at both unlimited and limited capacity.

ACKNOWLEDGEMENTS

- Funding support was provided by the Research Council of Norway through the ENERGIX Project No. 255116.
- This work was performed within MoZEES, a Norwegian Centre for Environment-friendly Energy Research (FME), co-sponsored by the Research Council of Norway (project number 257653) and 40 partners from research, industry and public sector.

REFERENCES

[1] Liu, N., et al., *Prelithiated Silicon Nanowires as an Anode for Lithium Ion Batteries.* ACS Nano, 2011. **5**(8): p. 6487-6493.

B Galvanostatic Cycling

B.1 Elecrochemical Prelithiation Program

Program name: 1cyc_C20_Lithiate_MR.sdu

Cycling steps:

1. OCV and rest for 18 h
2. IR measurement 1
3. Lithiation at C/20 with cut-off at 50 mV
4. IR measurement 2
5. OCV and rest for 30 min
6. Delithiation at C/20 with cut-off at 1 V
7. IR measurement 3
8. OCV and rest for 15 min
9. Lithiation at C/20 with cut-off at 50 mV
10. IR measurement 4
11. OCV and rest for 1 h

B.2 Standard Cycling Program

Program name: 3cyc_C20_100cyc_C10_MR.sdu

Cycling steps:

1. Open circuit voltage (OCV) and rest for 6 h
2. Internal resistance (IR) measurement 1
3. Three formation cycles:
   (a) Lithiation at C/20 with cut-off at 50 mV
   (b) IR measurement 2
   (c) OCV and rest for 30 min

   (d) Delithiation at C/20 with cut-off at 1 V
   (e) IR measurement 3
   (f) OCV and rest for 15 min
4. Loop with unlimited capacity cycling (100 cycles):
   (a) Lithiation at C/10 with cut-off at 50 mV
   (b) IR measurement 4
   (c) OCV and rest for 15 min
   (d) Delithiation at C/10 with cut-off at 1 V
   (e) IR measurement 5
   (f) OCV and rest for 15 min
5. OCV and rest for 30 min

B.3 Limited Capacity Cycling Programs

B.3.1 Limited Delithiation Cycling:

Program name: 1cyc_C20_500cyc_C5_LC-372_MR.sdu

Cycling steps:

1. OCV and rest for 6 h
2. IR measurement 1
3. Two formation cycles:
   (a) Lithiation at C/20 with cut-off at 50 mV
   (b) IR measurement 2
   (c) OCV and rest for 15 min
   (d) Delithiation at C/20 with cut-off at 1 V
   (e) IR measurement 3
   (f) OCV and rest for 15 min
4. Lithiation at C/20 with cut-off at 50 mV
5. IR measurement 4
6. OCV and rest for 15 min
7. Loop with limited capacity of 372 mAh/g (500 cycles):
   (a) Delithiation at C/5 with limited capacity of 372 mAh/g

   (b) IR measurement 5
   (c) OCV and rest for 15 min
   (d) Lithiation at C/5 with cut-off at 50 mV
   (e) IR measurement 6
   (f) OCV and rest for 15 min
8. OCV and rest for 30 min

B.3.2 Limited Lithiation Cycling:

Program name: 3cyc_C20_500cyc_C5_LC-372_Lithiation_MR.sdu

Cycling steps:

1. OCV and rest for 6 h
2. IR measurement 1
3. Three formation cycles:
   (a) Lithiation at C/20 with cut-off at 50 mV
   (b) IR measurement 2
   (c) OCV and rest for 15 min
   (d) Delithiation at C/20 with cut-off at 1 V
   (e) IR measurement 3
   (f) OCV and rest for 15 min
4. Loop with limited capacity of 372 mAh/g (500 cycles):
   (a) Delithiation at C/5 with cut-off at 50 mV
   (b) IR measurement 4
   (c) OCV and rest for 15 min
   (d) Lithiation at C/5 with limited capacity of 372 mAh/g
   (e) IR measurement 5
   (f) OCV and rest for 15 min
5. OCV and rest for 30 min

C Complete list of cells

TABLE C.1: Complete list of coin cells made during thesis work.

Cell	Cycling program	Load of active material (mg_{Si}/cm^2)	Comment
ref_01	standard	0.38	
ref_02	standard	0.42	
ref_03	standard	0.32	unsafe voltage
ref_04	standard	0.29	unsafe voltage
EP_01	standard	0.47	wrong C-rate
EP_02	standard	0.40	wrong C-rate
EP_03	standard	0.38	wrong C-rate
EP_04	standard	0.38	
EP_05	standard	0.32	
EP_06	standard	0.38	
EP_07	LC (delithiation)	0.42	
EP_08	LC (delithiation)	0.42	
EP_09	LC (lithiation)	0.37	
EP_10	LC (lithiation)	0.38	
MP_01	standard	0.34	wrong C-rate
MP_02	standard	0.34	wrong C-rate
MP_03	standard	0.33	wrong C-rate
MP_04	standard	0.38	
MP_05	standard	0.34	
MP_06	standard	0.40	unsafe voltage
MP_07	standard	0.42	
MP_08	standard	0.42	unsafe voltage
MP_09	standard	0.34	
MP_10	LC (delithiation)	0.36	
MP_11	standard	0.40	short-circuited
MP_12	standard	0.31	
MP_13	standard	0.34	
MP_14	LC (delithiation)	0.42	
MP_15	LC (delithiation)	0.40	
MP_16	LC (lithiation)	0.37	
MP_17	LC (lithiation)	0.45	

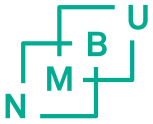

Norges miljø- og biovitenskapelige universitet
Noregs miljø- og biovitskapelege universitet
Norwegian University of Life Sciences

Postboks 5003
NO-1432 Ås
Norway